Introduction to X-ray Photoelectron Spectroscopy (XPS)

Emrah Özensoy

Bilkent University

Chemistry Department
Ankara, Türkiye

Turkish Soft **X**-ray **P**hoto**E**lectron **S**pectroscopy Project

TXPES SESAME

OzensoyLab
Catalysis for Energy, Environment and Sustainability

https://ozensoylab.bilkent.edu.tr/

An Introduction to XPS:

I. **XPS Operational Principles:**
   XPS Experiment & Instrumentation
   Photoemission Process
   Surface Sensitivity & Film Thickness Analysis
   Complex Spectral Features
   Spin Orbit Splitting
   Charge Compensation
   XPS Peak Fitting & Baseline Correction & Signal Deconvolution

II. **Common Types of Analysis via XPS:**
   Survey Scan & Surface Atomic % Composition Analysis
   Oxidation State & Functional Group Analysis (Chemical Shifts)
   Depth Profiling

Emrah Ozensoy, Bilkent University, Ankara, Türkiye

XPS Experiment & Instrumentation

Emrah Özensoy
Bilkent University

X-ray Photoelectron Spectroscopy (XPS)

Photon Source

- X-ray tube
- UV lamp
- Laser
- Synchrotron
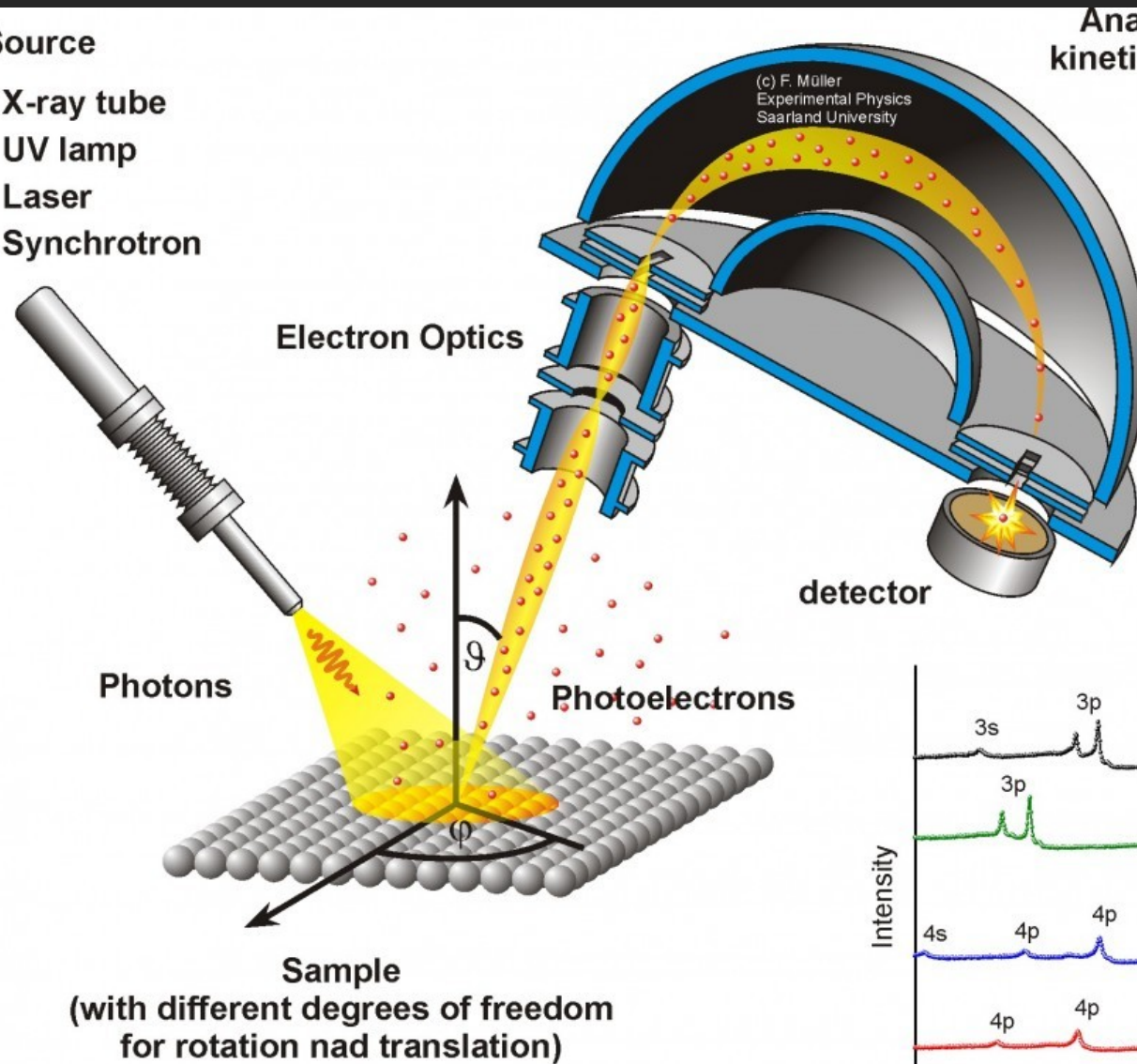
Also known as:

Photoelectron Spectroscopy (PES)
Photoemission Spectroscopy (PES)
Electron Spectroscopy for Chemical Analysis (ESCA)
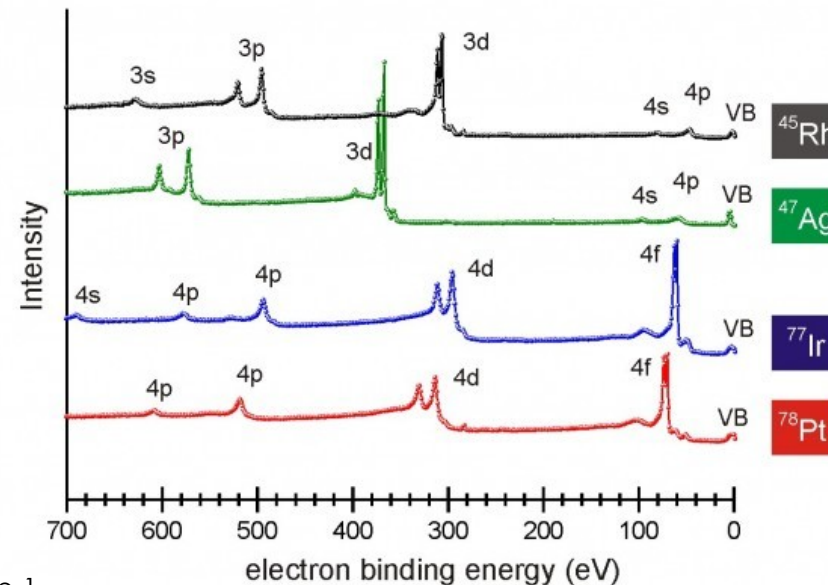
Emrah Özensoy
Bilkent University

XPS Spectrometer Components

Hemispherical analyser

Multi-channel Detectors (MCD)
Delay Line Detectors (DLD)
Pulse Counting CMOS Detectors

Detector

Surface Cleaning
Depth Profiling
Ion gun

$Ar^+(g)$ Sputtering Gun

X-ray Energy Resolution Enhancement
Monochromator crystal

Charge Compensation
During XPS Analysis
Flood gun

- Broad Area Electron Gun

- Al, Mg, Ag Anodes
- Synchrotron X-rays

X-ray source

Emrah Özensoy
Bilkent University

XPS Experimental Details
Hemispherical Electron Energy Analyzer

Energy Resolution of Analyzer

Small E_{pass} ←→ Large E_{retard}
High resolution
Low throughput (low count rates)
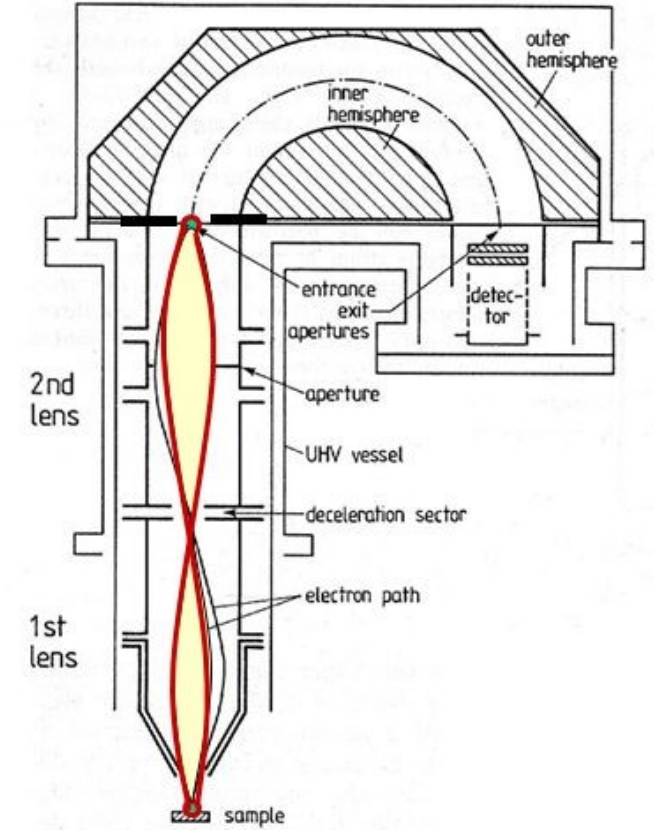
Large E_{pass} ←→ Small E_{retard}
Low resolution
High throughput (high count rates)

표면분석 2016 김정원

Retarding Field Analyzer (RFA)

**Emrah Özensoy
Bilkent University**

XPS: X-ray Sources

Mg/Al Dual Anode
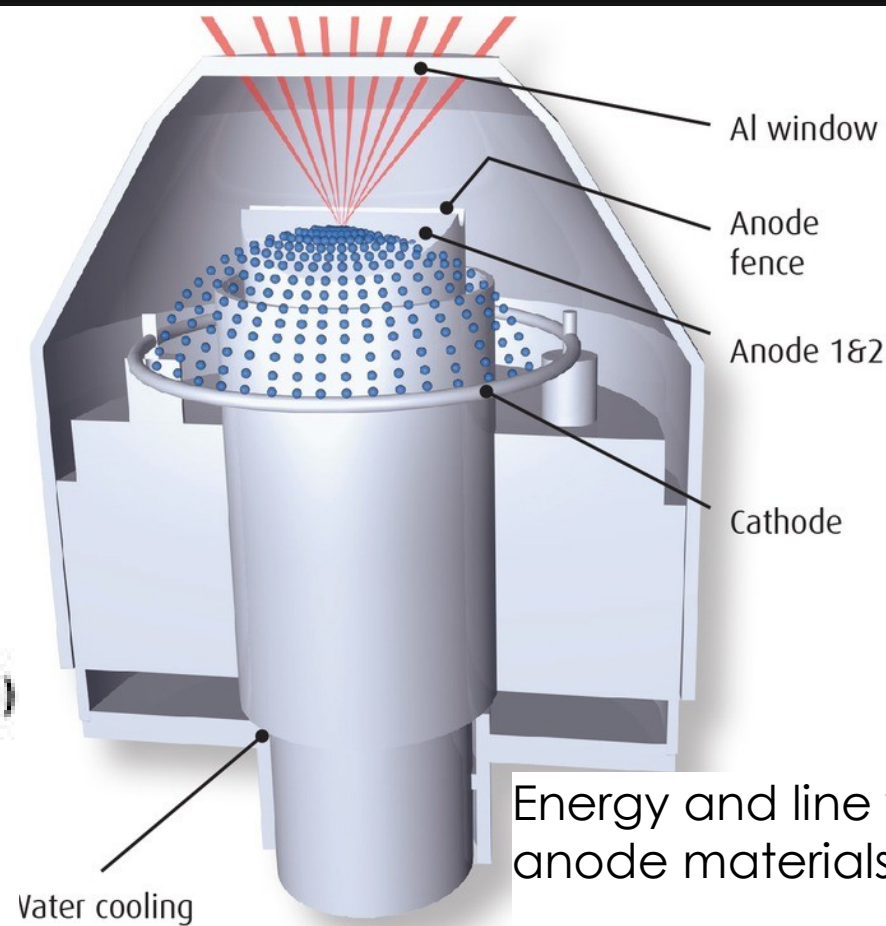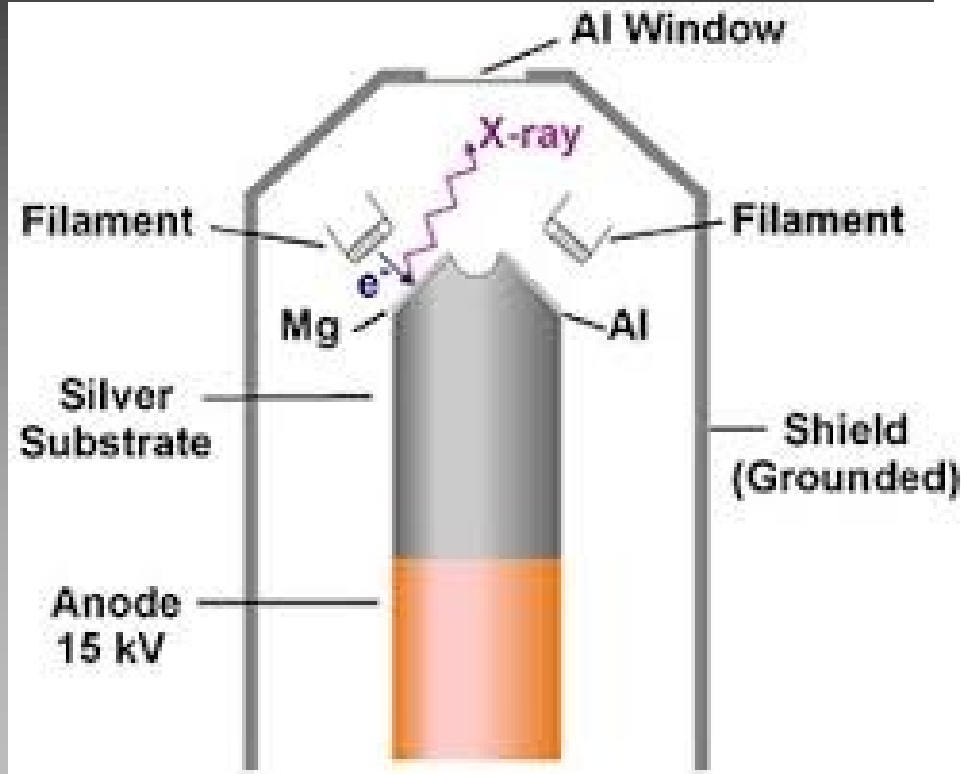
Emrah Özensoy
Bilkent University

Energy and line widths of available anode materials.

Anode	Radiation	Photon Energy (eV)	Line Width (eV)
Mg	Kα	1253.6	0.7
Al	Kα	1486.6	0.85
Zr	Lα	2042.4	1.6
Ag	Lα	2984.3	2.6
Ti	Kα	4510.9	2.0
Cr	Kα	5417	2.1

The most commonly employed X-ray sources:

Mg Kₐ radiation :
hv = 1253.6 eV

Al Kₐ radiation :
hv = 1486.6 eV

https://xpssimplified.com/xray_generation.php

Energy Resolution Enhancement viz Choice of X-ray Source

Non-monochromated X-ray Source

Monochromated X-ray Source
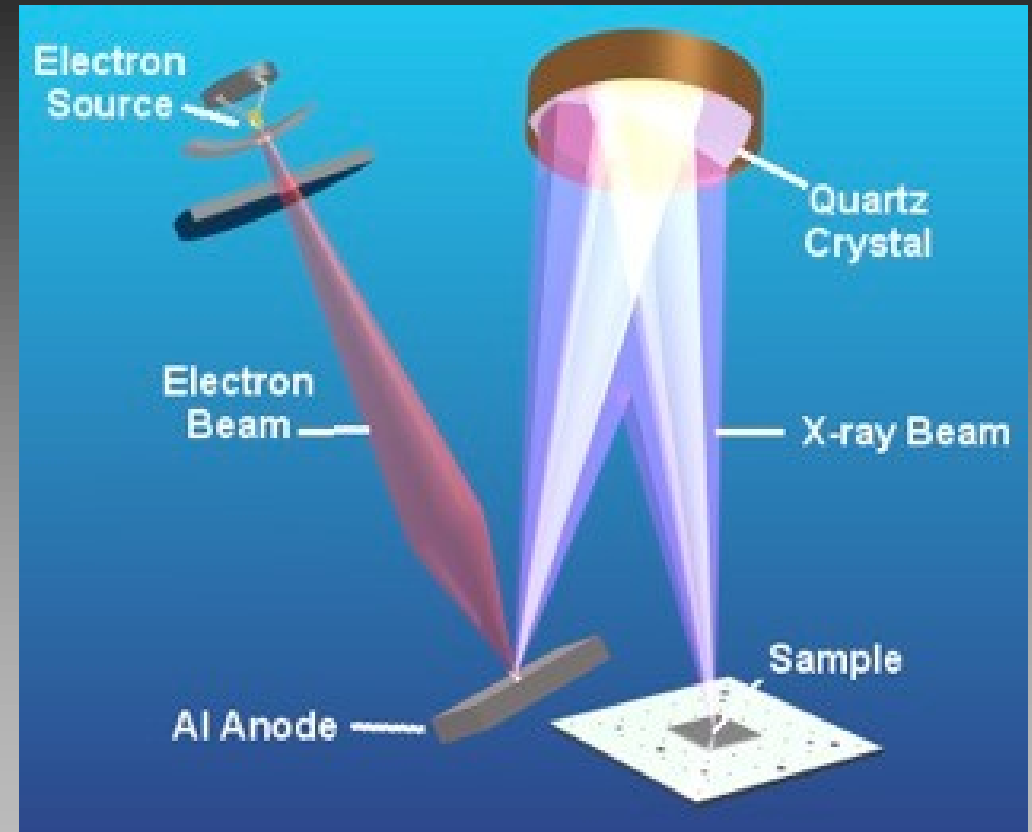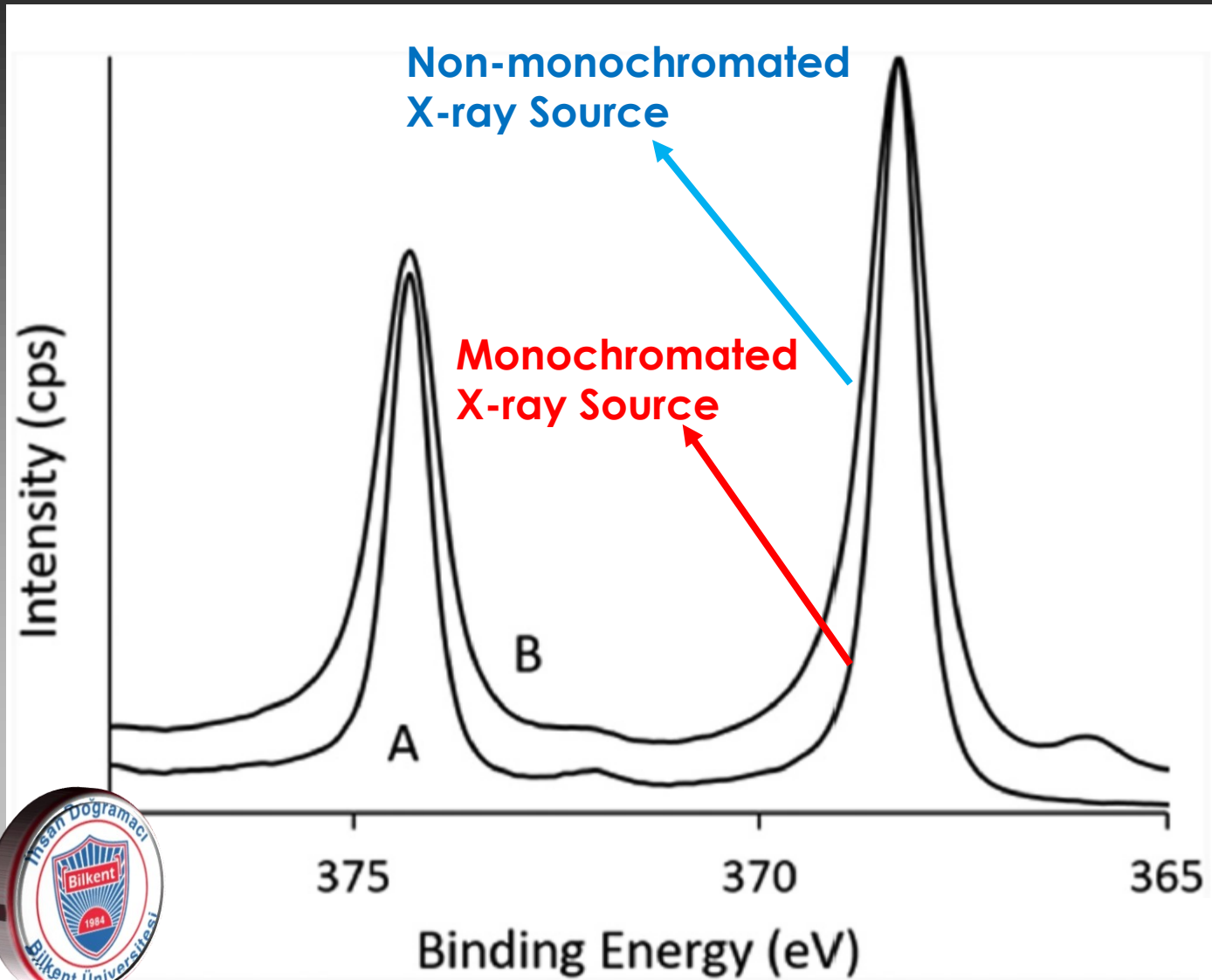
The most commonly employed benchtop X-ray sources:

Mg K_a radiation :
$h\nu = 1253.6$ eV

Al K_a radiation :
$h\nu = 1486.6$ eV

Stevie et al. J. Vac. Sci. Technol. A **38**, 063204 (2020)
https://doi.org/10.1116/6.0000412

Emrah Özensoy
Bilkent University

Why do we need Synchrotron (SR) based X-rays ?
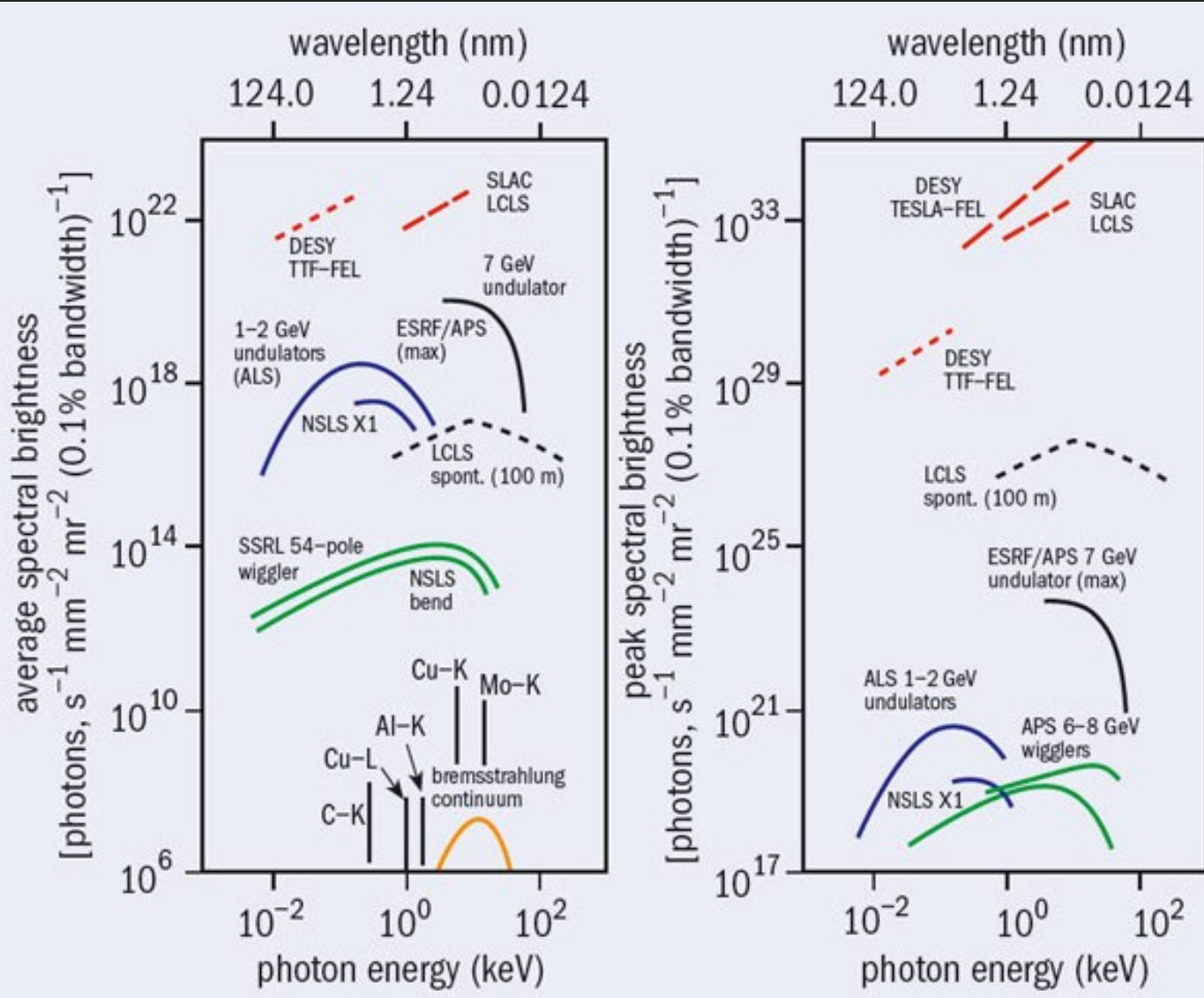
SR-based X-ray Sources offer:

- High Photon Flux (10^{14} photons s^{-1} mm^{-2} mr^{-2})
- High Energy Resolution (< 10 meV)
- High Spatial Resolution (< 50 μm)
- Tunable Wavelength
- Tunable Time Domain (Pulses)
- X-ray Polarization capabilities

- The **peak and average brightness** of lab-based sources, storage-ring based synchrotron radiation sources, and of the X-ray FELs.

https://cerncourier.com/a/making-x-rays-bright-times-ahead-for-fels/

Emrah Özensoy
Bilkent University

High Resolution XPS instead of Vibrational Spectroscopy ?
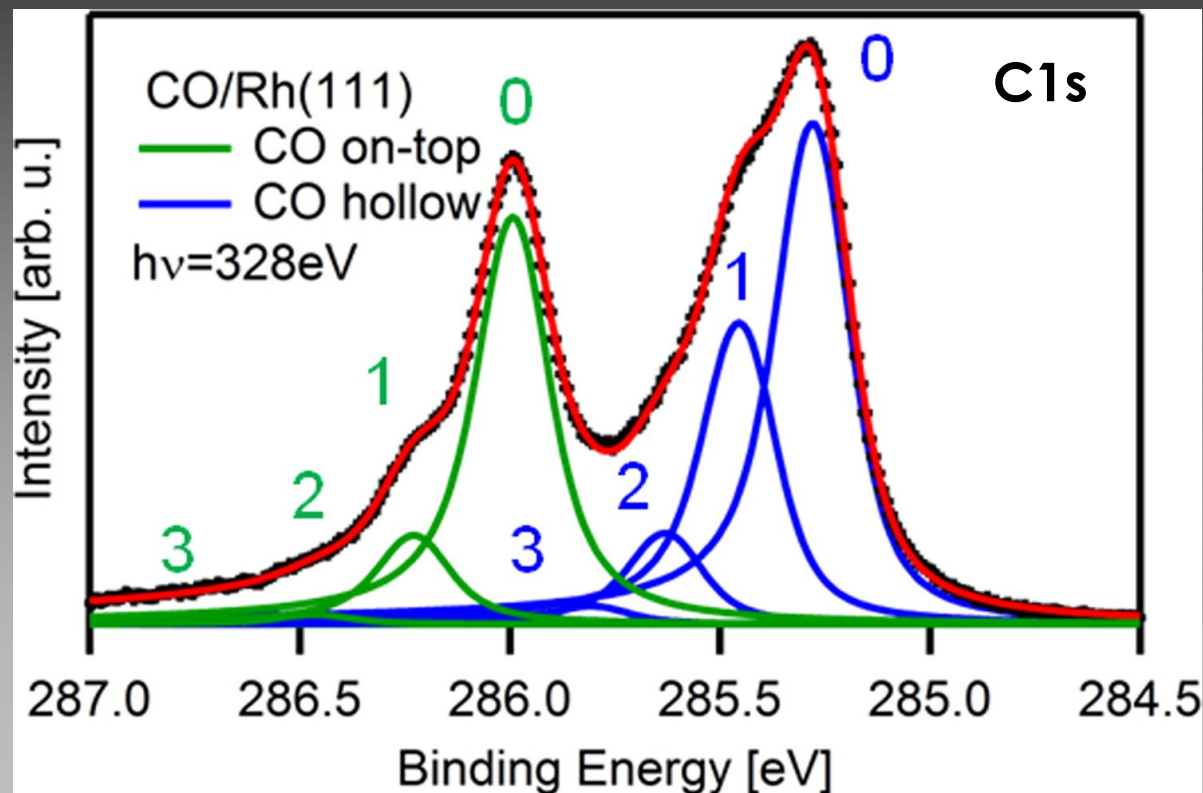
C1s spectrum of the saturated (2×2)-3CO layer on Rh(111), with a coverage of 0.75 ML. The spectrum was measured at MAX-Lab in Lund using a photon energy of 328 eV and a data collection time of 900 s.
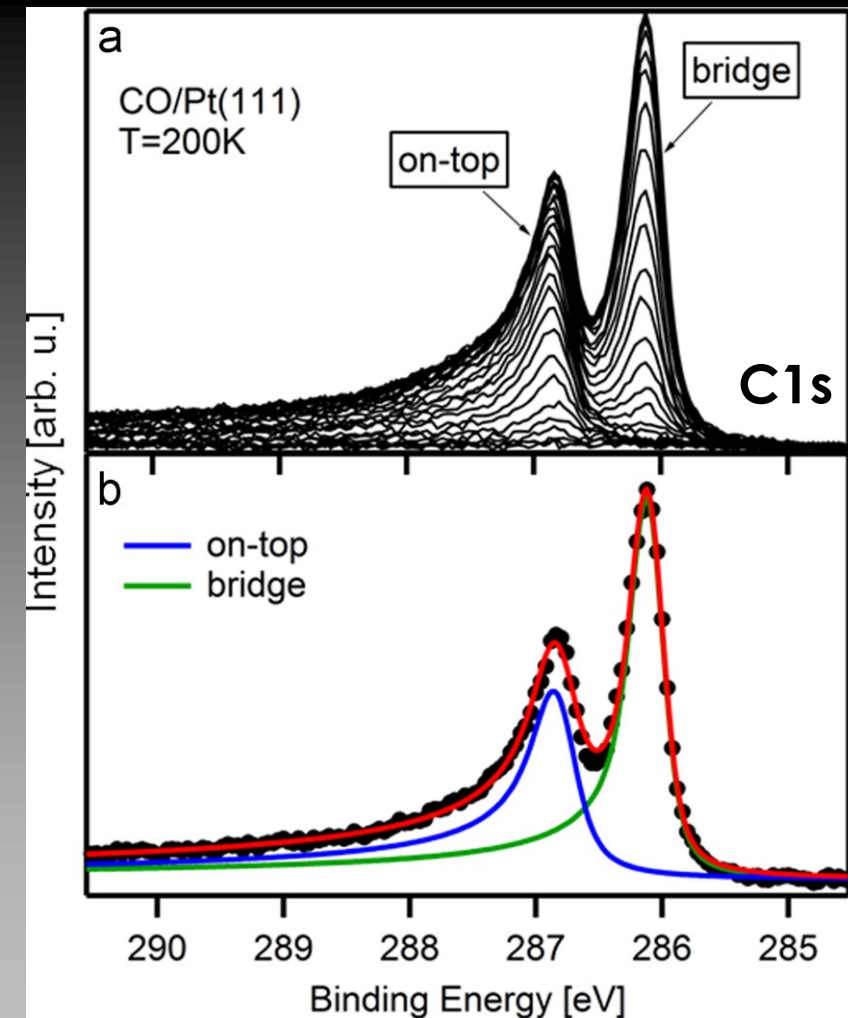
Normal emission C1s XP spectra taken during uptake of CO on Pt(111), using a photon energy of 380 eV; the topmost spectrum corresponds to a coverage of 0.5 ML and a c(4×2) LEED structure, observed after the measurement. Time between spectra 60 s, $p=1.7×10^{-9}$ mbar, time per spectrum 4.8 s

Steinrück et al. *Surface Science Reports* Volume 68, Issues 3–4, 2013, 446

Emrah Özensoy
Bilkent University

What kind of samples can be analyzed via UHV-XPS ?

- Solids
- Powders
- Films
- Polymers
- Inorganic salts
- Organic crystals
- Porous materials
- Selected Gases

- Conductors
- Insulators
- Semi-conductors

- Samples should be Ultra-High Vacuum, UHV (10^{-9}-10^{-10} Torr) compatible.

- Samples should not outgas severely.

- Samples should be dry/pre-dried

- No volatile organics/inorganics

- No liquids

Emrah Özensoy
Bilkent University

Photoemission Process

Emrah Özensoy
Bilkent University

Electron Energy Levels and Photoemission Process

Kinetic Energy

(a) Initial State before photon excitation

(b) Photoemission upon Core-hole formation (1 x e⁻ process)

(c) Auger transition upon Core-hole formation (3 x e⁻ process)

(d) X-ray Fluorescence upon Core-hole formation (2 x e⁻ process)

Emrah Özensoy
Bilkent University
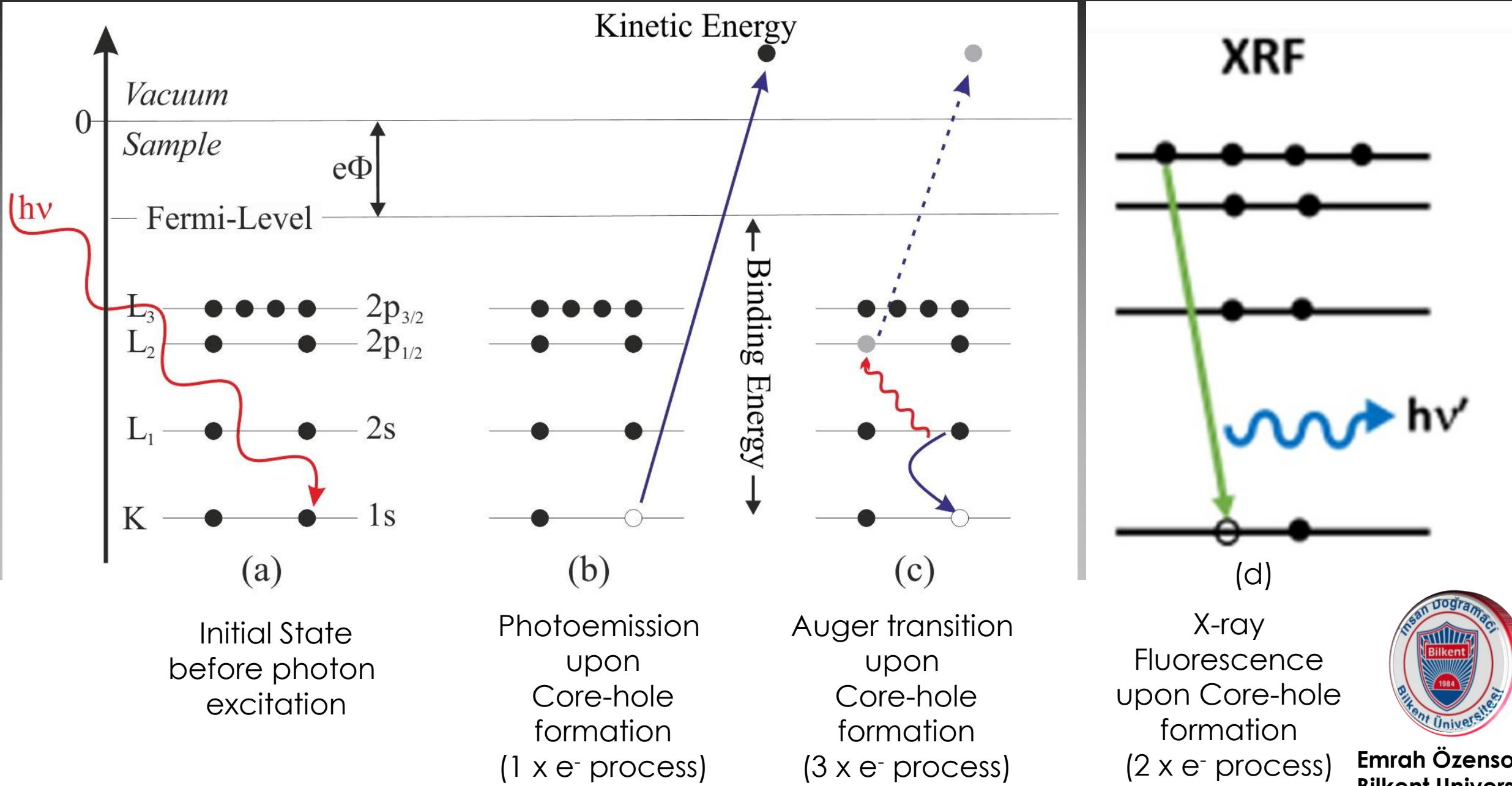
Electron Energy Levels and Photoemission Process

Binding Energy Reference

$$K.E. = h\nu - B.E._{.F} - \phi_{sample}$$

$$K.E. = h\nu - B.E._{.F} - \phi_{sample}$$
$$- (\phi_{spec} - \phi_{sample})$$
$$= h\nu - B.E._{.F} - \phi_{spec}$$

Vacuum level

e⁻

Vacuum level

Sample Work Function ϕ_{sample}

ϕ_{spec} Spectrometer Work Function

Fermi level   **Same level**   Fermi level

Binding Energy $B.E._{.F}$

Spectrometer

core level

Sample

Core electron Binding Energy	X-ray Photon Energy	Photoelectron Kinetic Energy	Spectrometer Work Function

$$B.E._{.F} = h\nu - K.E. - \phi_{spec}$$

Emrah Özensoy
Bilkent University

Electron Energy Levels and Photoemission Process

Emrah Özensoy
Bilkent University

Some of the Characteristic Aspects of XPS Spectra

Emrah Özensoy
Bilkent University

XPS Survey Spectrum
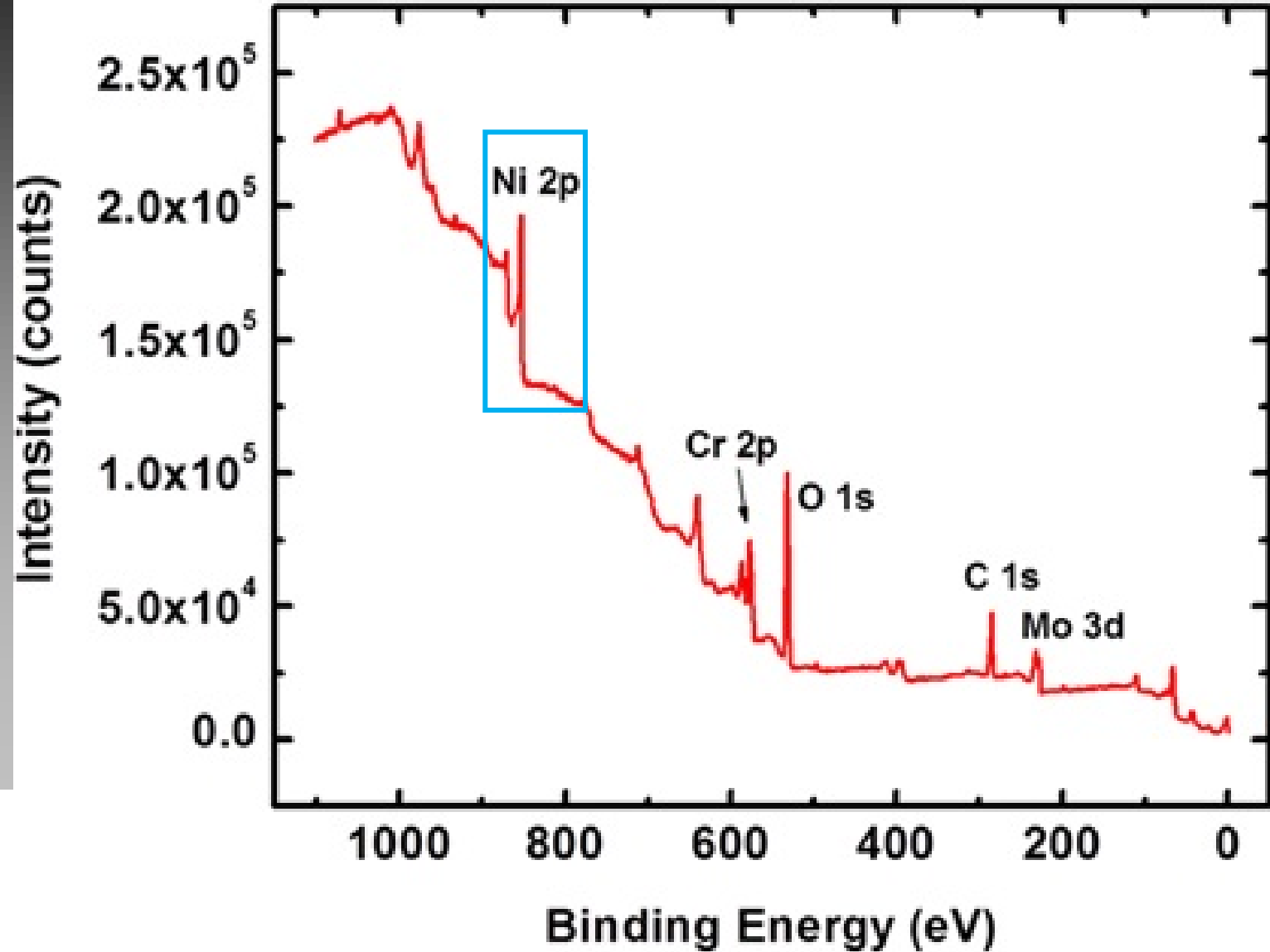
XPS Survey Spectrum:

- Low-energy resolution
- Quick data Acquisition
- Wide energy range
- Reveals all the elements within detection limit

https://www.xpsfitting.com/2016/12/advanced-quantification-combining.html

Emrah Özensoy
Bilkent University

High-Resolution XP-Spectrum for a given element: Ni

Emrah Özensoy
Bilkent University
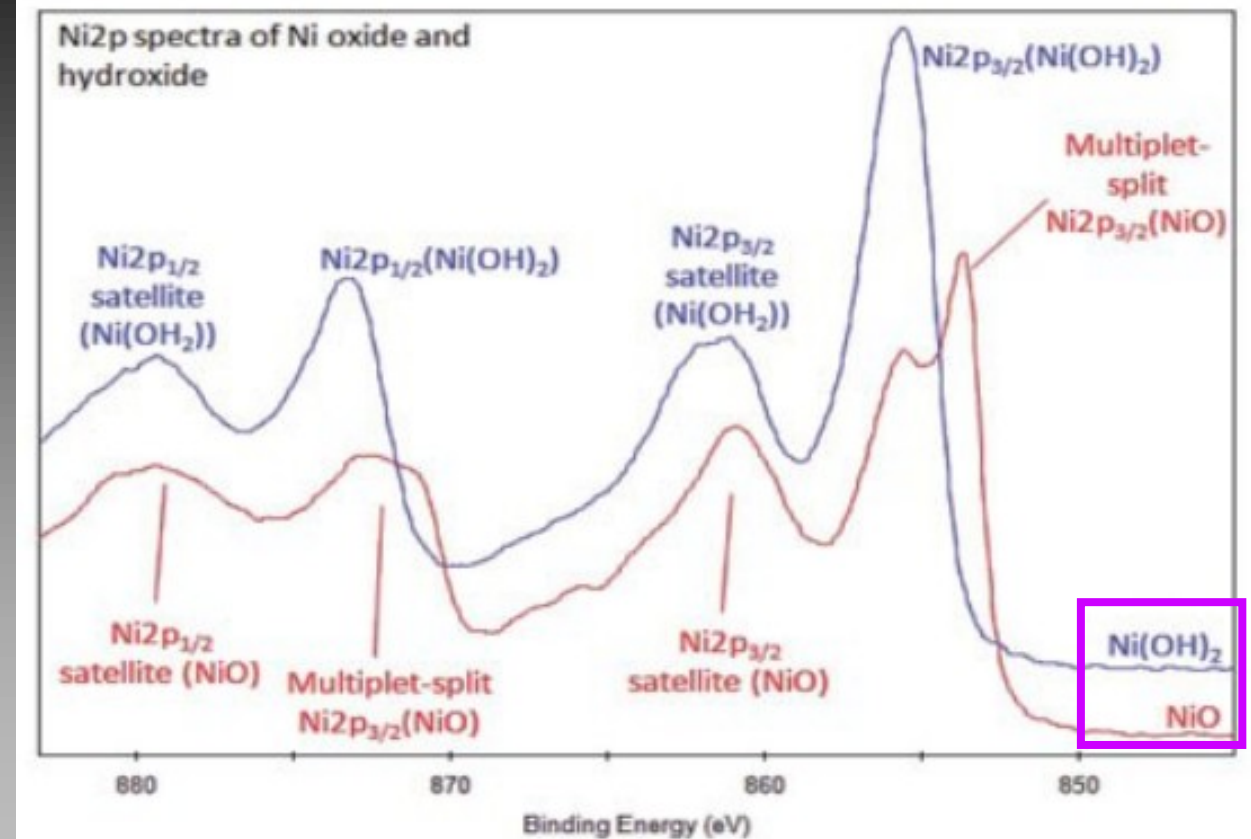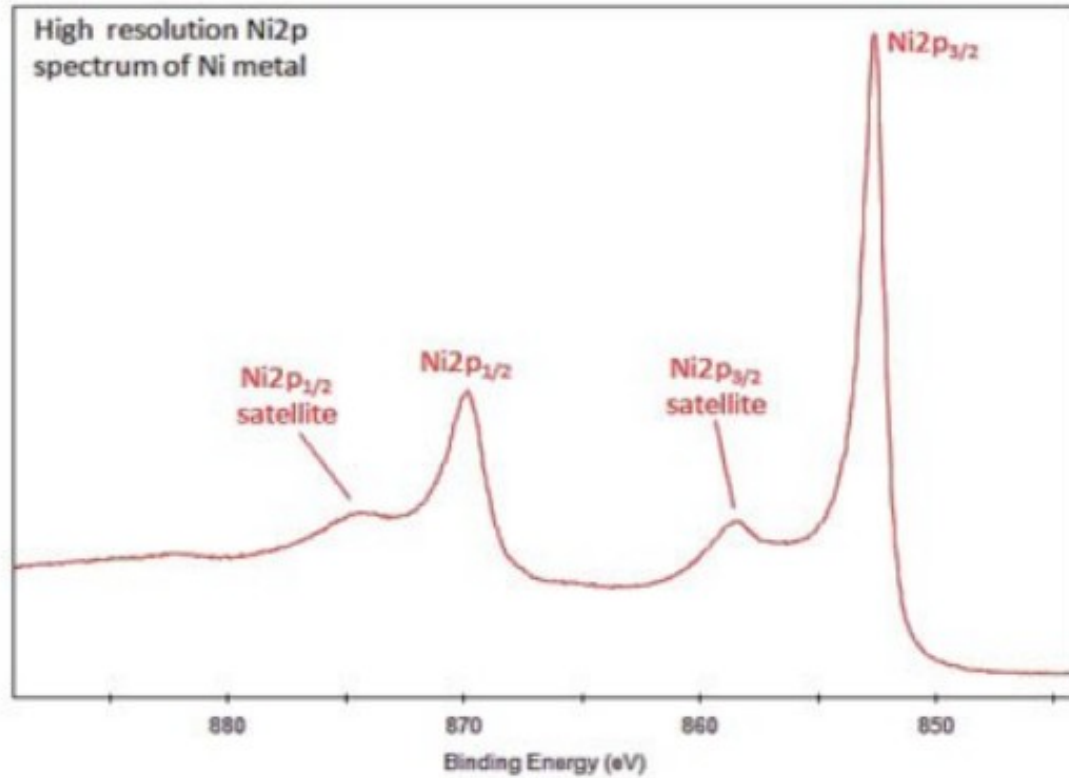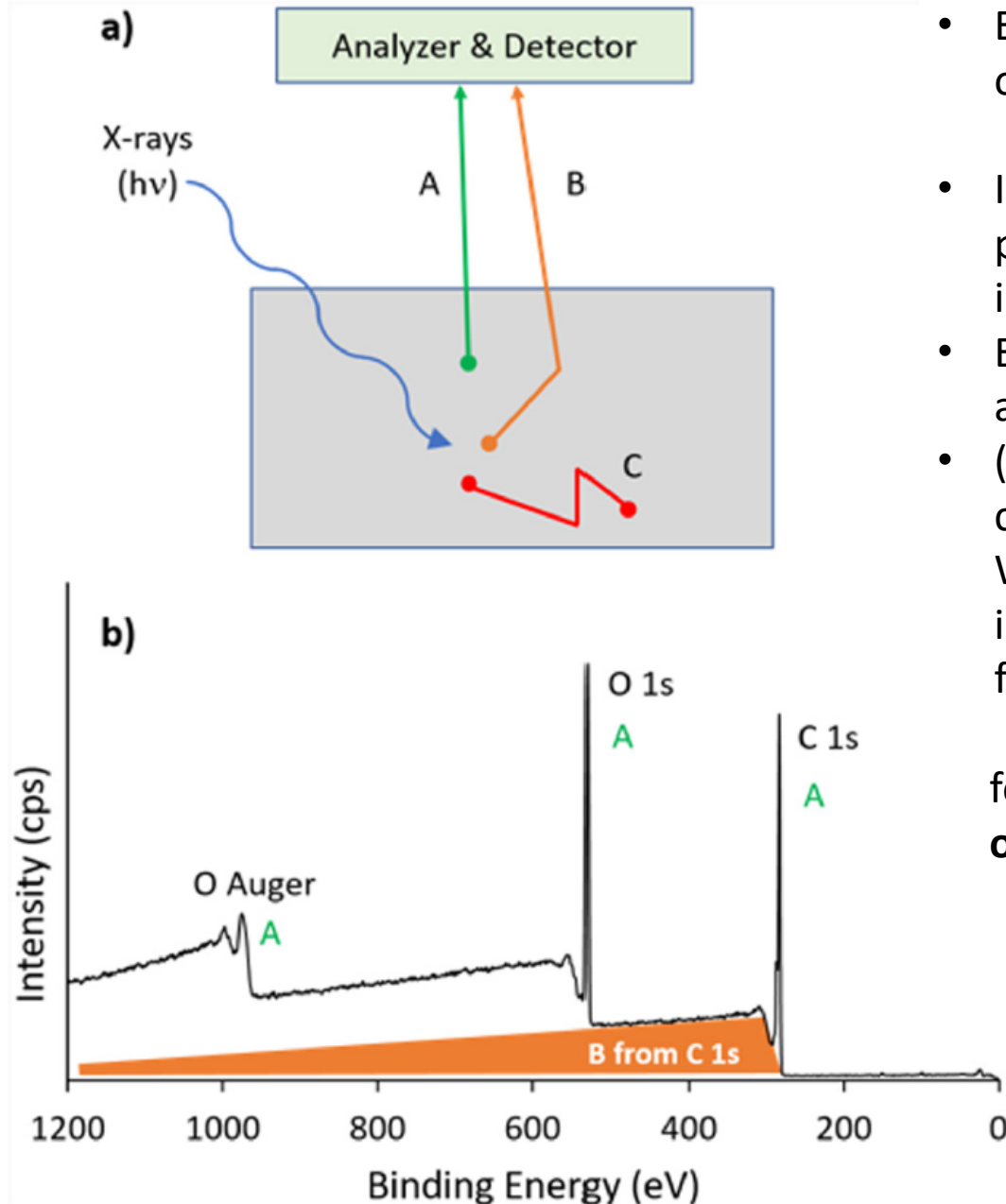
- Emitted electrons interact with the sample in different ways depending on the depth at which they are generated.

- In (a), electrons emitted without interaction, labeled A, produce XPS photoelectron and Auger peaks. Electrons which undergo at least one inelastic collision, labeled B, contribute to the background.
- Electrons that undergo multiple collisions and do not escape the sample are labeled C.
- (b) shows the XPS spectrum for PET. The orange area shows the contribution to the background signal that results from C 1s electrons. While only the contribution to the background from C 1s electrons is illustrated here, similar background contributions are made by electrons from O 1s and O Auger transitions as well:

forming the **vertical "steps" in the baseline observed for every major peak.**

Emrah Özensoy
Bilkent University

Survey vs High Resolution XP Spectra
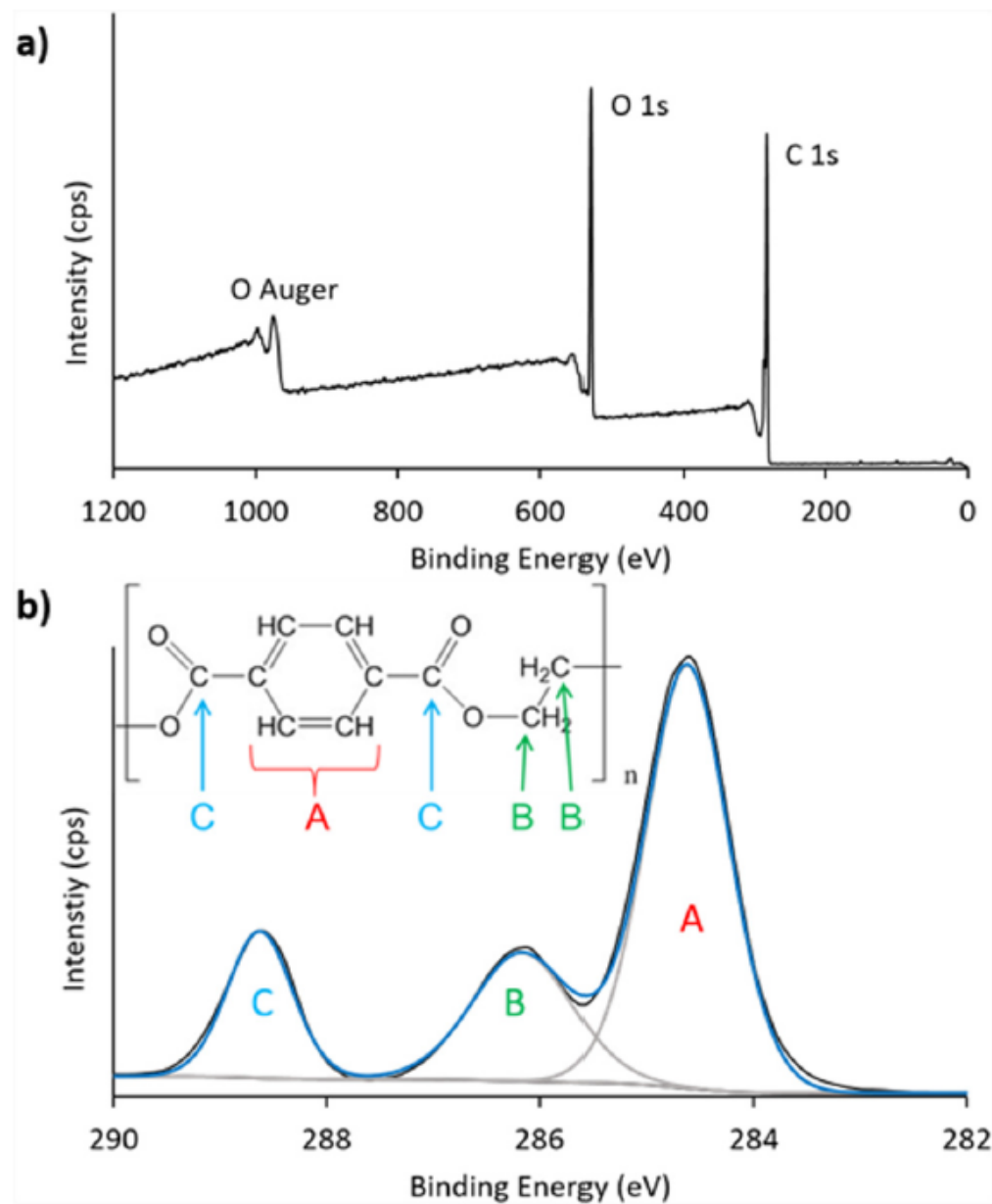
- XPS survey spectrum (a) and high-resolution C 1s spectrum (b) of PET.

- The inset of (b) shows the chemical structure of PET and the assignments of the three peaks in the C 1s spectrum.

**Emrah Özensoy
Bilkent University**

Chemical Shifts in XPS
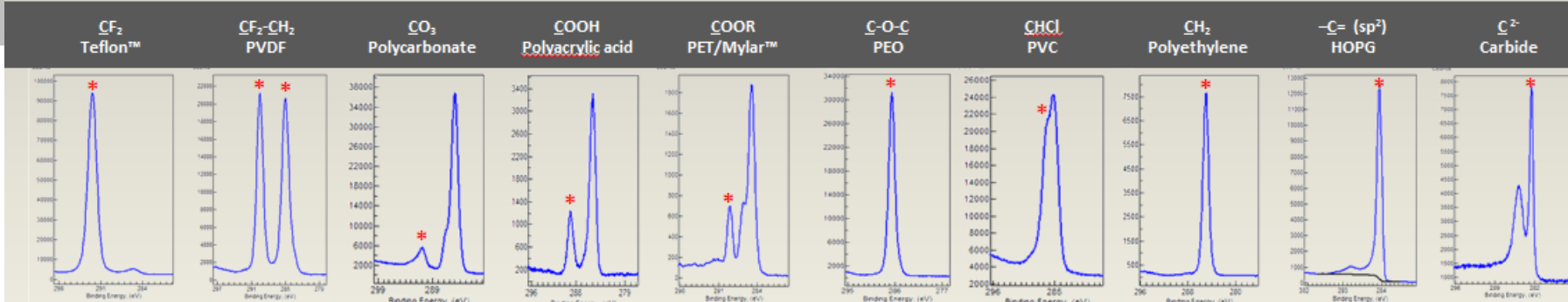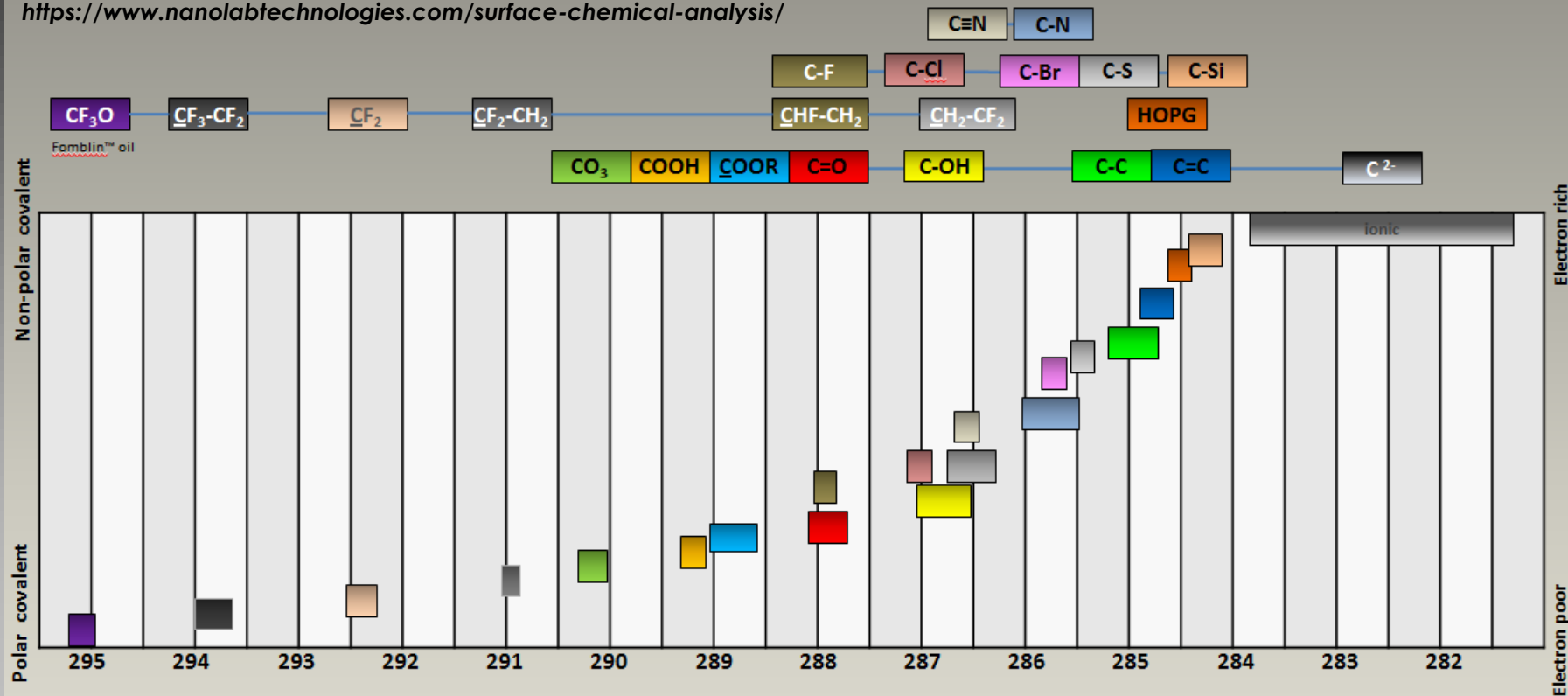
Emrah Özensoy
Bilkent University

Chemical Shifts in XPS

Oxidation States of Titanium

Titanium exhibits very large chemical shifts between different oxidation states of the metal; in the diagram below a Ti 2p spectrum from the pure metal (Ti ^{0}) is compared with a spectrum of titanium dioxide (Ti $^{4+}$).

Ti 2p XP Spectra — Mg Kα

Ti 2p$_{3/2}$
Ti 2p$_{1/2}$
Ti metal
Δ=6.05 eV for Ti(0)
Δ=5.72 eV for Ti(IV)
TiO$_2$
Binding Energy / eV
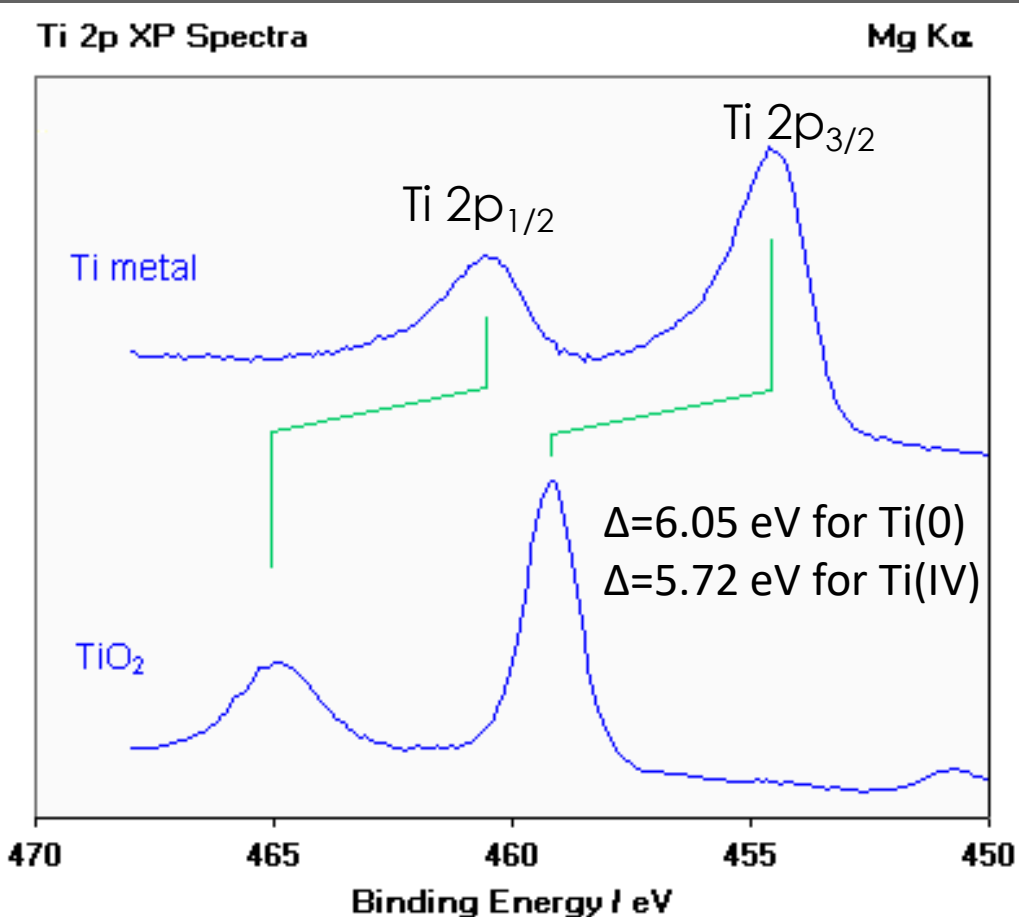
Note :

(i)   the two spin orbit components exhibit the same chemical shift (~ 4.6 eV)

(ii) **metals** are often *characterized by an asymmetric line shape*, with the peak tailing to higher BE

while **insulating oxides** yield *more symmetric peak profile*

(iii) the weak peak at ca. 450.7 eV in the lower spectrum arises because *typical x-ray sources also emit some x-rays of a slightly higher photon energy than the main Mg K$_a$ line*; *this satellite peak is a "ghost" of the main 2p$_{3/2}$ peak* arising from ionisation by these additional x-rays.

Adapted from Roger Nix (Surface Science, Queen Marry, University of London

Emrah Özensoy
Bilkent University

Chemical Shifts in XPS-II

Typically: *BE of elements increase w/ INCREASING Oxidation* *(Be aware of Exceptions !)*

XPS of Highly Oxidized Silver Films

TABLE 1: Summary of Structural Parameters and XPS BE Assignments for Silver Metal and Various Silver Oxides

	Ag^0	Ag^+	Ag^{2+}	Ag_3O_4	Ag_2O_3
structure	fcc	cubic cuprite[a]	monoclinic[b]	monoclinic[c]	square planar[c]
Ag charge state	Ag(0)	Ag(I)	1 × Ag(I) 1 × Ag(III)	1 × Ag(II) 2 × Ag(III)	Ag(III)
NN distance	2.89 Å	2.052 Å	Ag(I)−O: 2.176 Å Ag(III)−O: 2.010 and 2.053 Å	Ag(II)−O: 2.03 Å Ag(III)−O: 2.07 Å	2.02 Å average
BE Ag $3d_{5/2}$ (previous work)	368.1 ± 0.1 eV[d] 368.26 eV[e]	367.7 ± 0.1 eV[f]	367.3 ± 0.1 eV[g]		
BE Ag $3d_{5/2}$ [fwhm] (this work)	368.24 eV [0.63 eV]	367.3 eV [1.1 eV] (367.5−367.7 eV for $Ag_2O_{1-\delta}$)	Ag(III): 366.8 eV [0.8 eV] + 368.2 eV [1.2 eV] satellite		
BE O 1s (previous work)		529.0 ± 0.2 eV[f]	528.5 ± 0.1 eV[g]		
BE O 1s [fwhm] (this work)		529.0 eV [0.8 − 1.2 eV]	528.4 eV [0.8 eV]		

[a] Tjeng et al.[22] [b] Scatturin and Bellon.[25] [c] Waterhouse et al.[29] [d] Schon.[26] [e] Moulder et al.[48] [f] Hoflund et al.[32] [g] Hoflund et al.[33]

Decreasing B.E. with Oxidation !

Spectroscopic Evidence for Ag(III) in Highly Oxidized Silver Films by X-ray Photoelectron Spectroscopy

Tiffany C. Kaspar,*[,†] Tim Droubay,[†] Scott A. Chambers,[†] and Paul S. Bagus[‡]

Pacific Northwest National Laboratory, P.O. Box 999, Richland, Washington 99354, United States
Department of Chemistry, University of North Texas, 1155 Union Circle, # 305070, Denton, Texas 76203-5017, United States

The *Ag/AgO$_x$ system was the first reported negative BE shift of metal cations with increasing oxidation*,[26] although the phenomena was later observed in other systems.

E.g. **Cobalt**, where *Co(III) exhibits a lower BE than Co(II),*[34] and **Barium**, where *Ba(II) in BaO shifts to lower BE than Ba(0)*.[35]

Emrah Özensoy
Bilkent University

Baseline Correction and Peak Deconvolution

Emrah Özensoy
Bilkent University

Baseline Correction and Peak Deconvolution

W 4f

XPS Data analysis often involves fitting a baseline to the data and peak fitting:

(a) A **Shirley baseline** is shown

(b) three doublets are used to fit the W4f peak.

Emrah Özensoy
Bilkent University
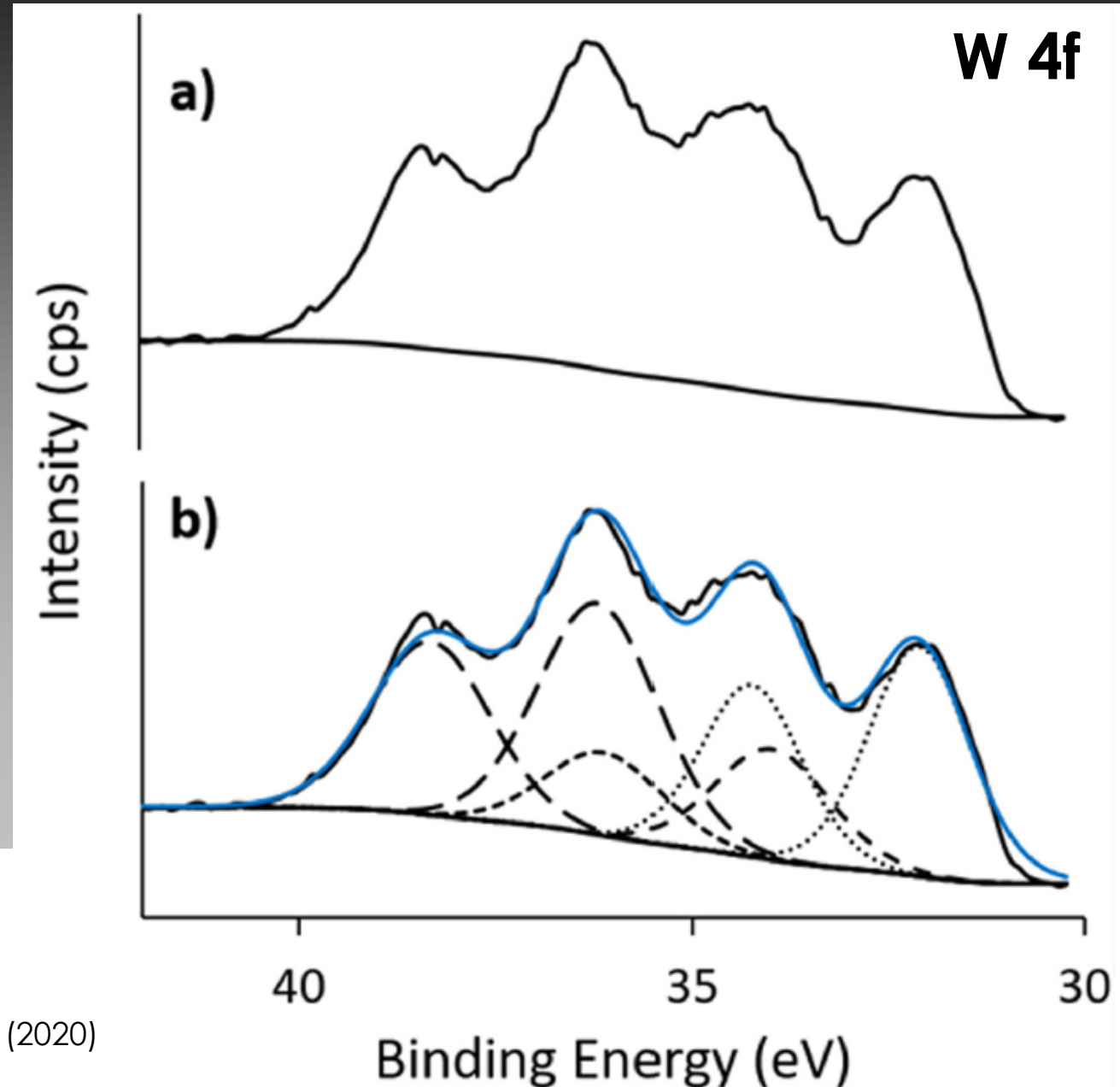
Peak Fitting & Deconvolution in XPS:
What to do and What NOT to do ?

Emrah Özensoy
Bilkent University
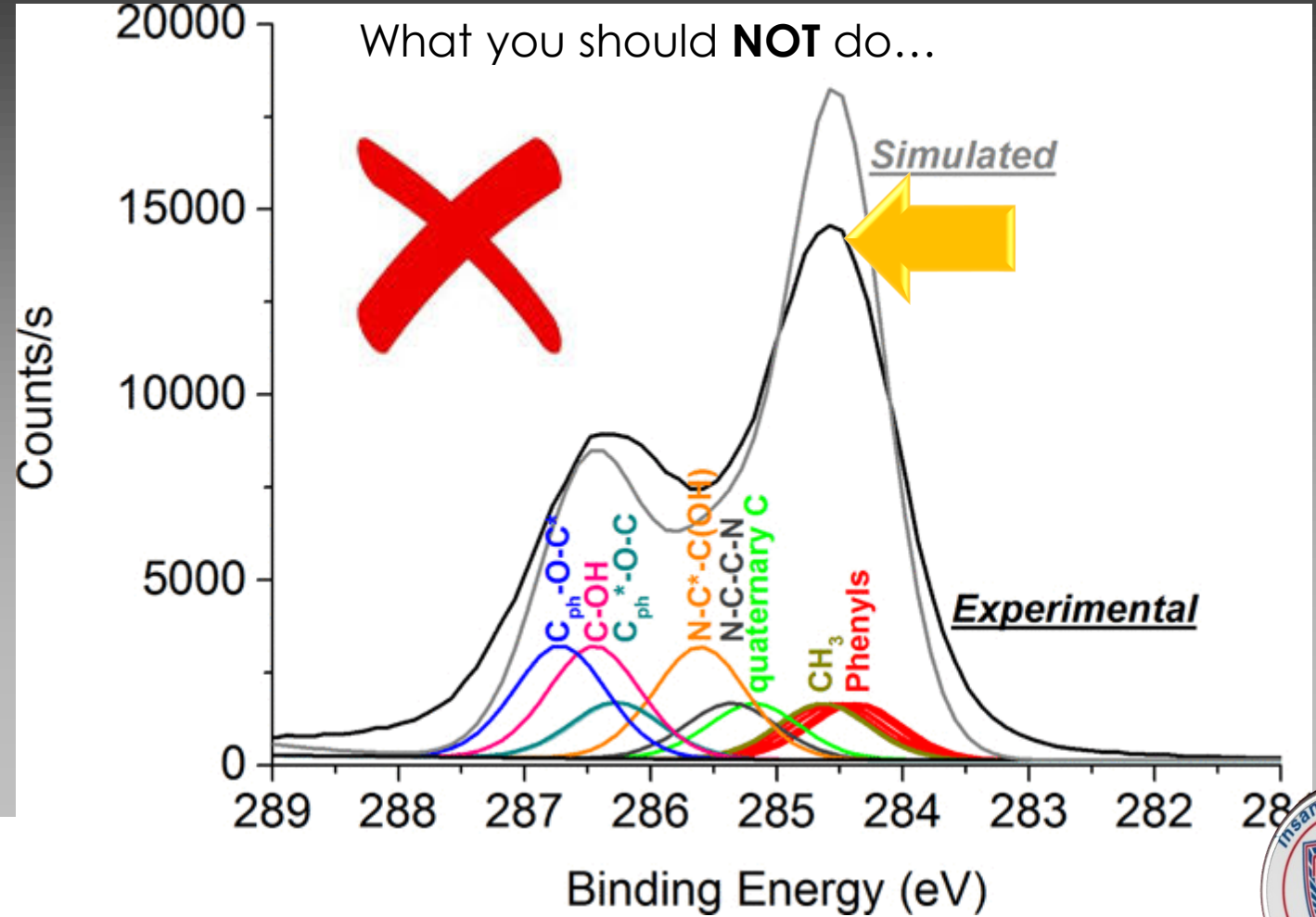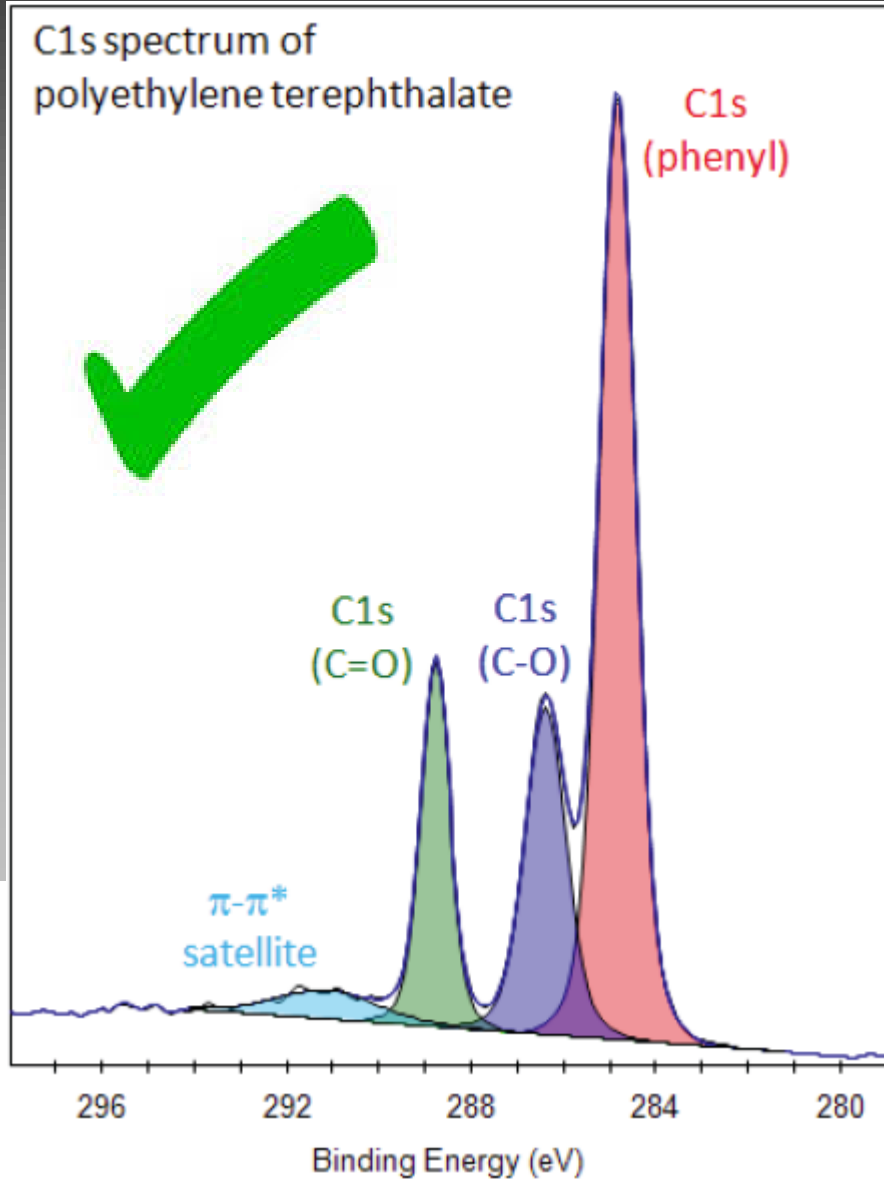
XPS Peak Line Shapes

XPS Peak Line Shapes can be simulated by using:

- **«Lorentzian» & «Guassian»** *and*

- *their combinations like* **«Voight»** line shapes
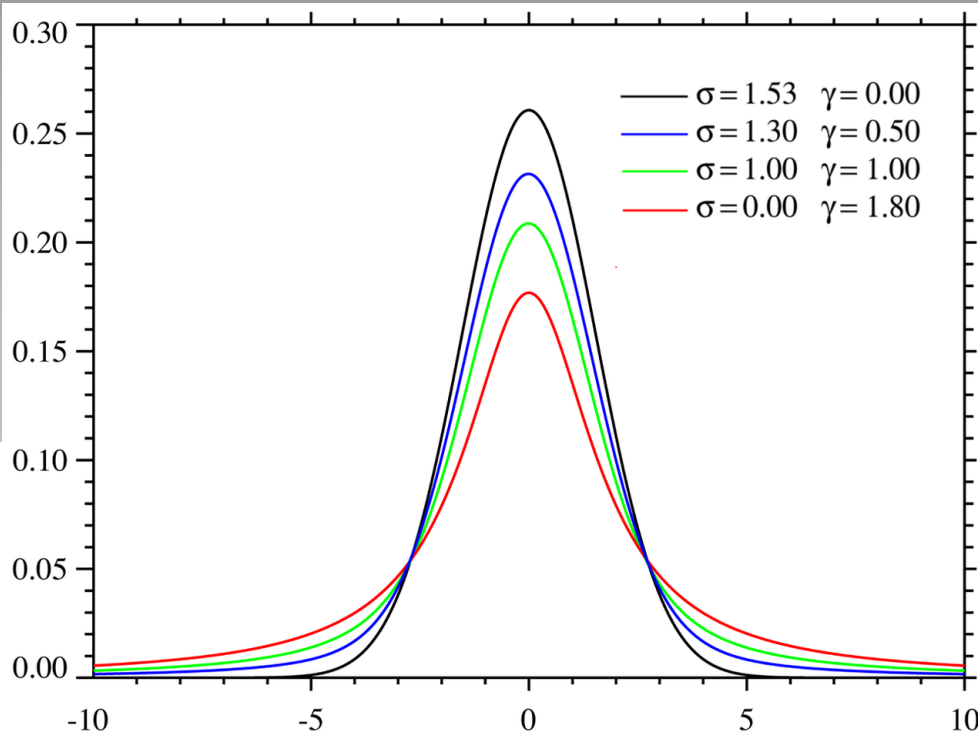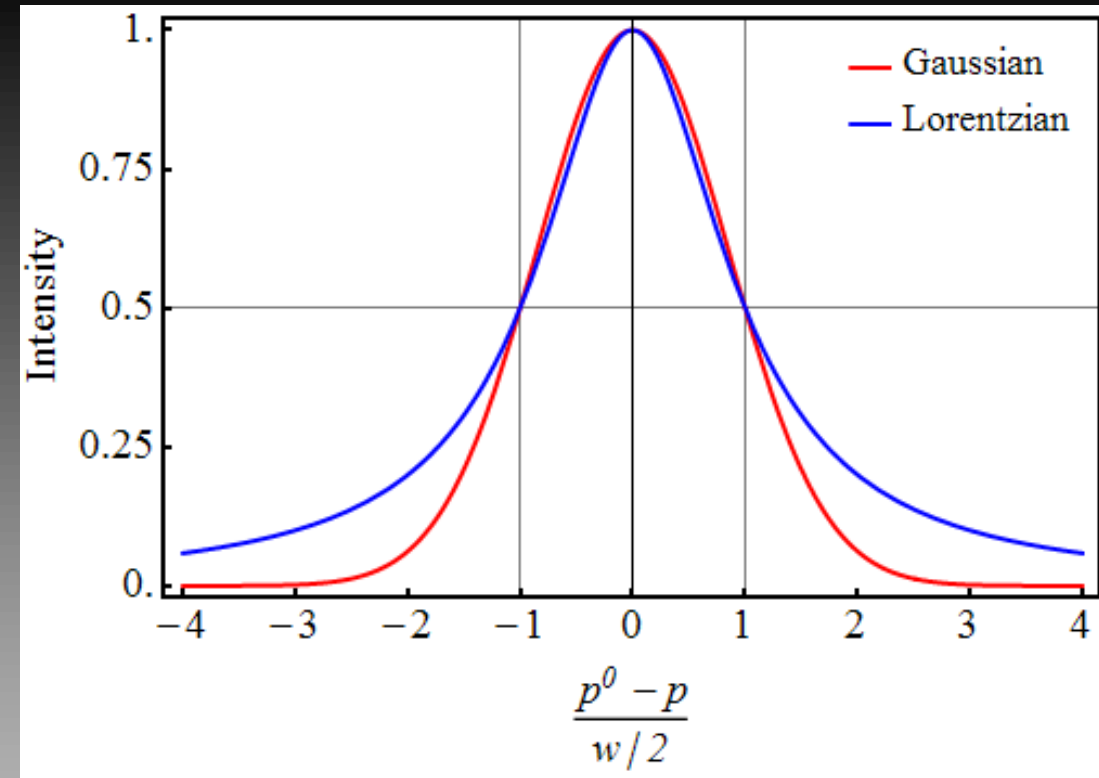
- Plot of the centered Voigt profile for four cases.
- Each case has a full width at half-maximum of very nearly 3.6.
- Black and Red profiles are the *limiting cases* of the **Gaussian (γ =0)** and the **Lorentzian (σ =0)** *profiles* respectively.

**Emrah Özensoy
Bilkent University**

Baseline Correction in XPS
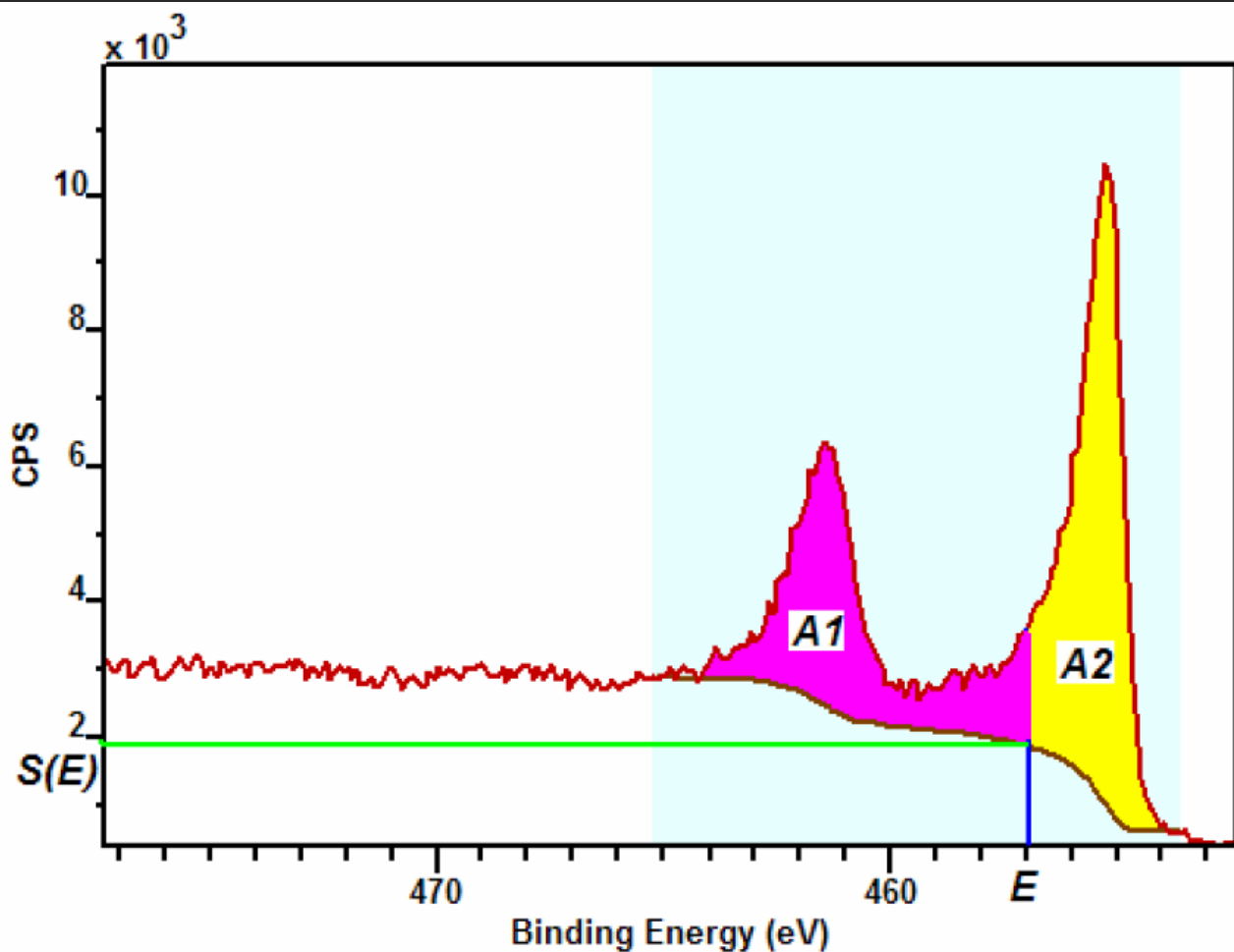
Figure 5: A Shirley background computed from a Ti 2p spectrum.
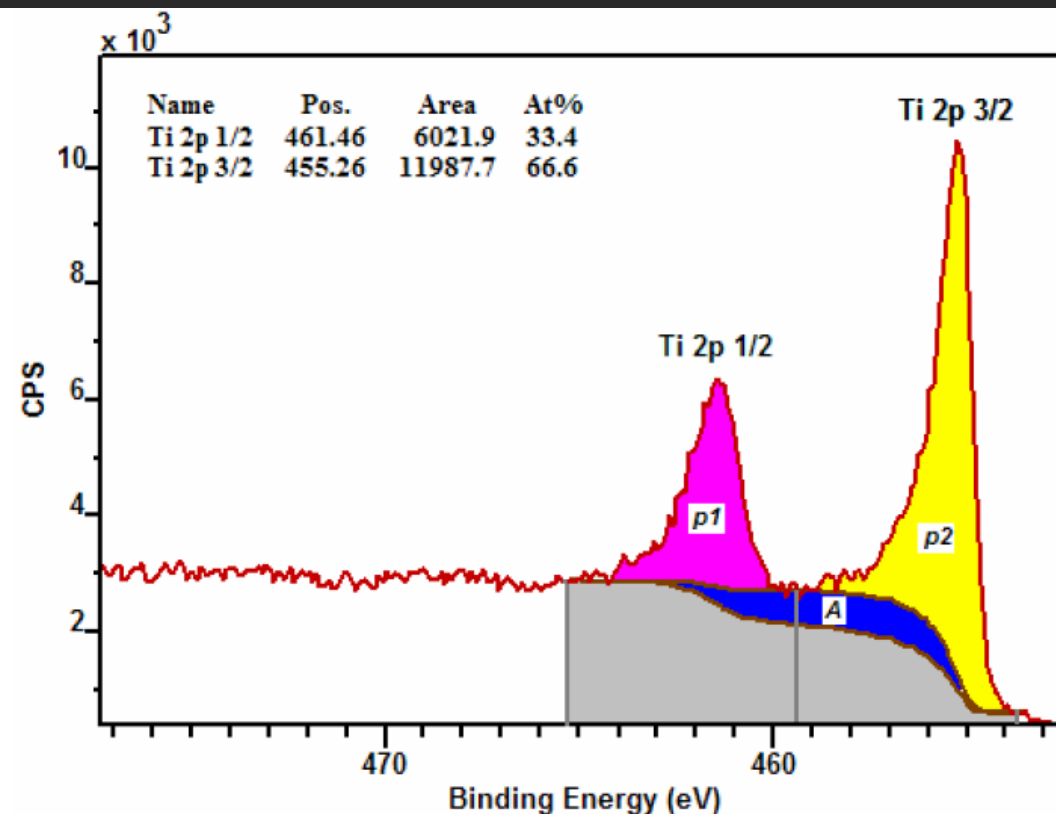
Name	Pos.	Area	At%
Ti 2p 1/2	461.46	6021.9	33.4
Ti 2p 3/2	455.26	11987.7	66.6

Figure 6: Metallic Ti modeled using two regions each defining a Shirley background (upper curve). The lower background curve is the Shirley background computed using the combined peaks. The At% column is computed using an RSF of unity for both peaks in the doublet pair, hence the 1:2 ratio in peak areas *p1* and *p2*.

CASAXPS Peak Fitting Manual

**Emrah Özensoy
Bilkent University**

Complex Spectral Features in XPS Data

Emrah Özensoy
Bilkent University

Spin-Orbit Splitting

The **Russell-Saunders (L+S)** coupling approximation is best applied **only to light atoms** and this splitting can alternatively be described using individual electron *l-s* coupling.

In this case the resultant angular momenta arise from the single hole in the *d*-shell; a *d*-shell electron (or hole) has *l* = 2 and *s* = 1/2, which again gives permitted *j*-values of 3/2 and 5/2 with the latter being lower in energy.

If we consider the final ionised state of Pd within the *Russell-Saunders coupling approximation*, the $(3d)^9$ configuration gives rise to two states (ignoring any coupling with valence levels) which *differ slightly in energy* and *in their degeneracy ($g_J = 2J + 1$)...*

$3d_{5/2}$ $g_J = 2 \times \{5/2\} + 1 = 6$

$3d_{3/2}$ $g_J = 2 \times \{3/2\} + 1 = 4$

These two states arise from the *coupling of the L = 2 and S = 1/2 vectors to give permitted J values of 3/2 and 5/2 via*

$J = L \pm S$, *where 2S+1 = multiplicity* (e⁻ state degeneracy due to spin Q#)

The *lowest energy final state* is the one with maximum *J* (since the shell is more than half-full), i.e. *J = 5/2*, hence this gives rise to the "lower binding energy" peak.

The relative intensities of the two peaks reflects the degeneracies of the final states $(g_J = 2J + 1)$, which in turn *determines the probability of transition to such a state during photoionization*.

Spin-orbit splitting is not evident with s-levels (l = 0), but is seen with **p,d & f core-levels.**
For heavier atoms the splitting is larger.

Complex Peak Features in XPS: Shake-up, Satellite, Multiplet, Tail

(a) Shakeup peak in the C 1s spectrum of PET due to the π→π* transition

(b) Shakeup peaks due to the excitation of plasmon lines in Si

(c) Tailing on a metallic peak for Pt 4f, due to shakeup excitations into a continuum of states above the Fermi level

(d) Multiplet splitting and shakeup peaks in the Ni 2p spectrum from NiO. Multiplet splitting of core level peaks occurs when there are unpaired electrons in the valence levels and often results in unexpected peak splitting. This affects the s orbitals of some transition metals [Mn(II), Cr(II), Cr(III), Fe(III)] and also can be observed for some p and d orbitals

Emrah Özensoy
Bilkent University
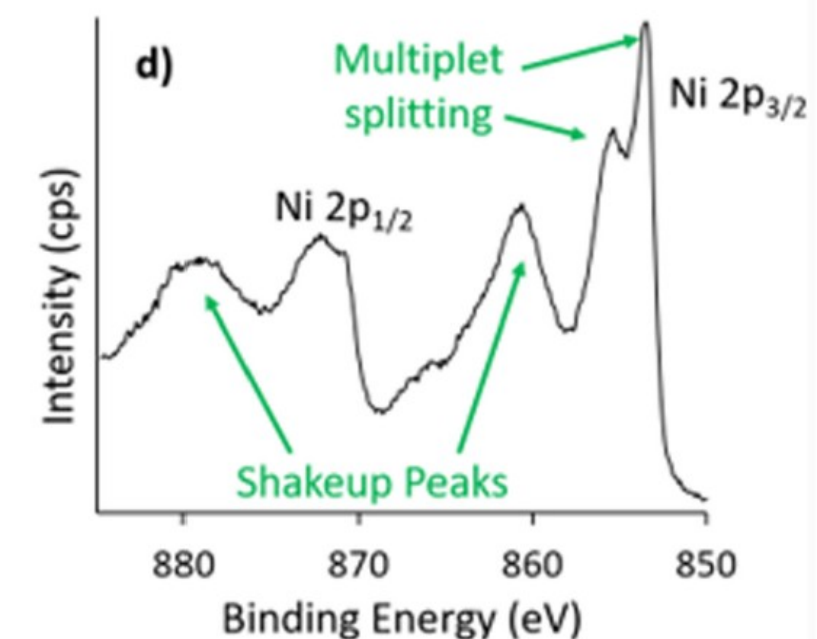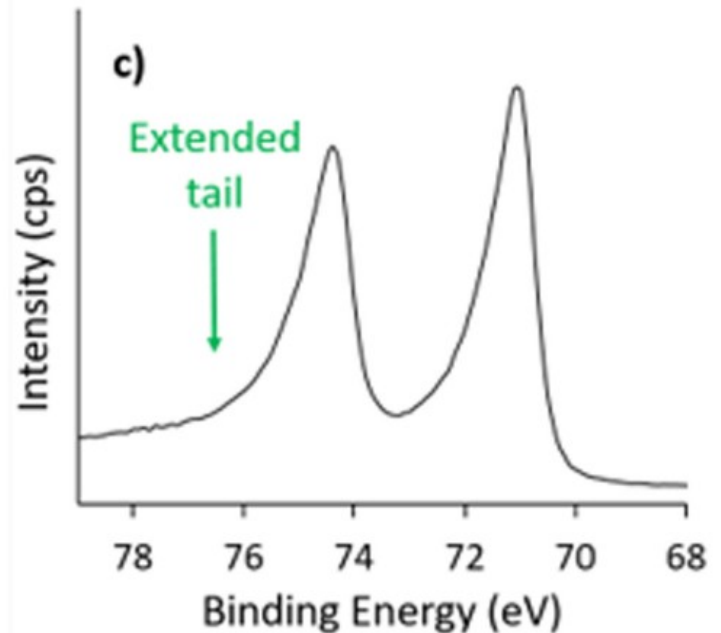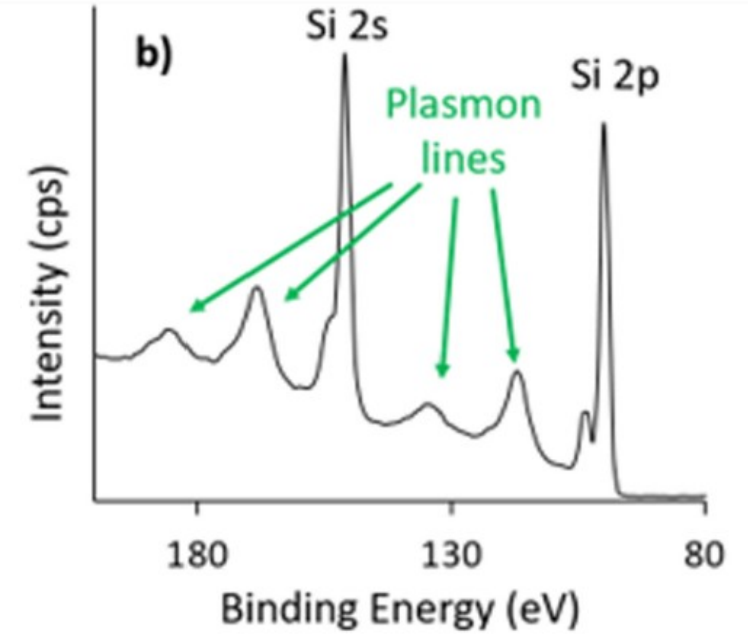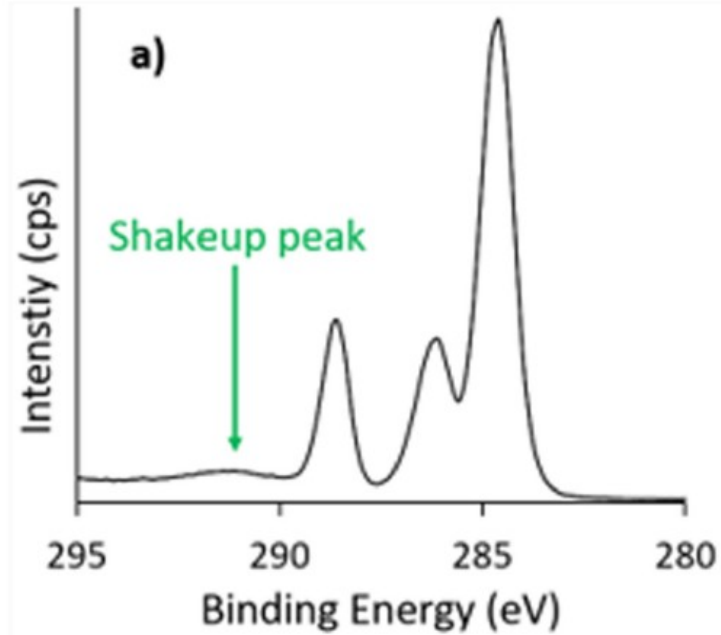
Complex Peak Features in XPS: Use in Oxidation State Assignment

- Cu2p peak has significantly split spin-orbit components (Δ=19.75 eV, intensity ratio= 0.508).

- It is possible to distinguish Cu oxidation states using satellite features of Cu2p.

- Cu(II) has an observable collection of satellite features at 943 eV.

- Cu2p$_{3/2}$ peak in Cu(II) oxide is shifted and is much broader compared to Cu(I) oxide.

- In Cu(I) oxide, there is only a very weak satellite at 945 eV.

- Cu2p$_{3/2}$ peak in Cu(I) oxide is NOT shifted, but is broader compared to Cu metal.

Emrah Özensoy
Bilkent University

https://www.thermofisher.com/tr/en/home/materials-science/learning-center/periodic-table/transition-metal/copper.html
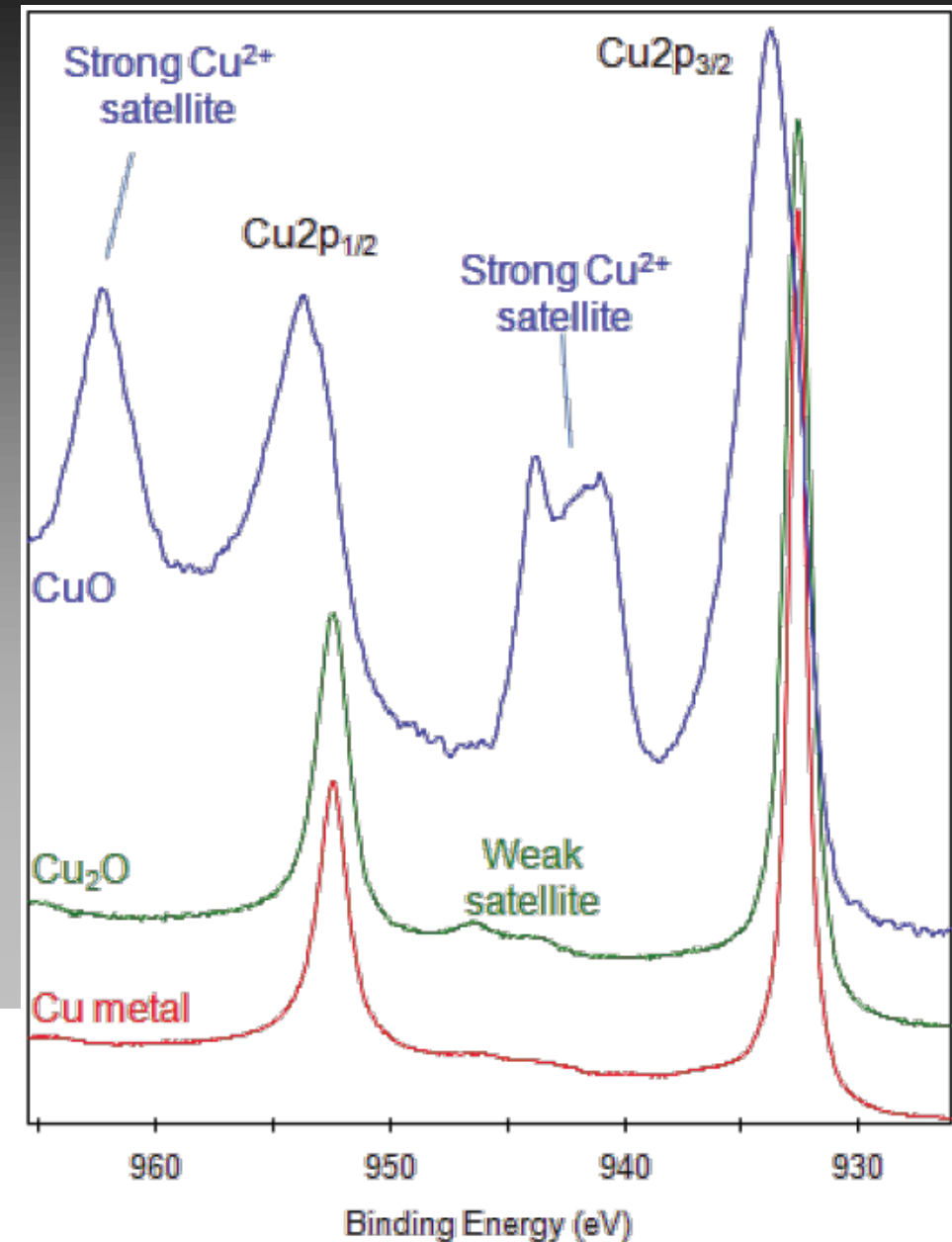
Detection of Auger Peaks in XPS Spectra

a) Mg source

b) Monochromatic Al source
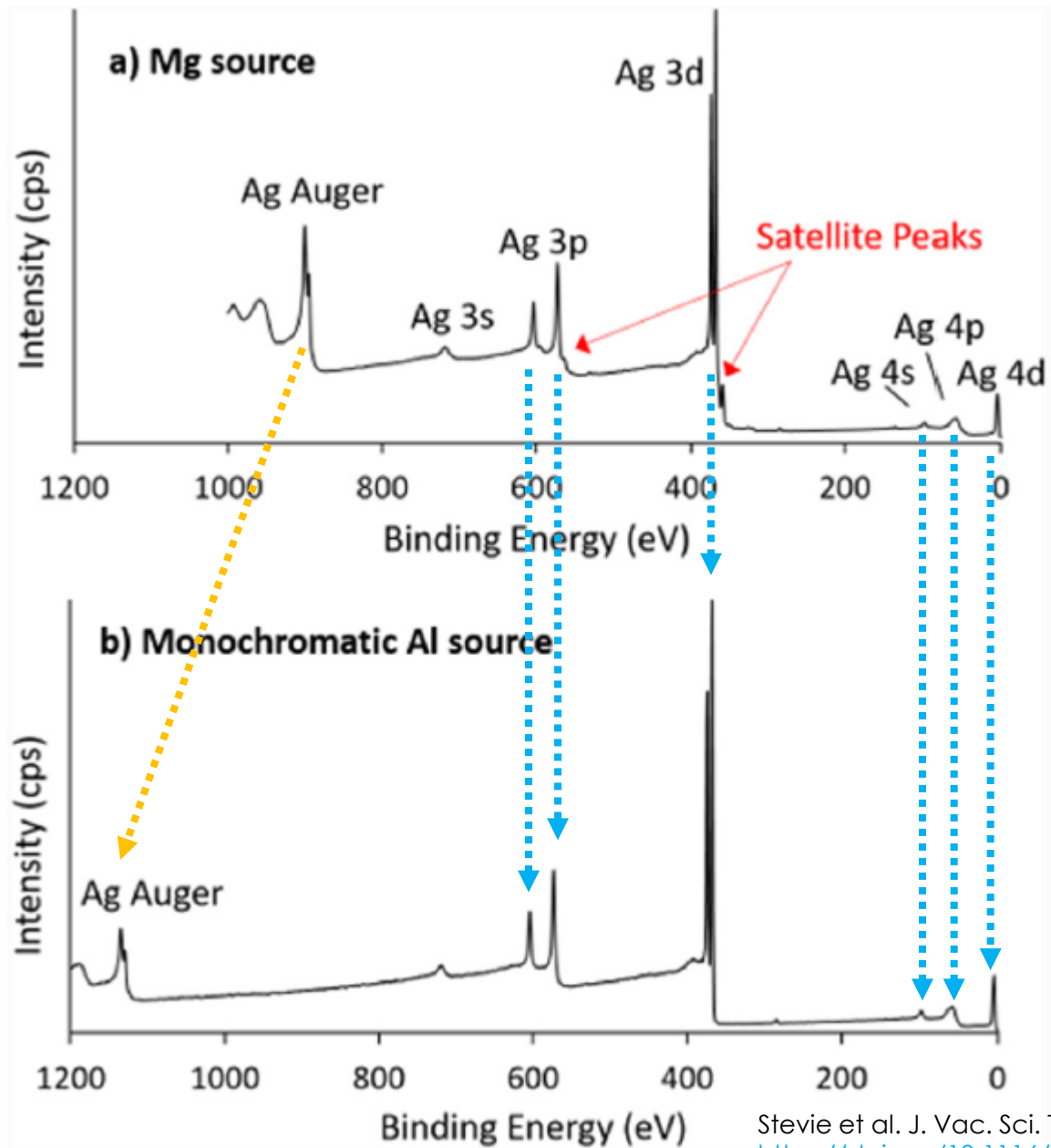
- (a)Nonmonochromatic Mg and (b)monochromatic Al sources show how the photoelectron peaks are at the same BE.
- But, the Auger peaks shift with the use of different sources.

(Note that the satellite peaks are removed by the **monochromator source**)

- In special cases, Auger peaks can be useful for oxidation state analysis where XPS signals are deconvoluted/difficult to resolve.
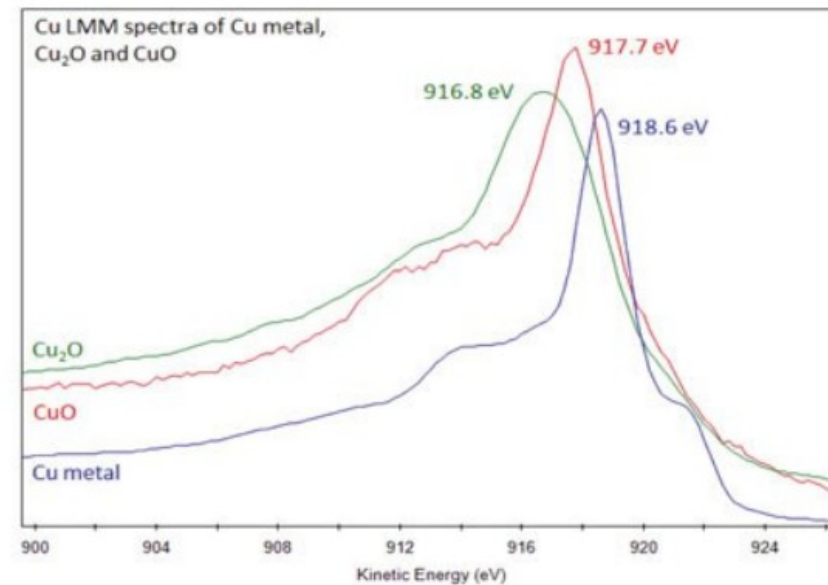
Cu LMM spectra of Cu metal, Cu_2O and CuO

Stevie et al. J. Vac. Sci. Technol. A **38**, 063204 (2020)
https://doi.org/10.1116/6.0000412

https://www.thermofisher.com/tr/en/home/materials-science/learning-center/periodic-table/transition-metal/copper.html

Emrah Özensoy
Bilkent University

Cl2p for NaCl

No charging
a)

Slight charging
b)

Moderate charging
c)

Severe charging
d)

Intensity (cps)

Improving Charge Compensation

Low Energy Electron Flood Gun

~2eV-20eV

filament

Electrons optics

e⁻

Binding Energy (eV)
205   200   195
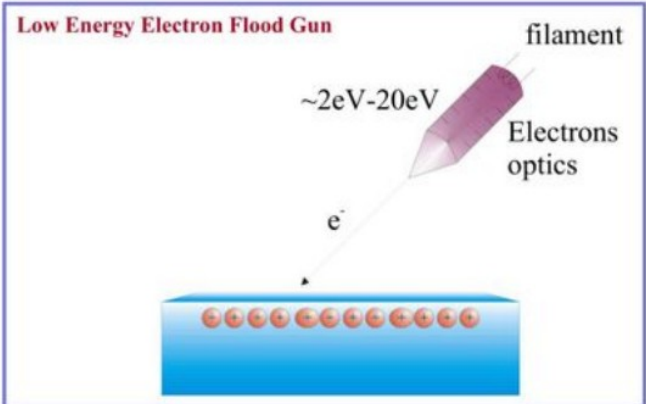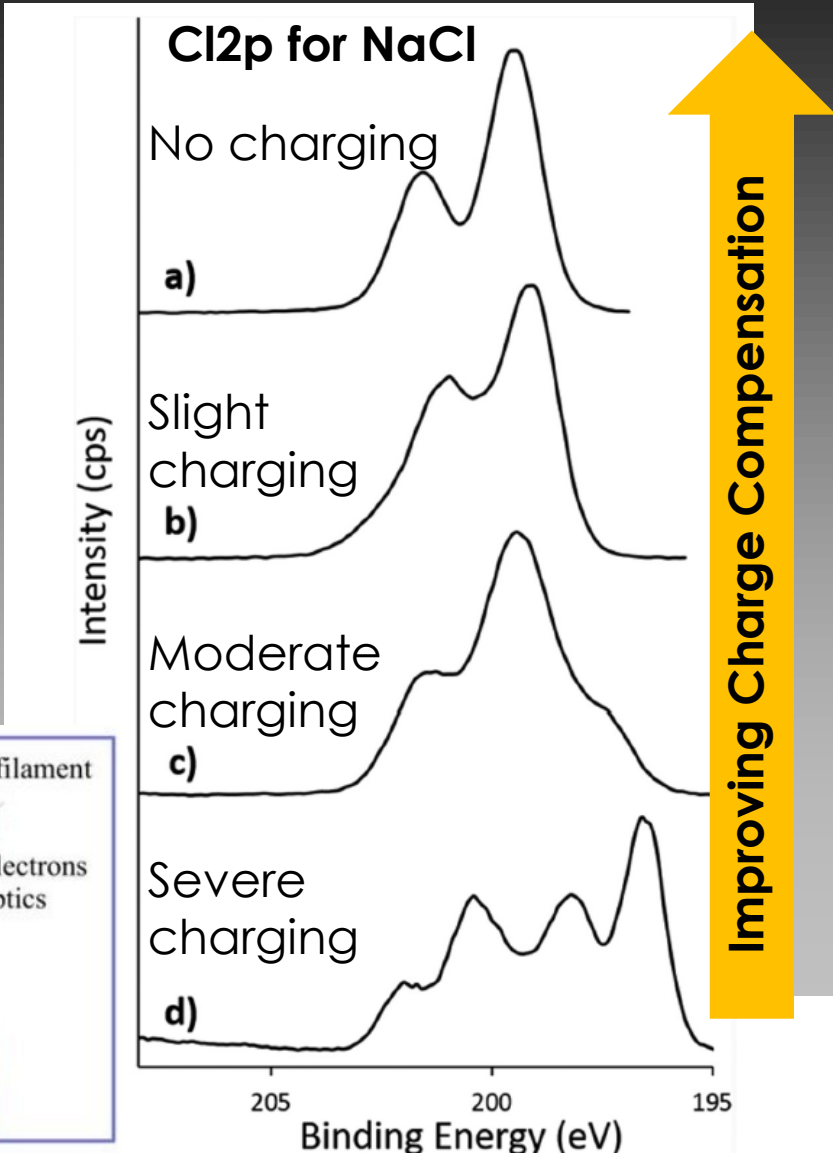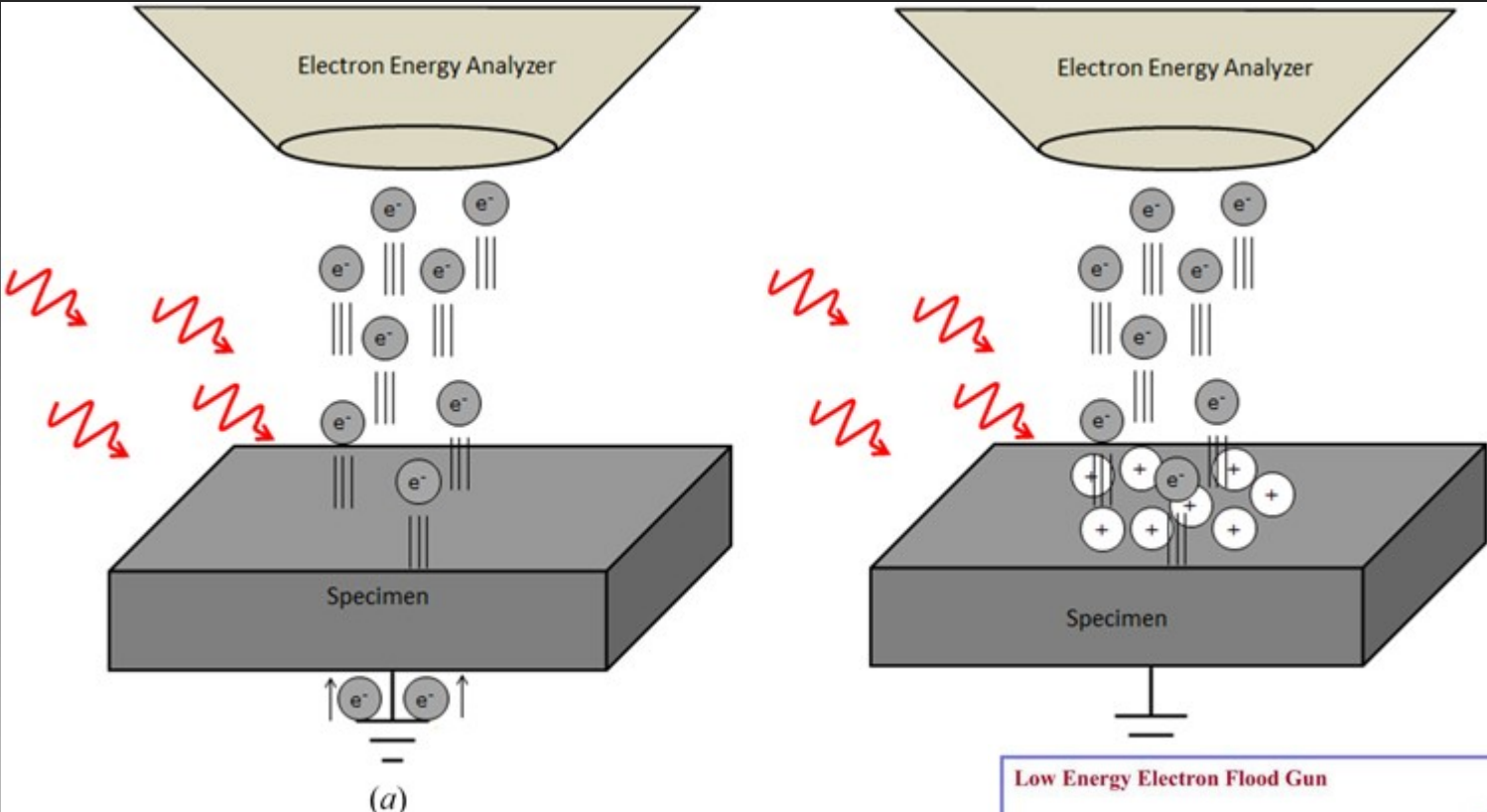
FIG. 9. Cl 2p high resolution spectra from a NaCl sample were obtained using different charge neutralizer conditions. The examples show (a) absent, (b) slight, (c) moderate, and (d) severe charging.

Electron Energy Analyzer

Specimen

(a)

Electron Energy Analyzer

Specimen

Adventitious Carbon

- A thin layer of carbonaceous material is usually found on the surface of most air exposed samples.

- This layer is generally known as **adventitious carbon**.

- Even small exposures to atmosphere can produce these films.

- Adventitious carbon is generally comprised of a variety of (relatively short chain [1]) hydrocarbons species with small amounts of both singly and doubly bound oxygen functionality.
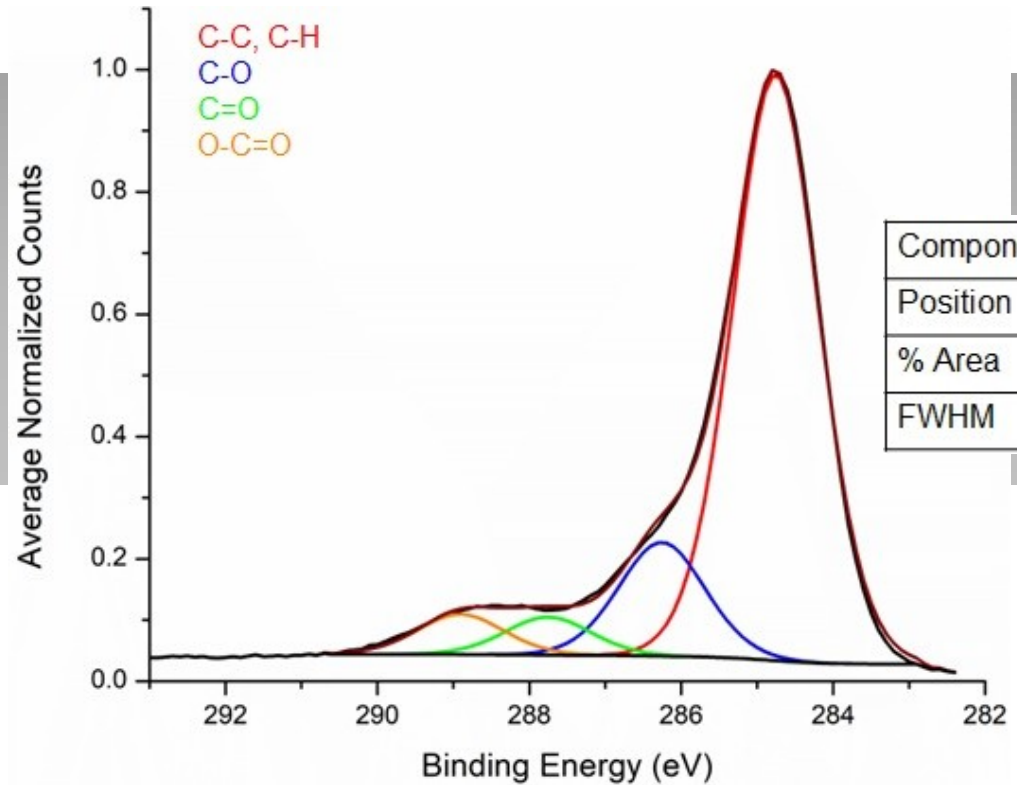
Component	C-C, C-H	C-O	C=O	O-C=O
Position	A	A+1.5	A+3	A+4.15
% Area	74.8	14.7	5.1	5.5
FWHM	1.33	1.33	1.33	1.33

Emrah Özensoy
Bilkent University

Enhancing S/N of XPS Data by Averaging (Scanning) Longer Durations of Time

Merit of Collecting More Scans

Figure of Merit (Y axis) = (Rel Increase in S/N Ratio) / (Expt S/N Ratio X Time Spent)

S/N=2, 4 scans

Derived from noise in the baseline data for the 386-406 eV BE range of survey spectra on Silver.

S/N=3
9 scans

S/N=4
16 scans

S/N=5
25 scans

S/N=7
49 scans

S/N=10
100 scans

S/N=1.4

Figure of Merit (ROI)
ROI = Return on Investment

S/N =1
1 scan

Conclusion:
For this XPS system, the most time effective S/N ratio (aka: figure of merit) is achieved for 4 scans.
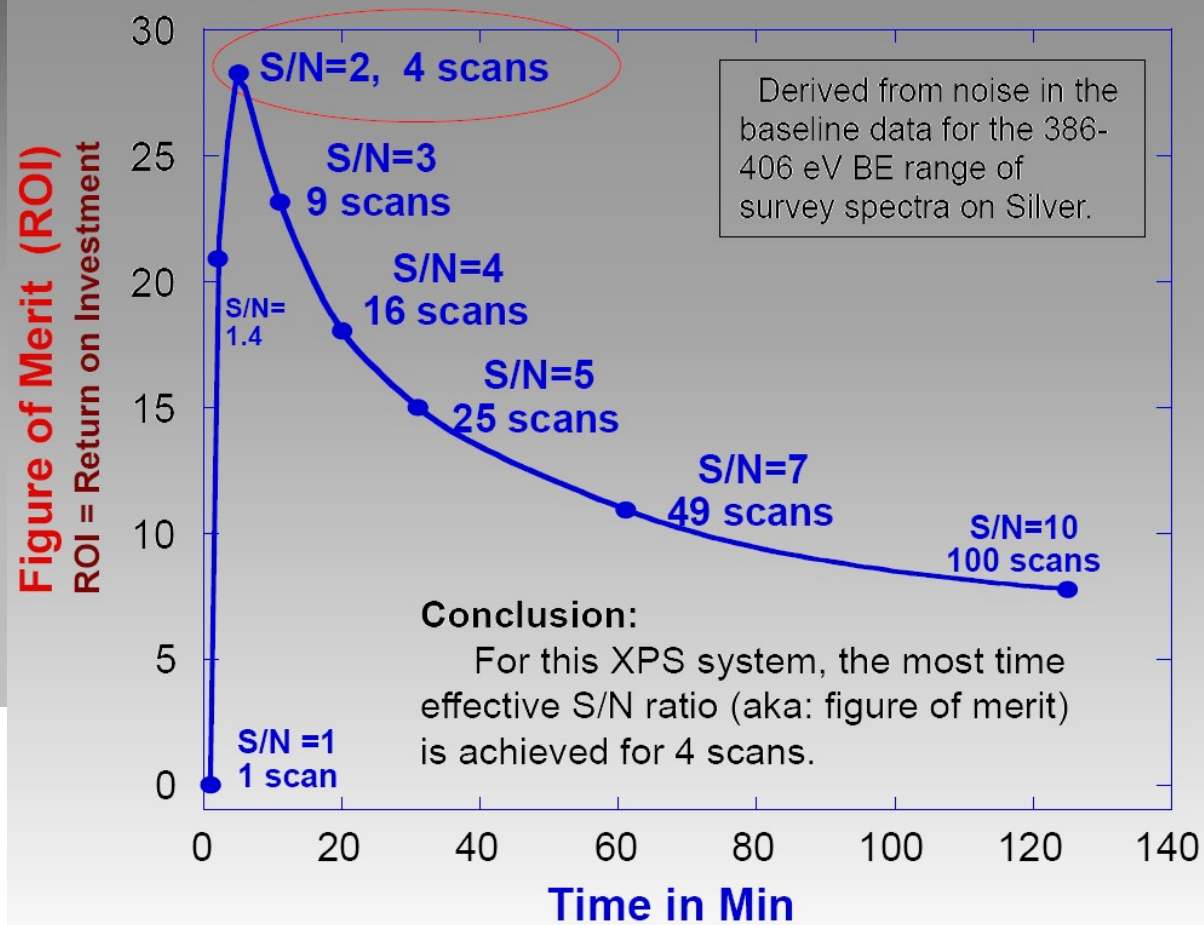
# Scans	Time (min)
1 scan	1.25 min.
2 scans	2.50 min.
4 scans	5.00 min.
9 scans	11.25 min.
16 scans	20.00 min.
25 scans	31.25 min.
49 scans	61.25 min.
100 scans	125.00 min.

400 uM Spot
PE = 200 eV
1 eV/point
50 ms/point

Time in Min

https://www.nanolabtechnologies.com/visual-guide-charts/

Emrah Özensoy
Bilkent University

Common Types of Surface Chemical Analysis via XPS

Emrah Özensoy
Bilkent University

Surface Sensitivity of XPS

In XPS, ***most of the signal comes from within a few atomic layers of the surface***, Thus, XPS is described as a **surface sensitive** technique.

"Universal Curve" of inelastic electron mean free paths
M.P. Seah, W.A. Dench *Surf. Interface. Anal.* 1, 2 (1979)
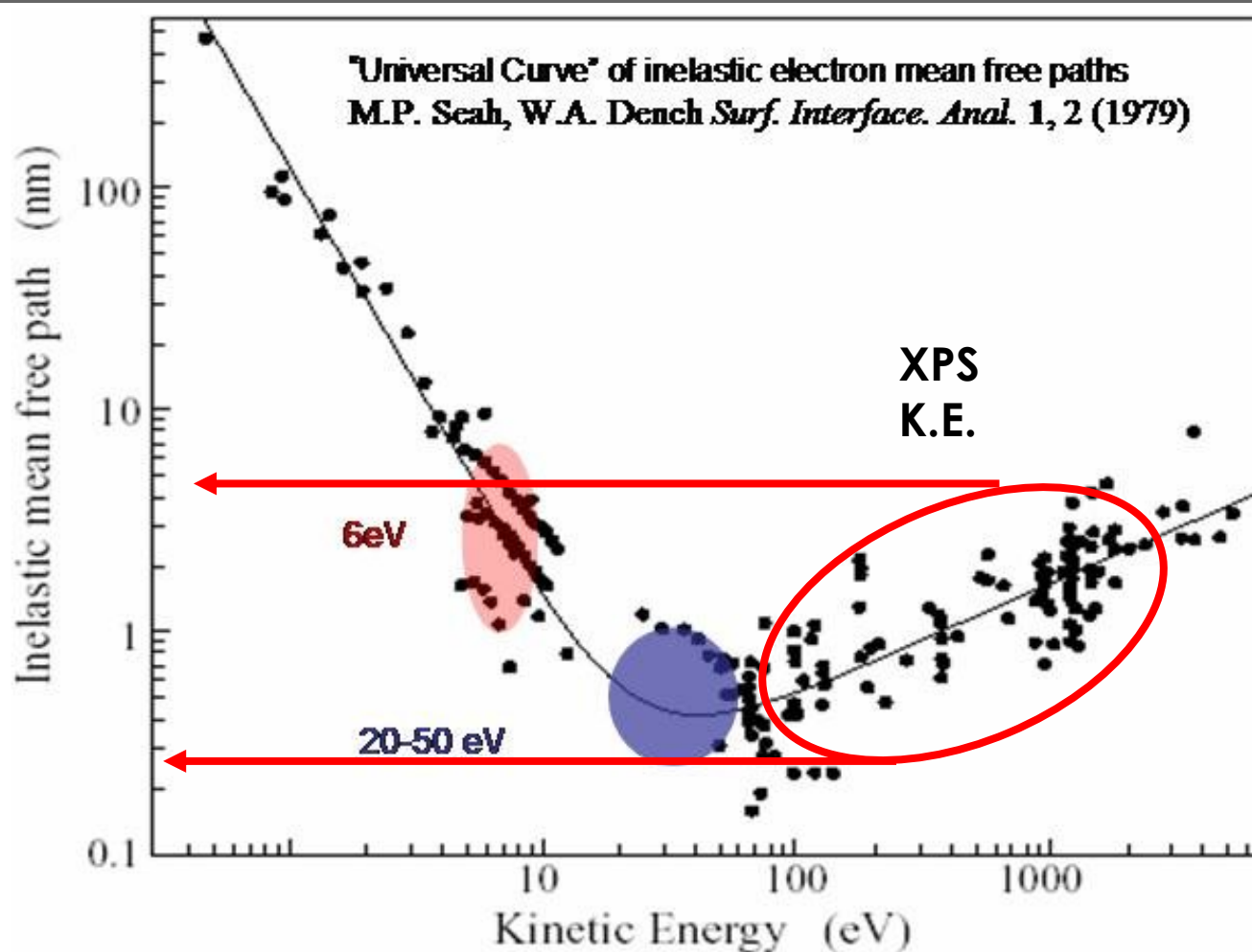
Inelastic Mean Free Path (λ) of electrons: *average distance travelled by an electron through a solid before it is inelastically scattered.*

Depends on:
• The ***initial kinetic energy of the electron***.
• The ***nature of the solid***
 (but *most elements show very similar IMFP vs E*)

• Virtually ***all* (> 95%)** of the electrons detected in XPS come from within **3 x λ** of the surface:

Detected XPS signal comes from
Top $\leq$ 10 nm of surface !

Emrah Ozensoy, Bilkent University, Ankara, Türkiye

Film Thickness Analysis via XPS

Film

A

t

B

Substrate

I

I_o
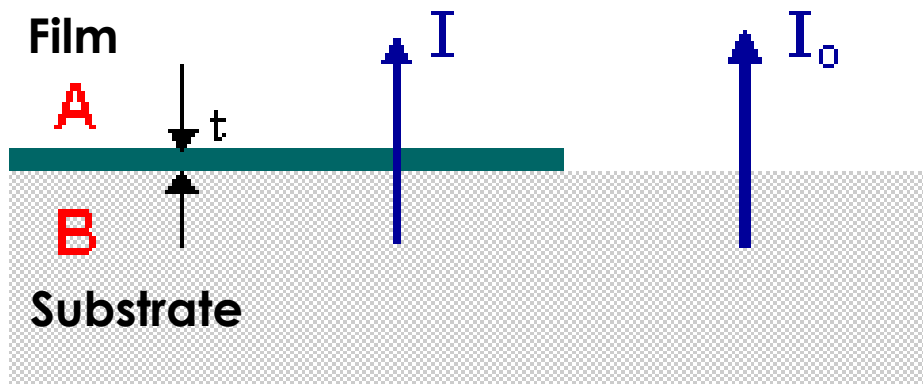
Initial XPS signal (I_o) due to clean Substrate (B) is reduced to (I) due to the presence of the surface film (A) by:

$$I = I_o \exp (- t / \lambda)$$

t: Thickness of surface film (A)
λ: IMFP of photoelectrons used in XPS analysis in substrate (B)

If **I & I_o of B** are measured via XPS, film thickness can be estimated.

Consider, photoelectron emission at angle θ to the surface normal.

Detector

x

θ

d

Angular Variation of XPS Signal Ratio

I_A/I_B

Sample I

Sample II

Emission Angle, θ
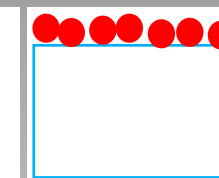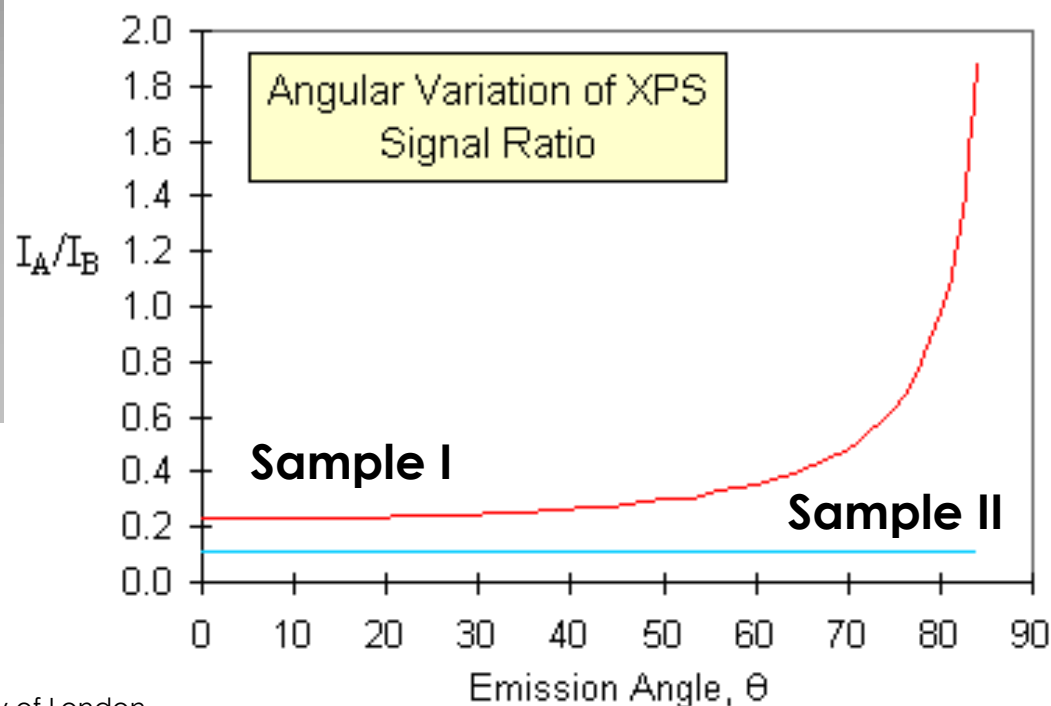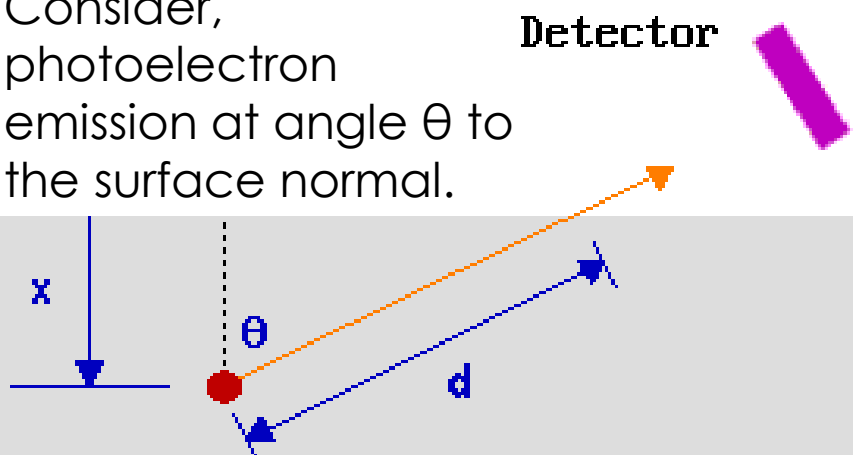
Sample I: Substrate with a Surface Film

Sample II: Uniform alloy A&B

Emrah Özensoy
Bilkent University

Film Thickness Analysis via XPS-II

XPS data can be used to estimate **the thickness, "d",** of an **overlayer "A"** on top of a **substrate "B"** :

$$I_A = I_A^{\infty}(1 - e(-d/\lambda^A{}_{imfp}(E_A)\cos\alpha))$$

$$I_B = I_B^{\infty}(e(-d/\lambda^A{}_{imfp}(E_B)\cos\alpha))$$

- I_A and I_B are the intensities from the overlayer and substrate.

- $I_A\infty$ and $I_B\infty$ are the intensities from pure A and pure B.

- $\lambda^A imfp(E_A)$ is the IMFP or attenuation length of electrons traveling through A, with kinetic energies characteristic of the electrons originating from A.

- $\lambda^A imfp(E_B)$ is the IMFP or attenuation length of electrons traveling through A, with kinetic energies characteristic of the electrons originating from B.

- α is the angle of emission of electrons

**Emrah Özensoy
Bilkent University**

Angle-Dependent XPS Thin Film Analysis

Depth of Analysis:

d~10 nm   d~8.7 nm   d~5 nm

θ

SiO₂
Si

$I_{surface}/I_{bulk}$ = Small

$I_{surface}/I_{bulk}$ = Large

Si Bulk Substrate

I_{Bulk}

$I_{Surface}$

SiO₂ Surface Coating

θ

2013 Casa Software Ltd.
www.casaxps.com
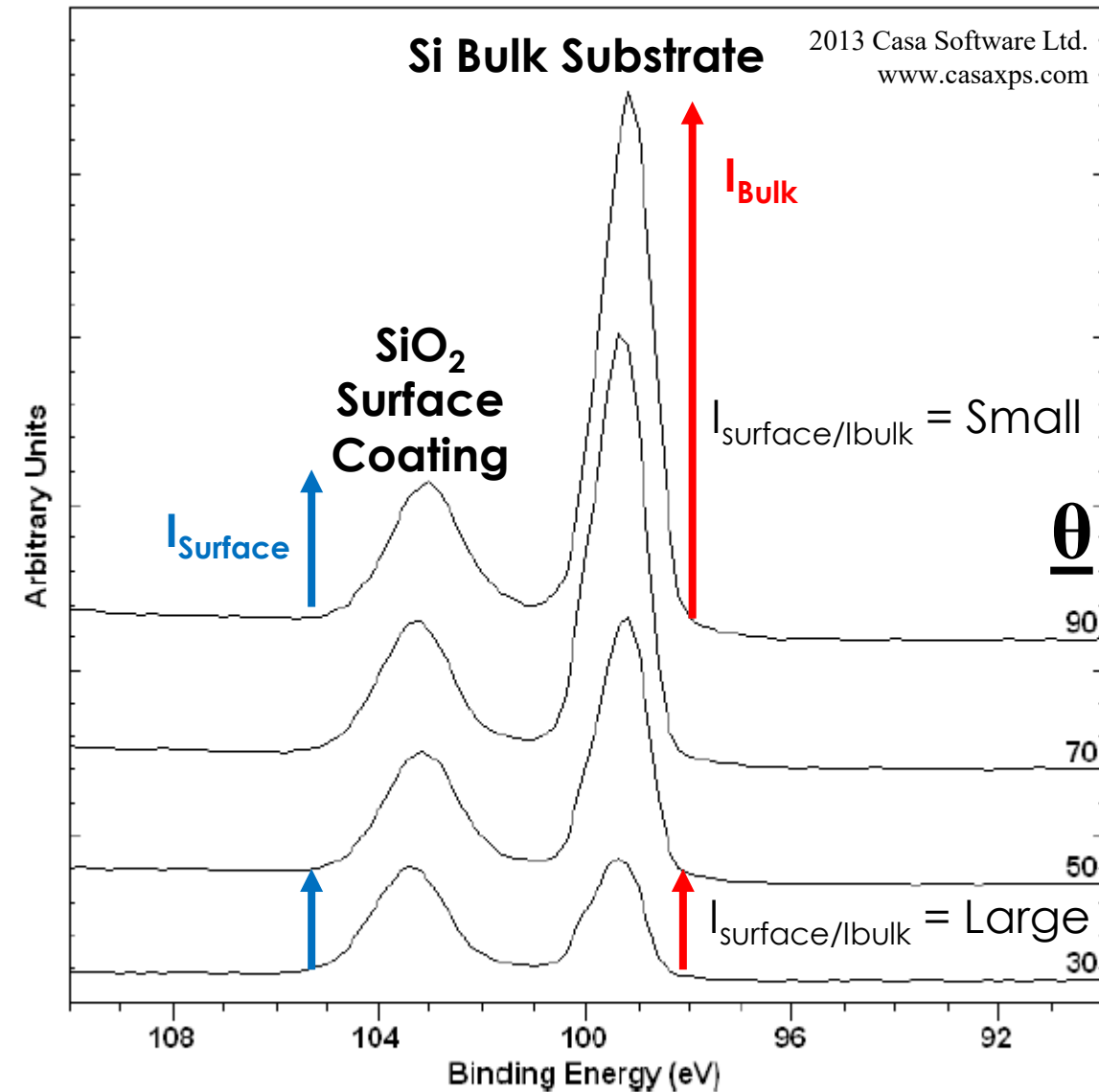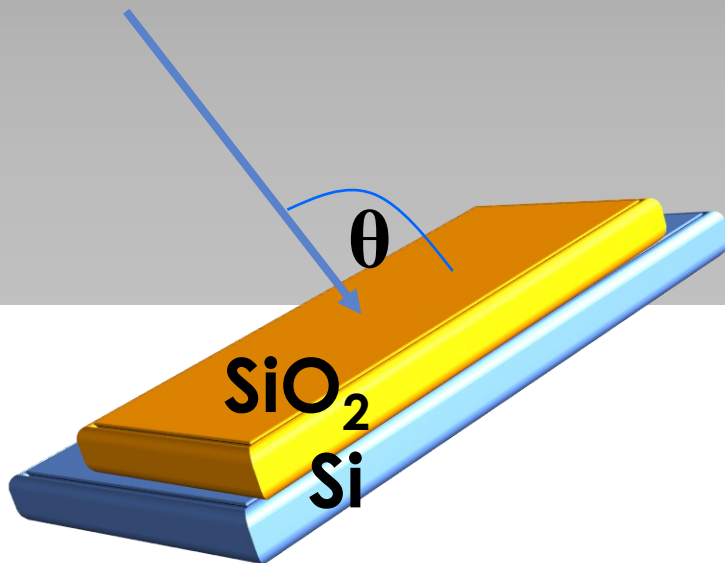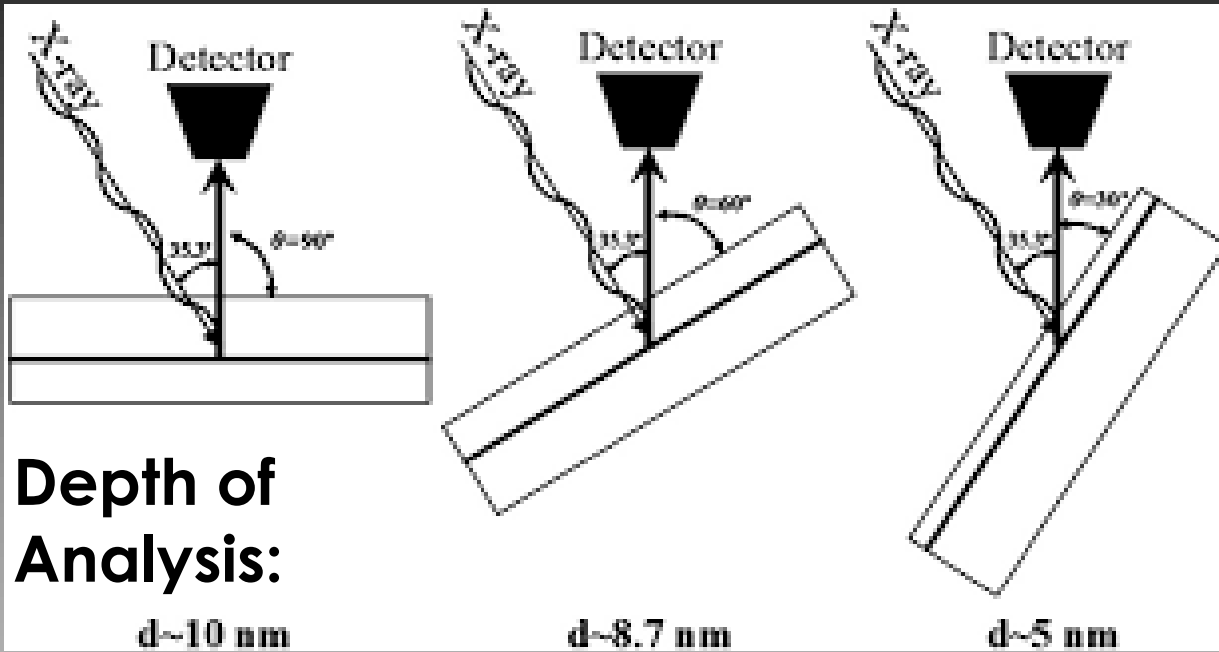
Figure 5: Angle resolved Si 2p spectra showing the changes to the spectra resulting from tilting the sample with respect to the analyser axis.

Emrah Özensoy
Bilkent University

Angle-Dependent XPS Thin Film Analysis

Emrah Özensoy
Bilkent University
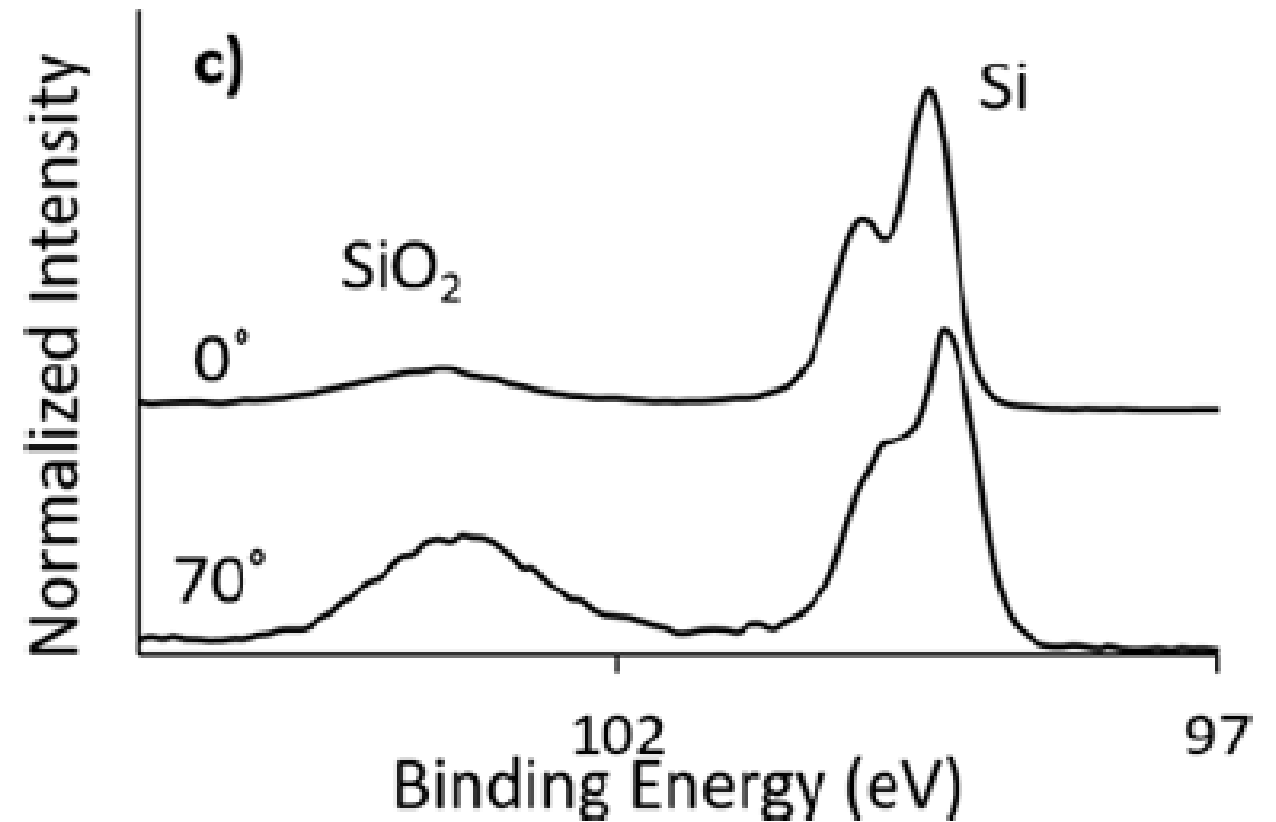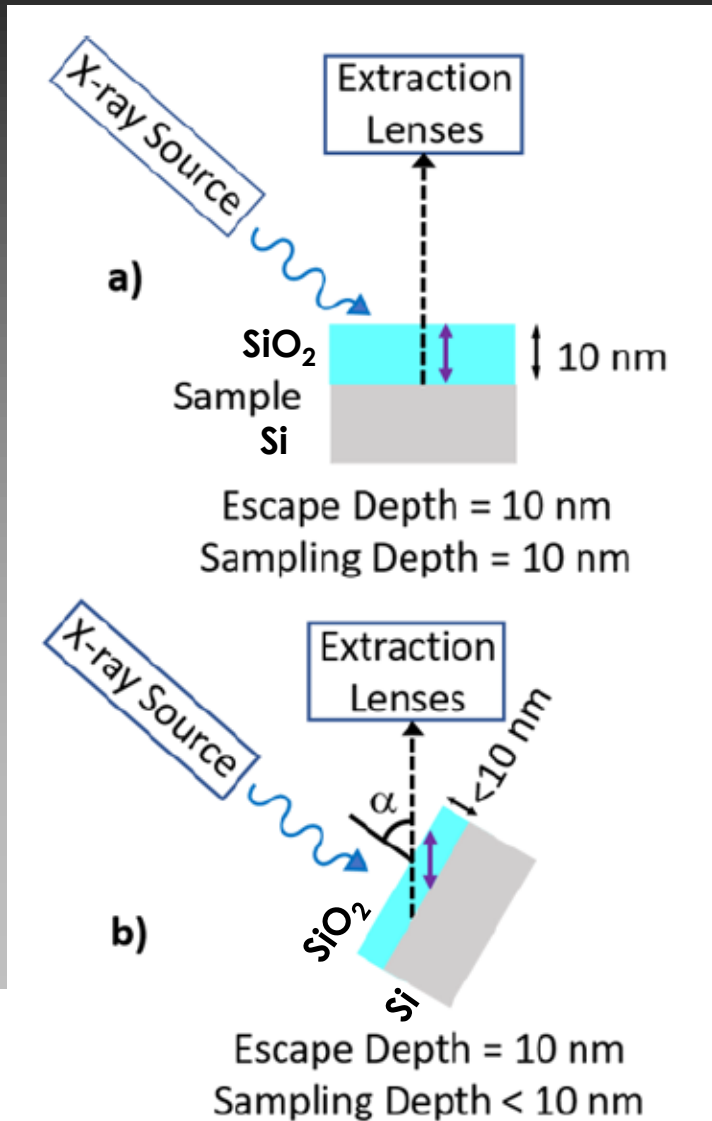
Film Growth Analysis via XPS: Layer by Layer growth of BaO_x on Al_2O_3/NiAl(100)

Ozensoy & Szanyi et al. J. Phys. Chem. B, 2006, 110, 17001

Emrah Özensoy
Bilkent University
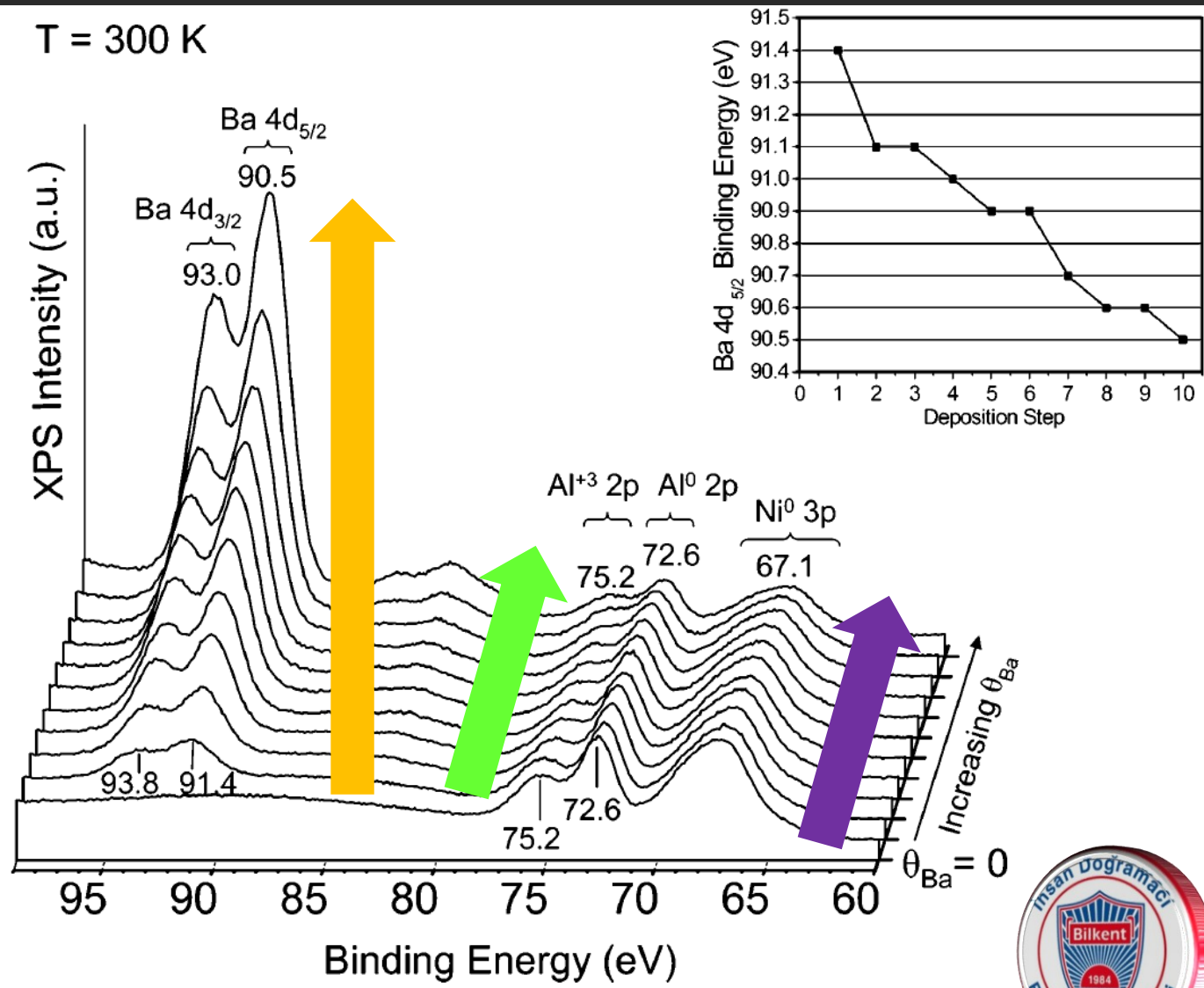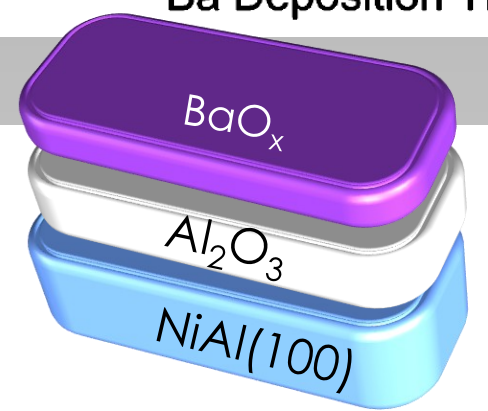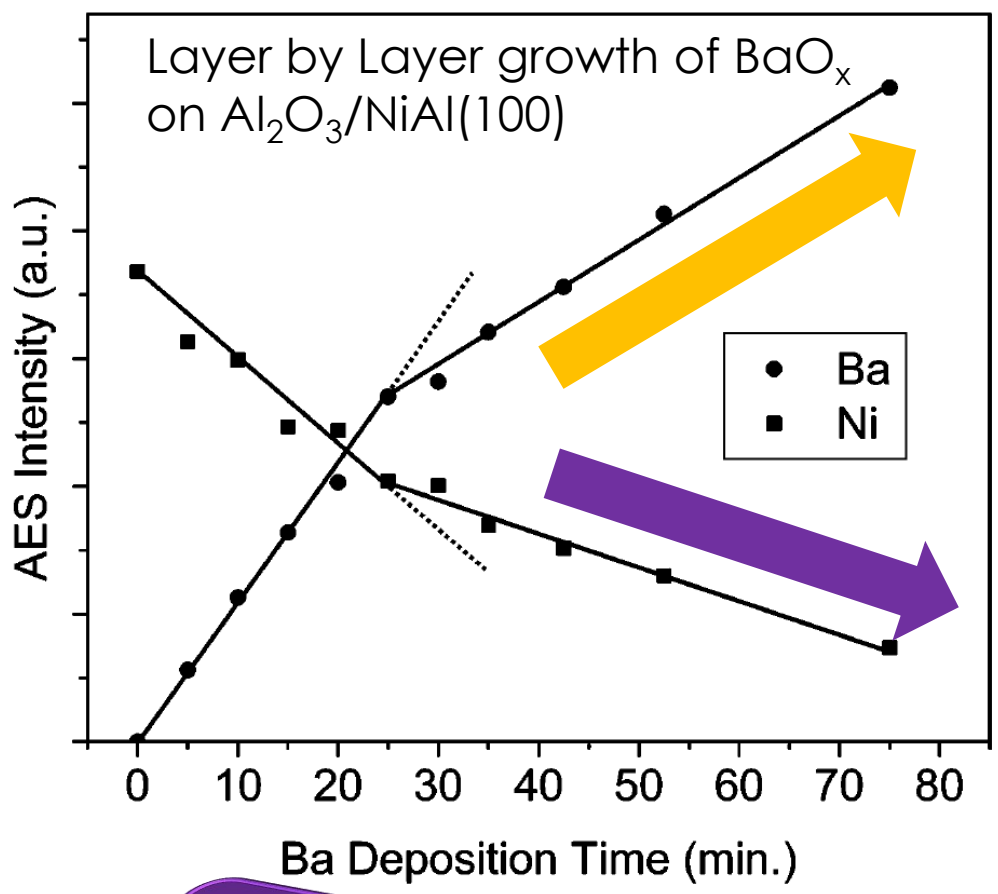
Depth Profiling via XPS

Emrah Özensoy
Bilkent University
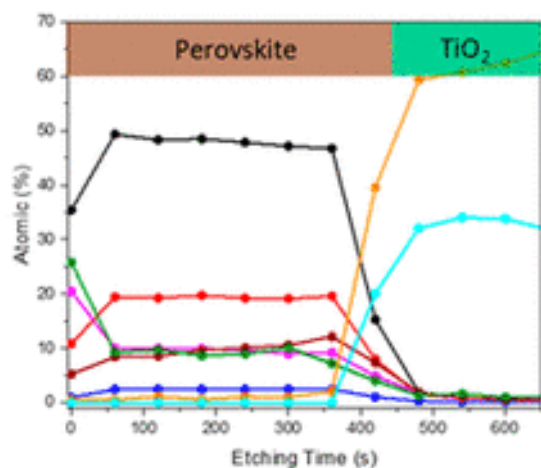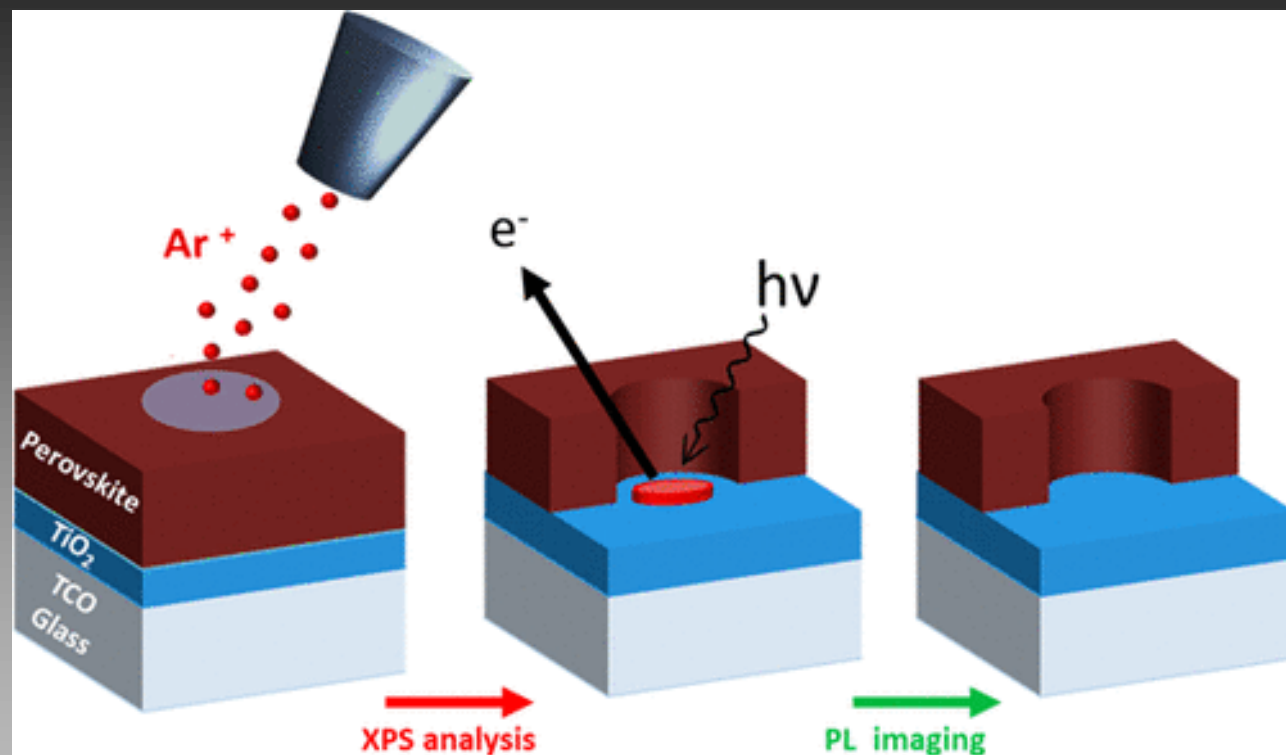
Depth Profiling via XPS
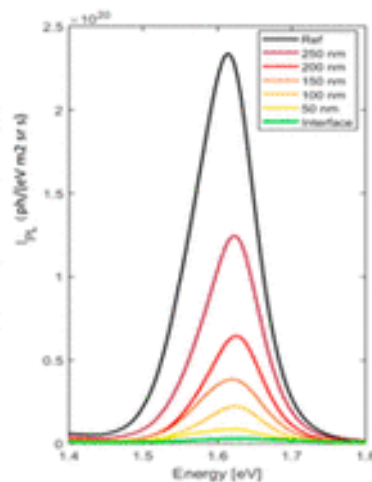
Cacovich et al.
ACS Appl. Mater. Interfaces 2022, 14, 30, 34228

Emrah Özensoy
Bilkent University

Depth Profiling via XPS:

SiO$_x$/Si
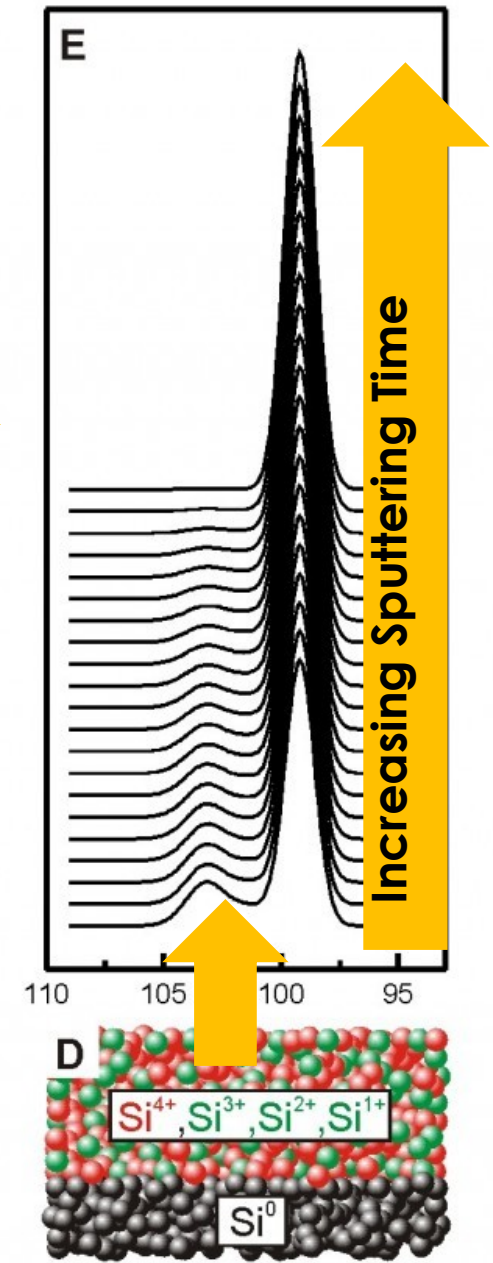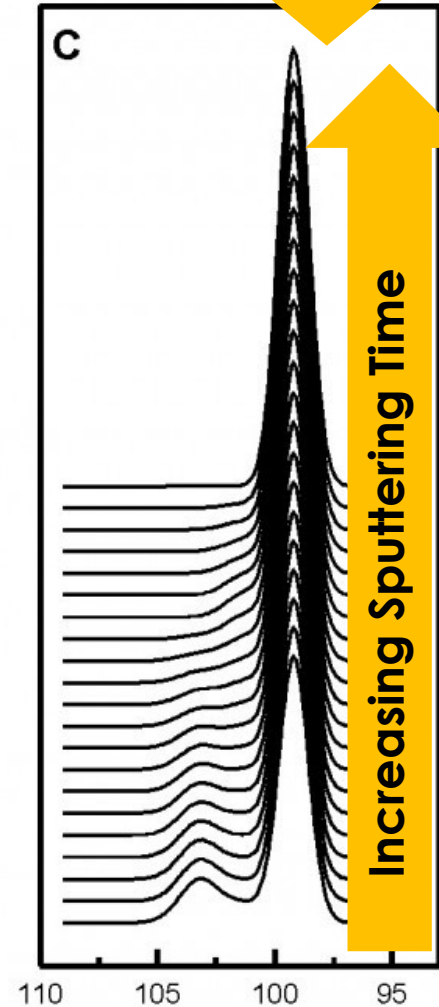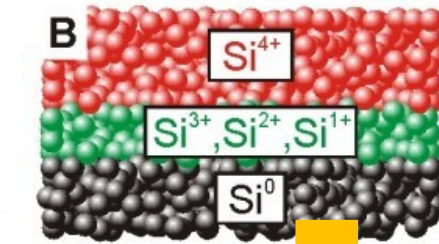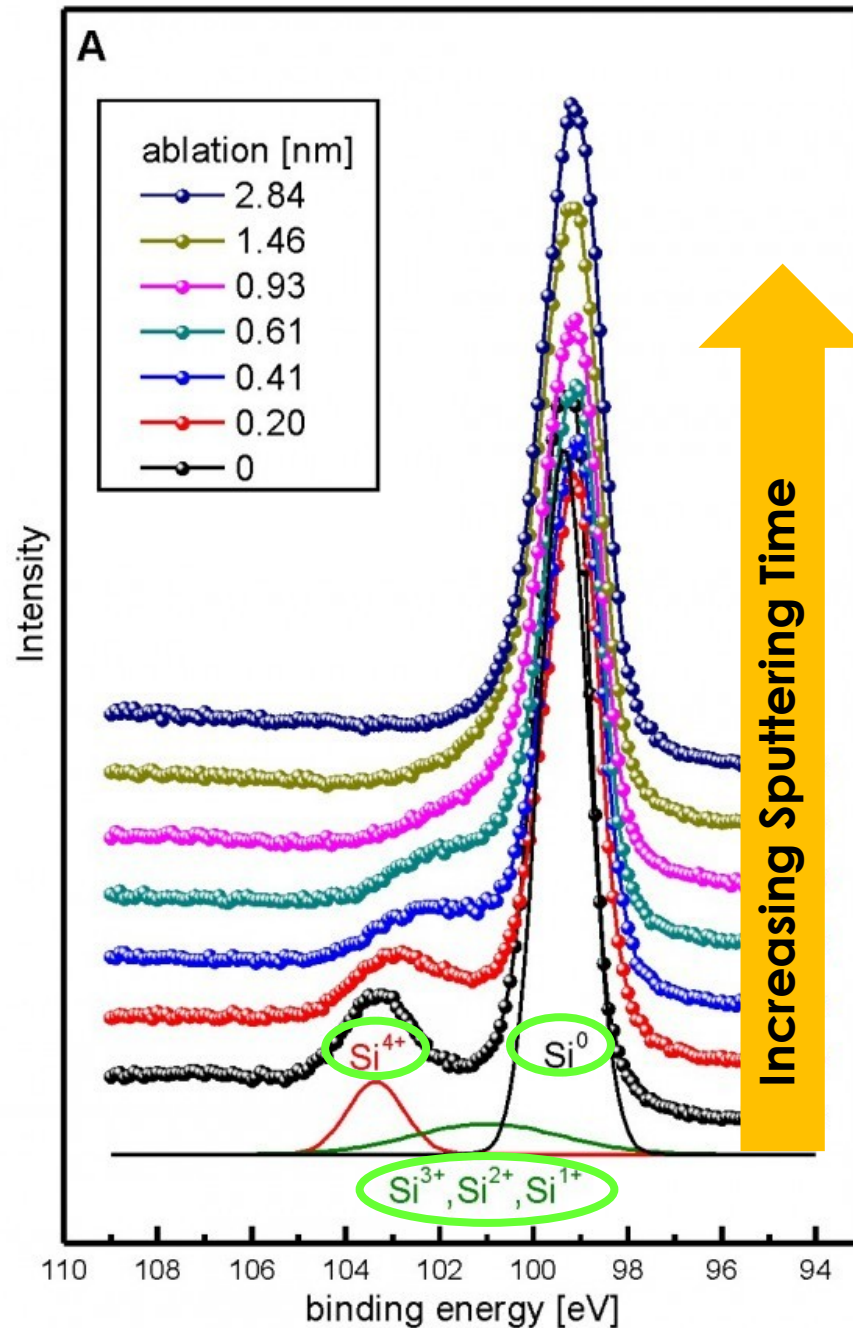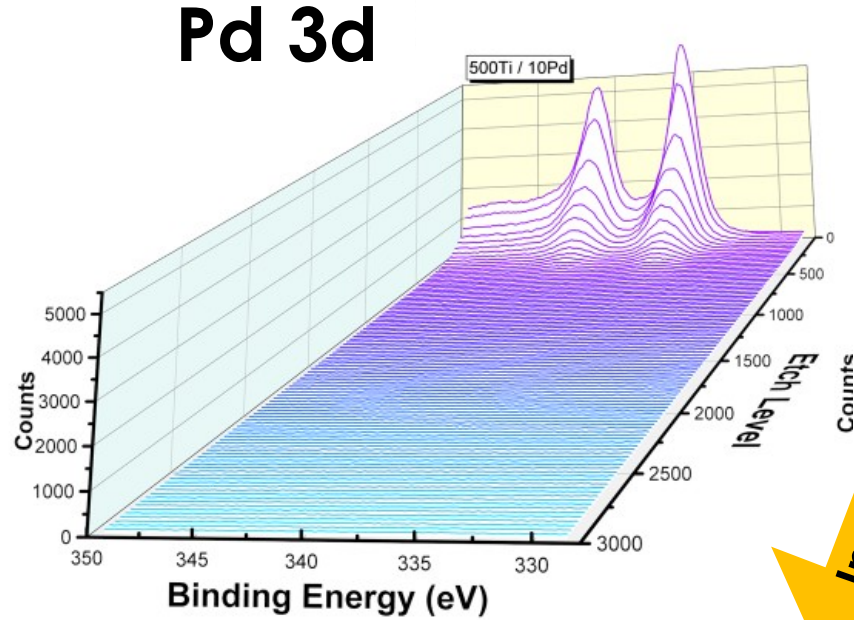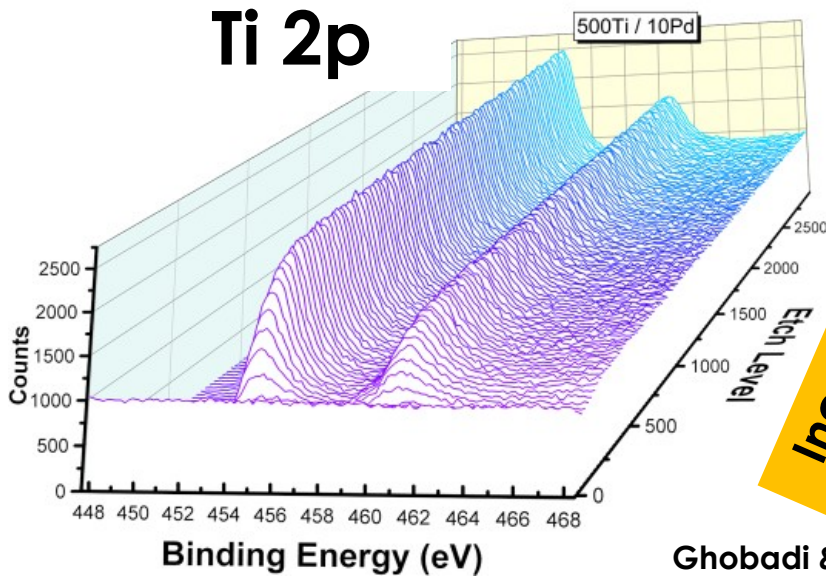
Emrah Özensoy
Bilkent University
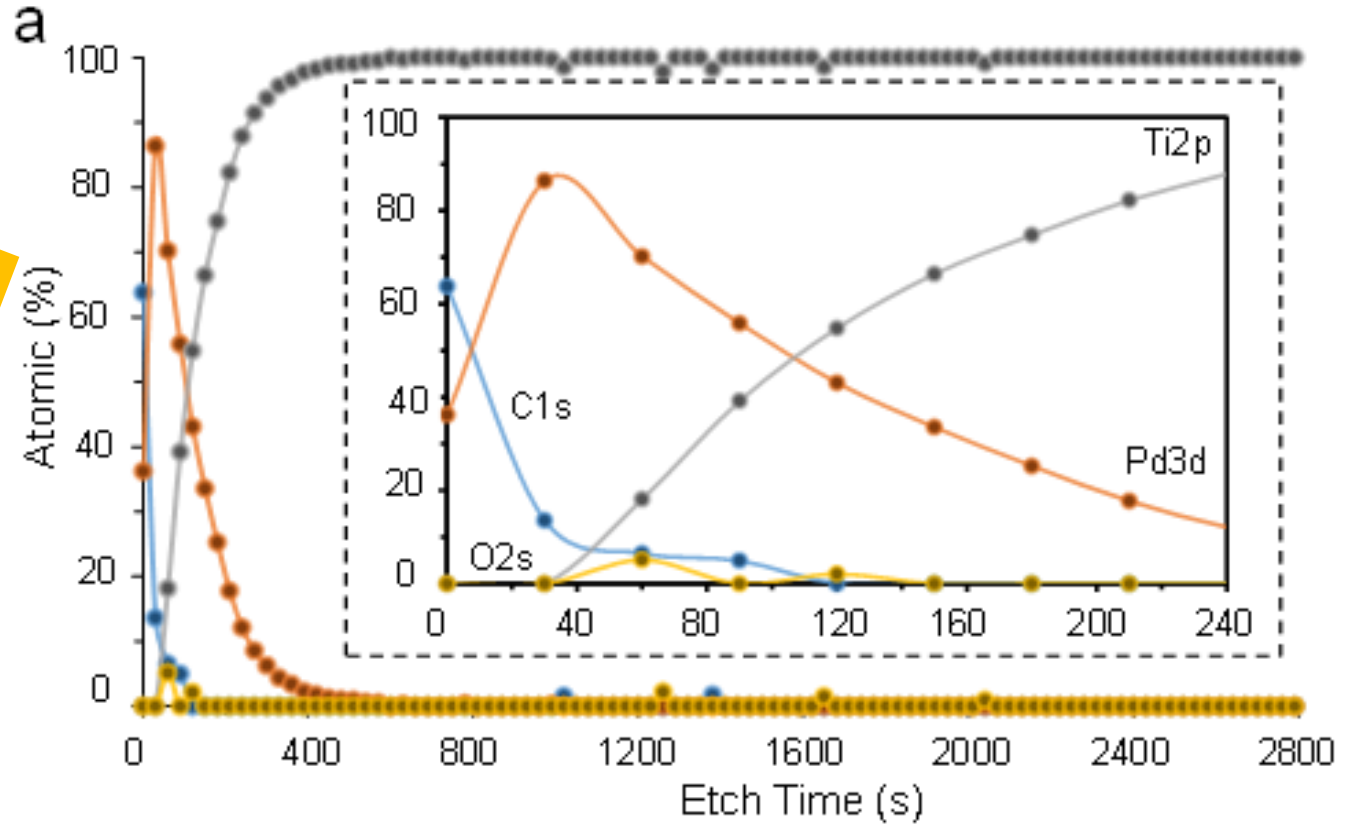
Ghobadi & Ozensoy et al. *Applied Materials & Interfaces*, 2023, 15, 34, 40459

**Emrah Özensoy
Bilkent University**
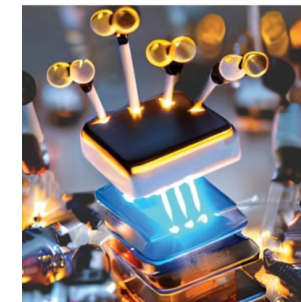
Quantitative XPS Analysis

Emrah Özensoy
Bilkent University

Determination of Surface Atomic concentrations without the use of standards

- After baseline subtraction, the area under a peak (I_i) can be measured.
- But raw areas alone cannot be used to determine relative concentrations.
- Instead, a sensitivity factor (S_i) that is specific for each transition must be considered to obtain atomic concentration (C_x):

$$C_X = (I_X/S_X)/(\Sigma(I_i/S_i))$$

E.g., if a survey spectrum showed the presence of both Au & C, and the Au 4f and C 1s peaks had the same intensity, there would be ~17.4 times more C than Au ($S_{Au\ 4f}/S_{C\ 1s} = 17.4/1$)

There are two types of **relative sensitivity factors (RSFs)**: empirical RSF determined with the aid of reference materials and theoretical RSF. Theoretical RSF values will account for all of the area produced by the electrons from a particular orbital, including the main photoemission peak, but also all satellite, shakeup, shakeoff, and multiplet splitting lines as well. Some of these features can be quite far from the main line [as for the Si plasmon lines], and thus the experimental data acquisition should account for this wider scan to capture all of the relevant features. Empirical RSF values often only include the intensity from the main photoemission line.
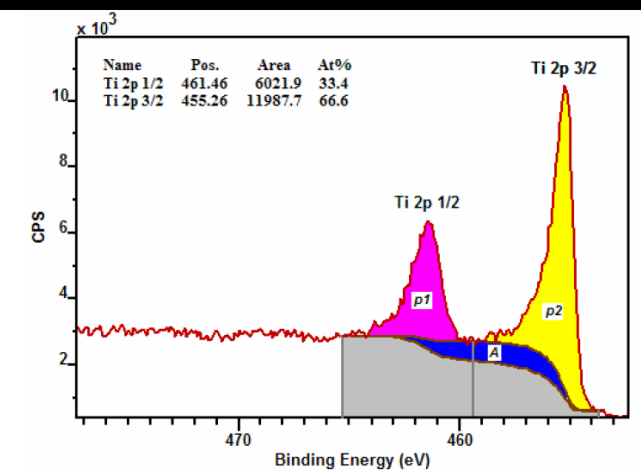
Figure 6: Metallic Ti modeled using two regions each defining a Shirley background (upper curve). The lower background curve is the Shirley background computed using the combined peaks. The At% column is computed using an RSF of unity for both peaks in the doublet pair, hence the 1:2 ratio in peak areas *p1* and *p2*.

TABLE IV. Sensitivity factors for some commonly analyzed elements (Ref. 102), derived and reprinted with permission from Scofield, J. Electron Spectrosc. Rel. Phenom. **8**, 129 (1976). Copyright 1976, Elsevier.

Element	Sensitivity factor	Element	Sensitivity factor	Element	Sensitivity factor
C 1s	1.00	Ca 2p	5.13	Ag 3d	18
N 1s	1.77	Cr 2p	11.5	In 3d	22.4
O 1s	2.85	Ni 2p	21.1	Sn 3d	24.7
F 1s	4.26	Ni 2p 3/2	13.9	Hf 4f	7.95
Na 1s	7.99	Ni 2p 1/2	7.18	Ta 4f	9.07
Al 2p	0.5735	Cu 2p	24.1	W 4f	10.3
Si 2p	0.865	Ga 2p	31	Pt 4f	15.9
Cl 2p	2.36	Mo 3d	9.74	Au 4f	17.4

Emrah Özensoy
Bilkent University

Words of Caution Regarding of Surface Atomic Concentration Determination: Use of Different XPS Features
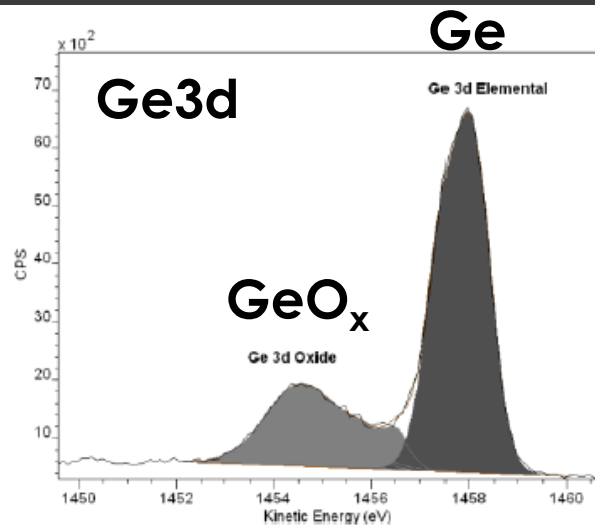
Figure 4: Germanium Oxide relative intensity to elemental germanium measured using photoelectrons with kinetic energy in the range 1452 eV to 1460 eV.
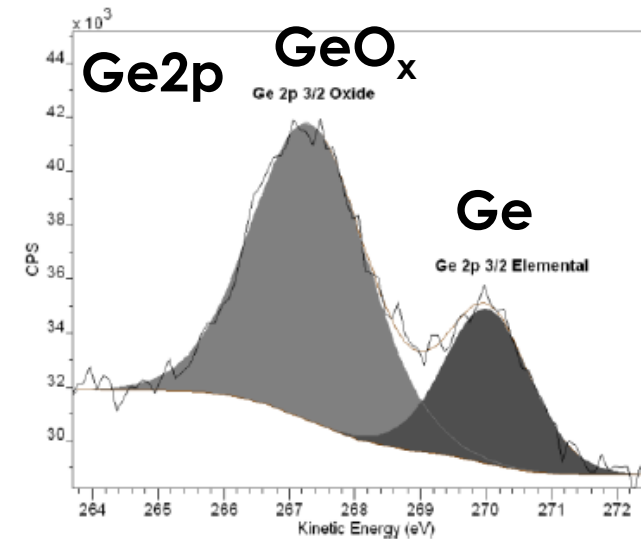
Figure 3: Germanium Oxide relative intensity to elemental germanium measured using photoelectrons with kinetic energy in the range 262 eV to 272 eV.

- *Low energy photoelectrons (270 eV) from the elemental Ge2p line are attenuated due to GeO_x covering Ge.*

- *This results in a shallower sampling depth in Ge2p XPS data as compared to Ge3d (1450 eV).*

- *Surface atomic concentration estimations may differ.*

CASA XPS Manual 2013 Casa Software Ltd. www.casaxps.com

Emrah Özensoy
Bilkent University

XPS Analysis Research Examples from Ozensoy Group

Emrah Özensoy
Bilkent University

Catalyst Deactivation by Thermal Diffusion of BaO$_x$ Overlayers into TiO$_2$ Substrate
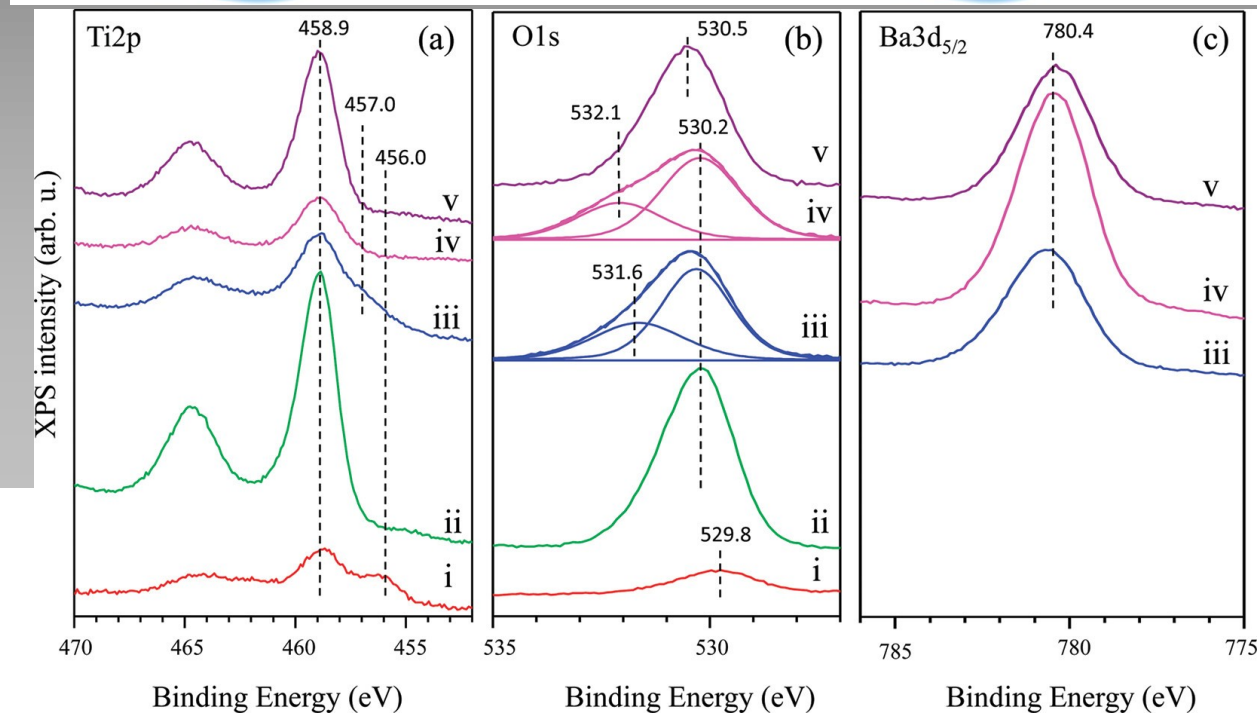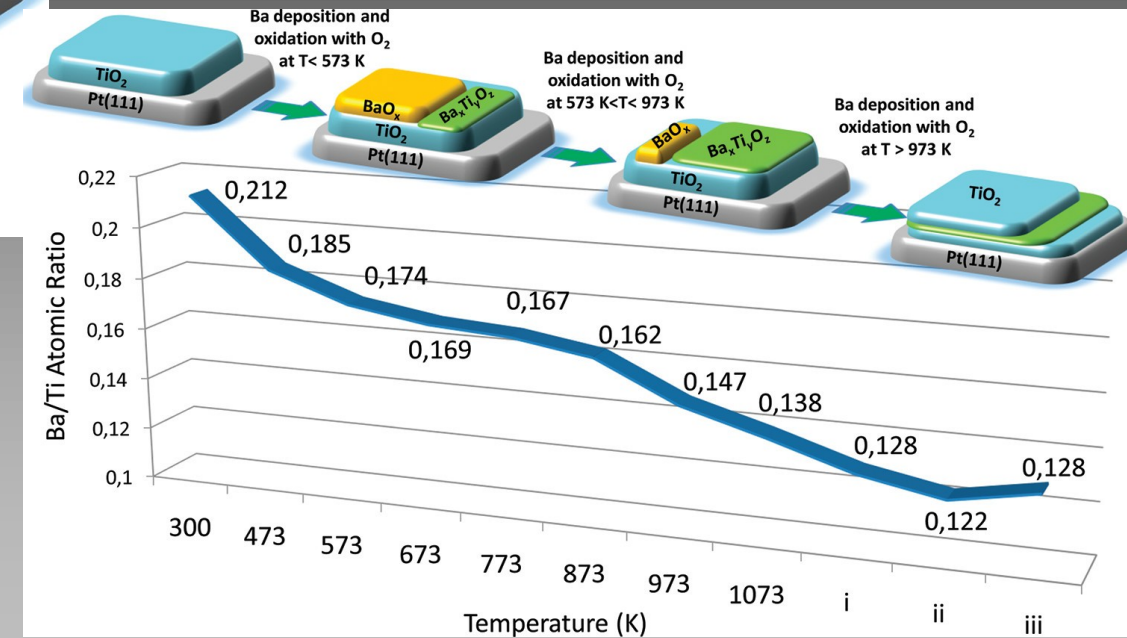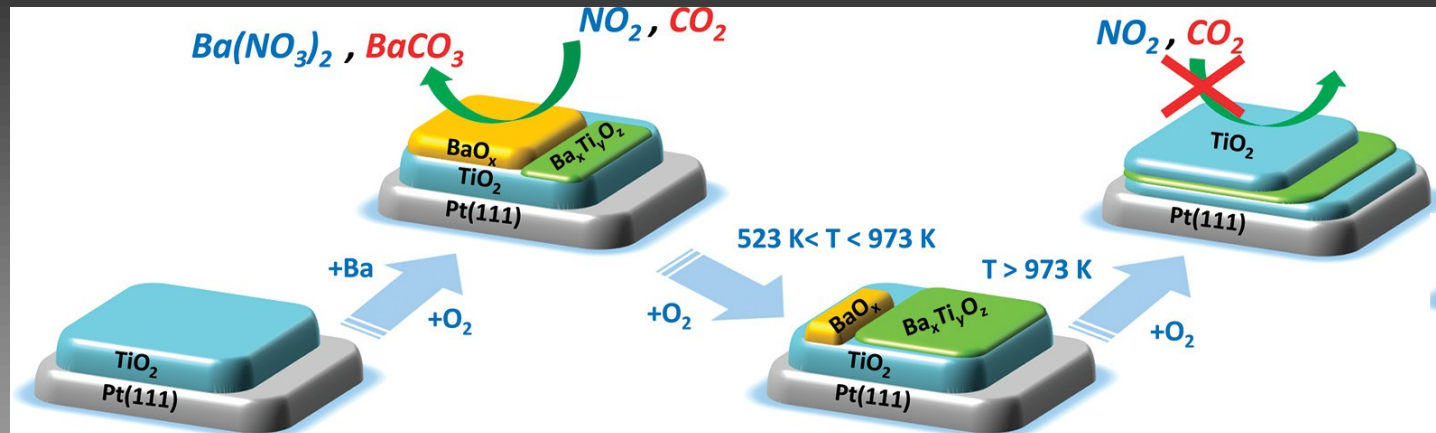
Emmez & Ozensoy et al. J. Phys. Chem. C 2011, 115, 45, 22438

Emrah Özensoy
Bilkent University

Quantitative determination of surface atomic composition of Sulfur-Poisoned & Regenerated Perovskite Emission Control Catalysts:

Emrah Özensoy
Bilkent University
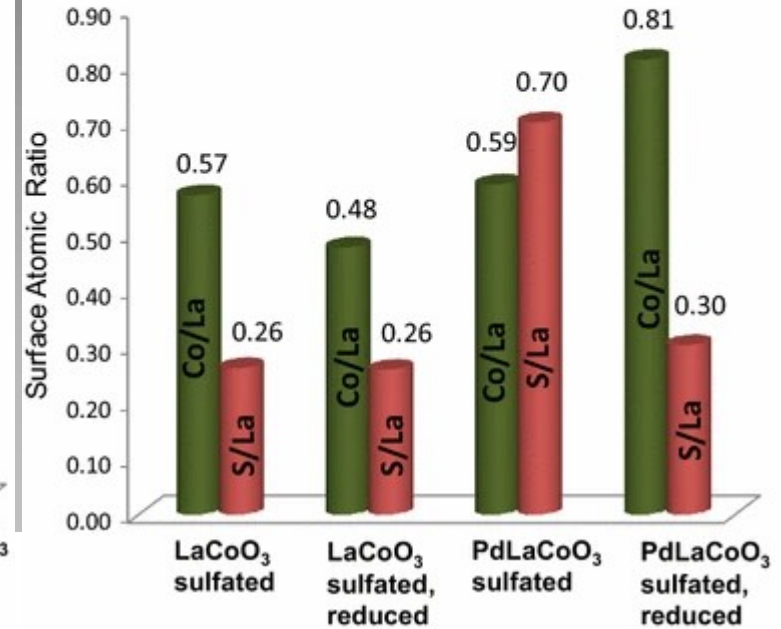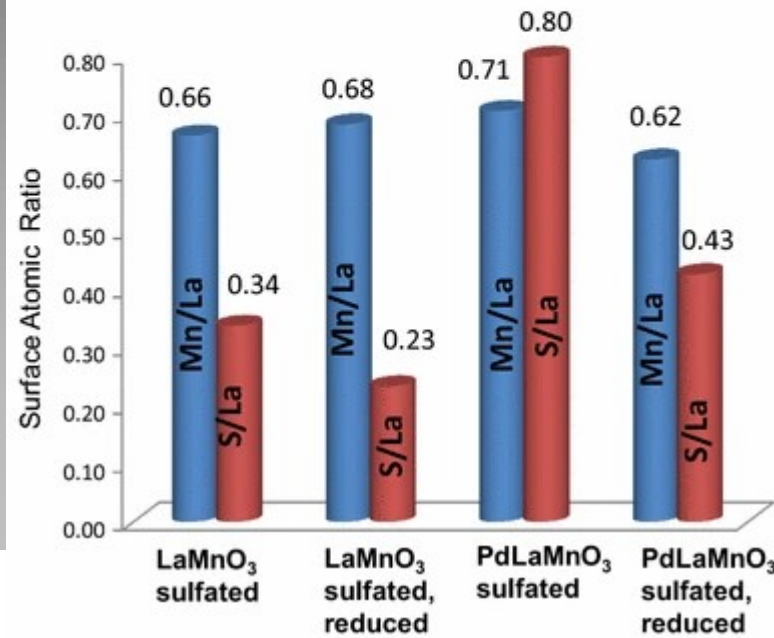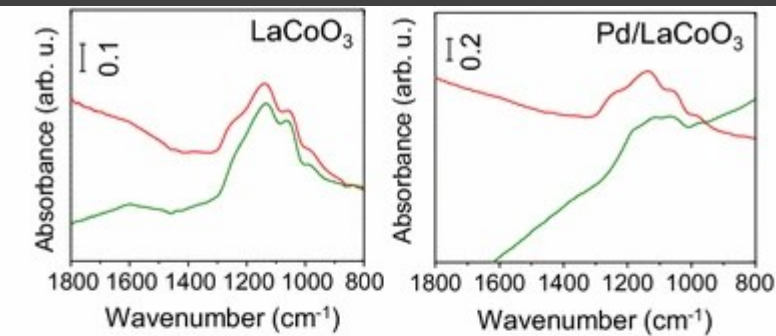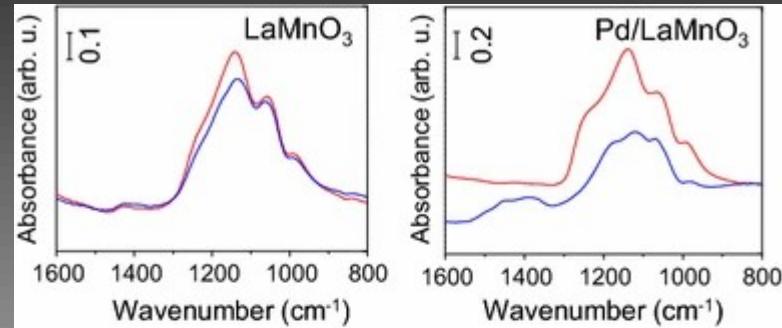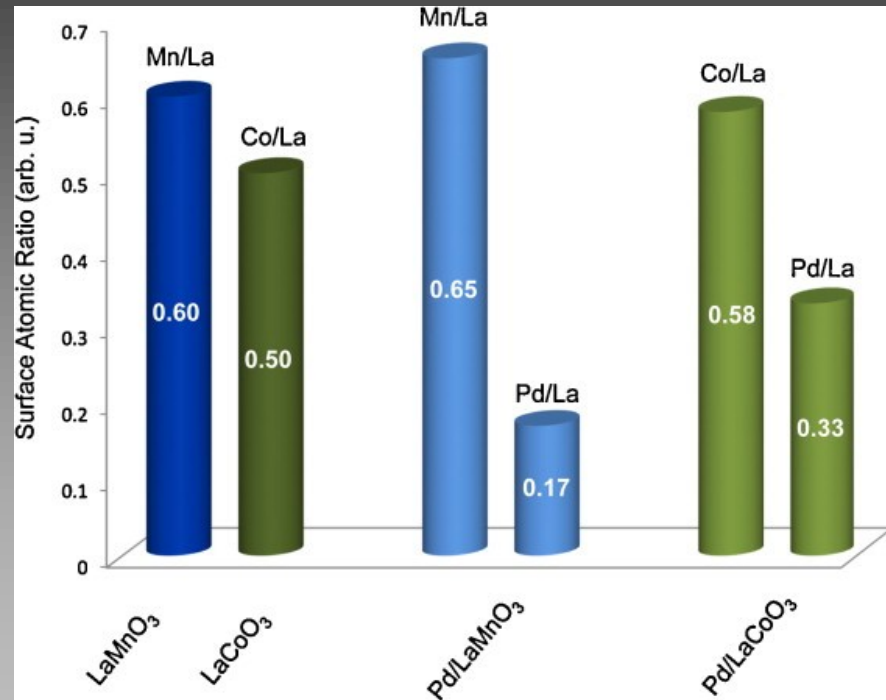
Monitoring Thermal Reduction & Activation of Perovskite Catalysts for Alkylaryl Oxidation
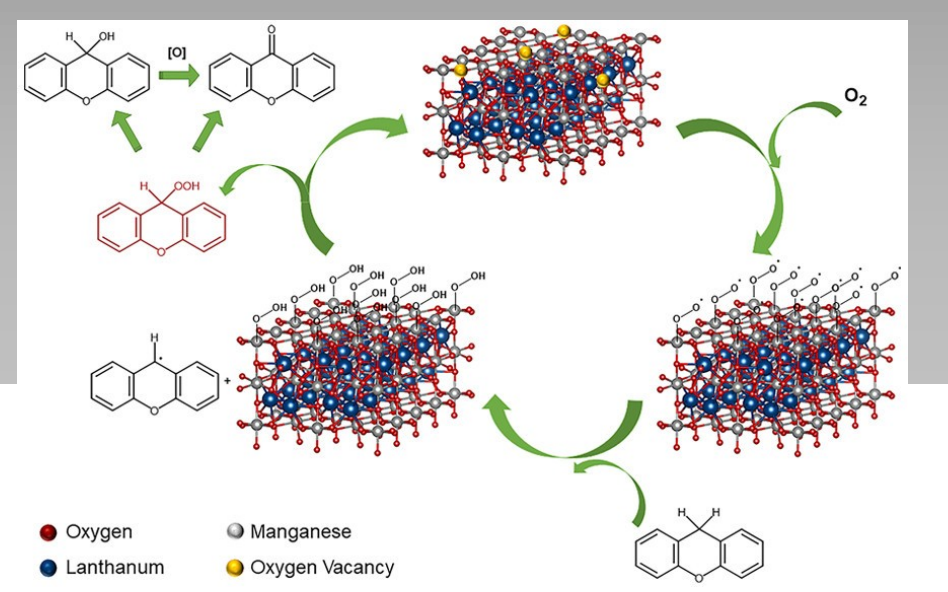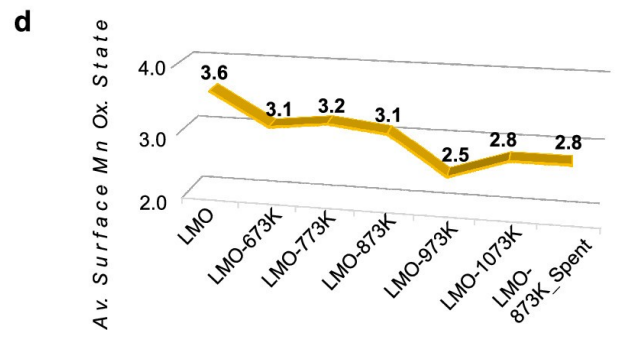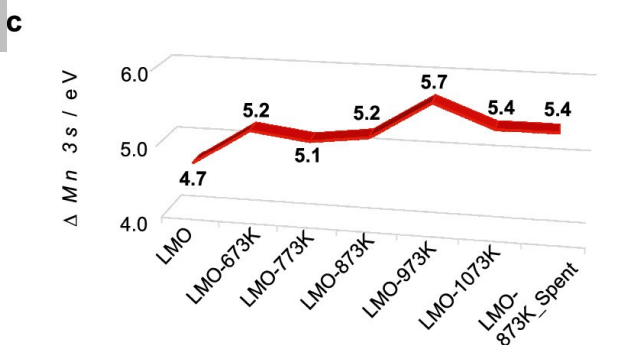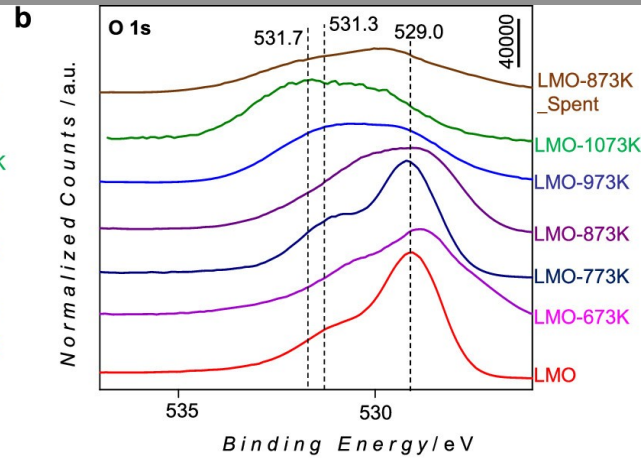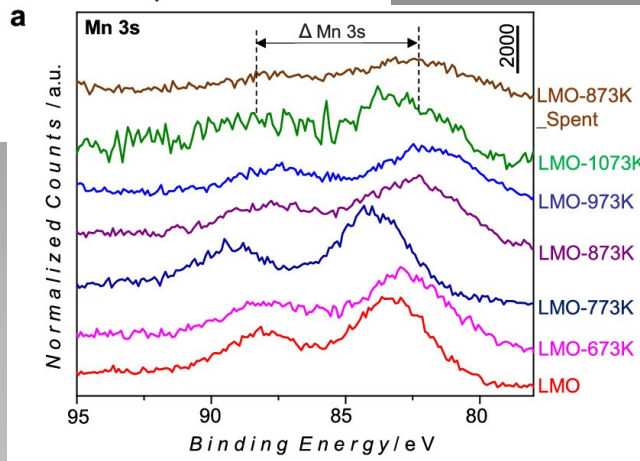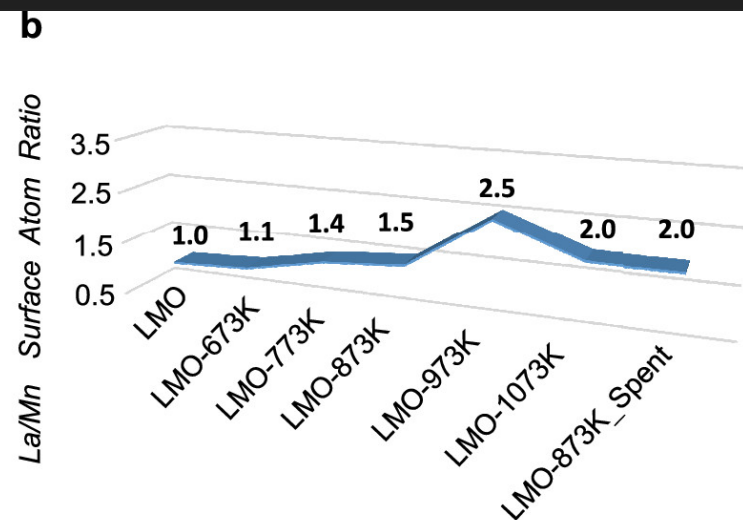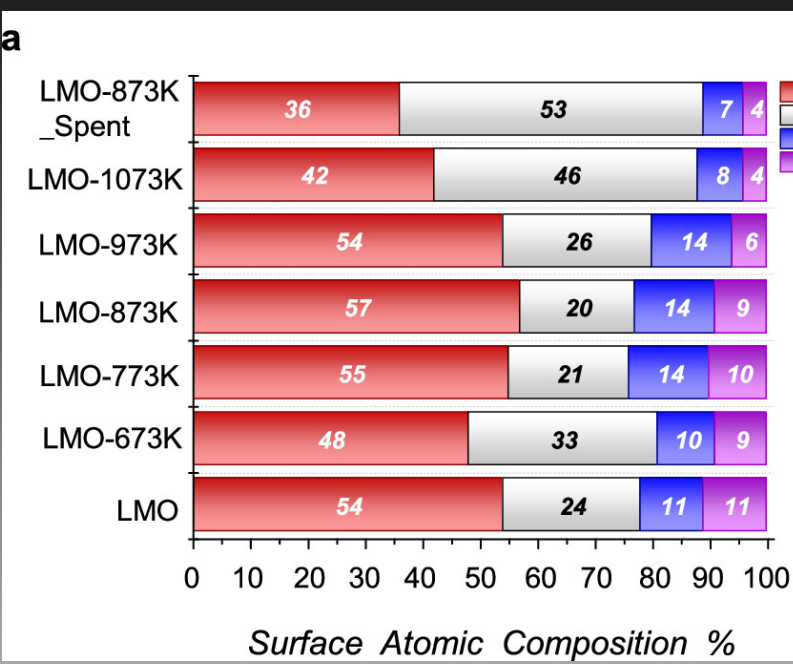
Emrah Özensoy
Bilkent University

Sahin & Ozensoy et al.
ACS Appl. Mater. Interfaces 2021 (13) 5099

Unraveling Surface Chemistry of 2D-Layered Double Hydroxide Catalysts

$Ni_{0.6}Mn_{0.4}(OH)_y$ Layered Double Hydroxide (LDH) 2D-Nanoplatelet
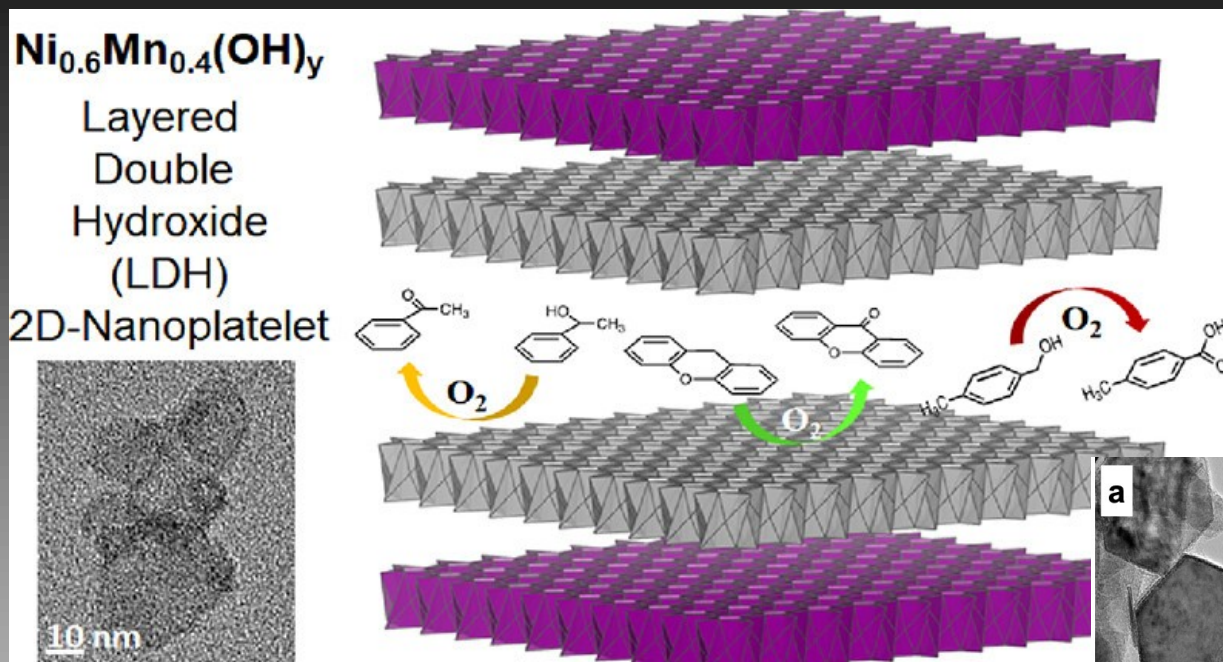
Nartey & Ozensoy et al.
ACS Appl. Nano Mater. 2022, 5, 12, 18855
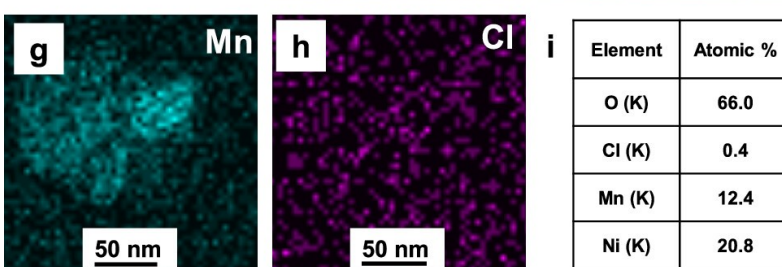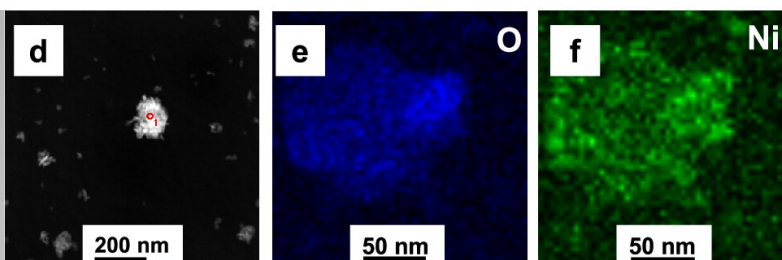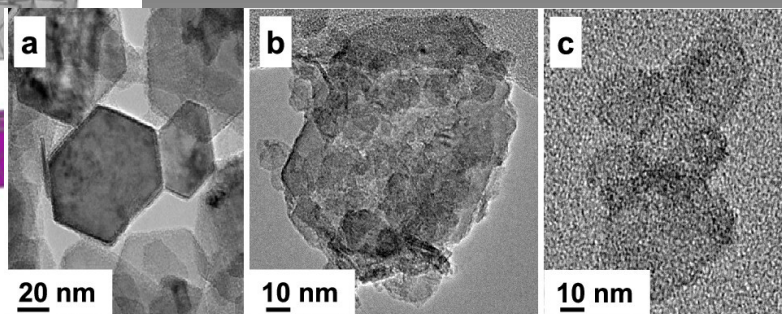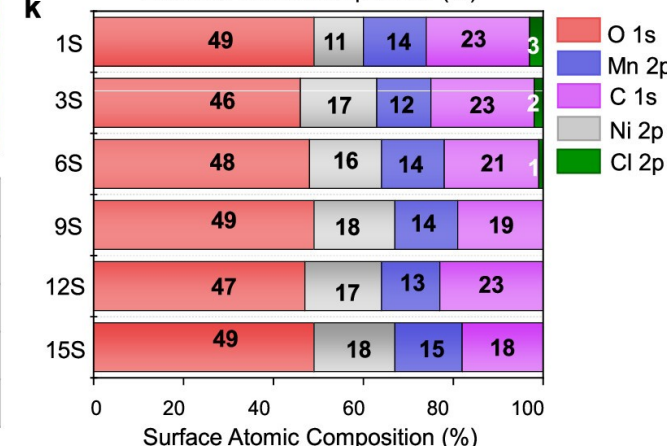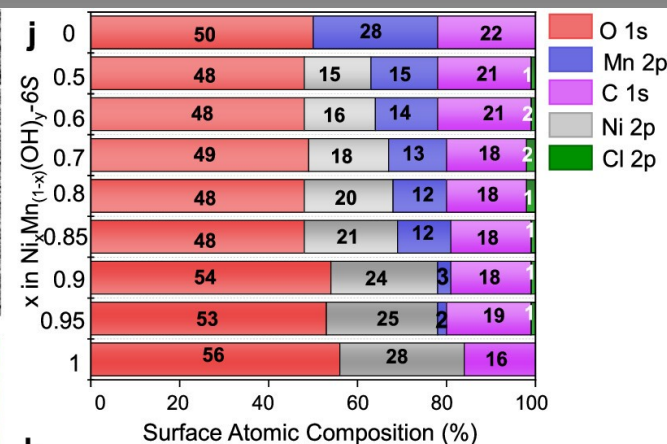
Emrah Özensoy
Bilkent University

Detection of Surface Na⁺ Promoters on Mixed Metal Hydroxide Catalysts
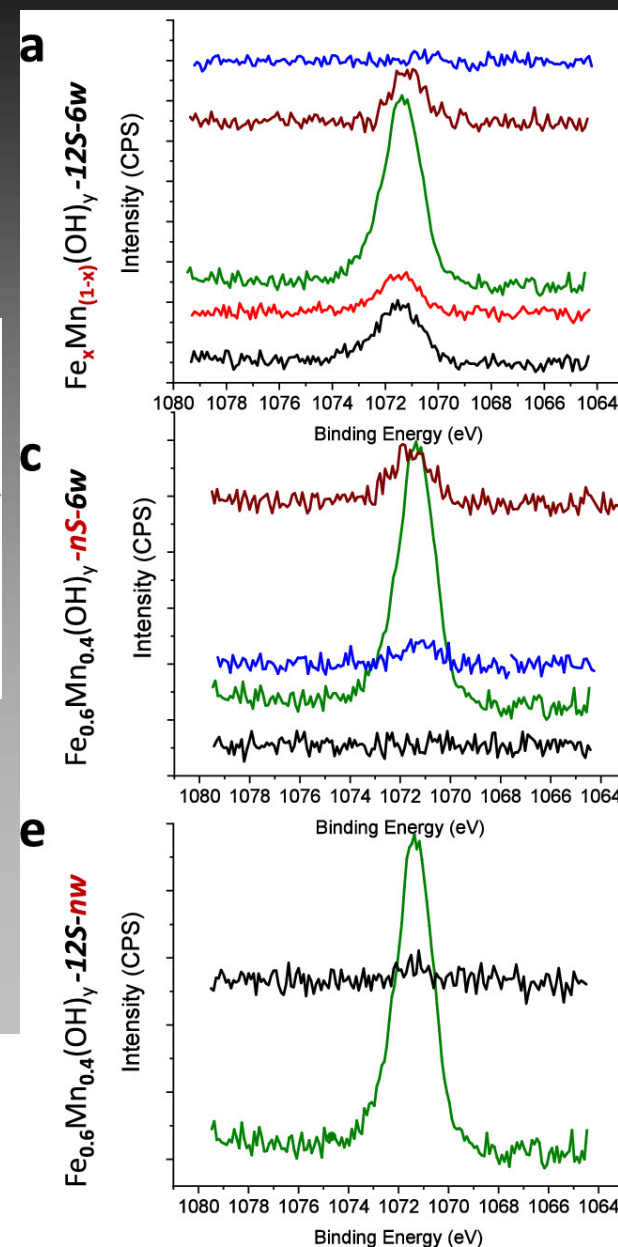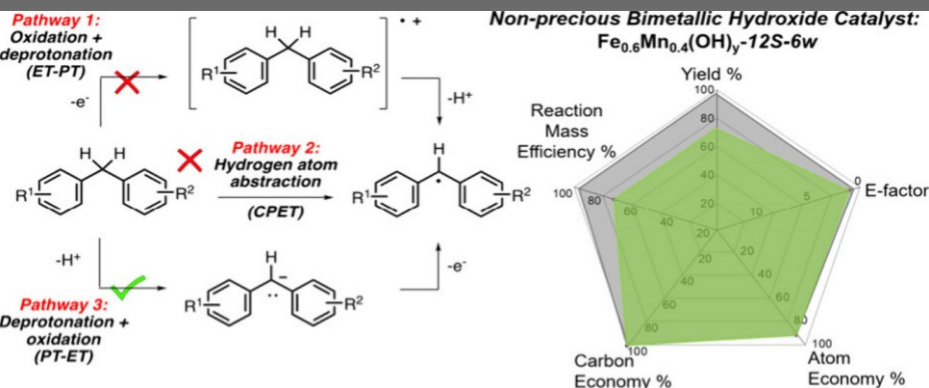
Emrah Özensoy
Bilkent University

Erdivan & Ozensoy et al.
ACS Appl. Mater. Interfaces 2024, 16, 44, 60151
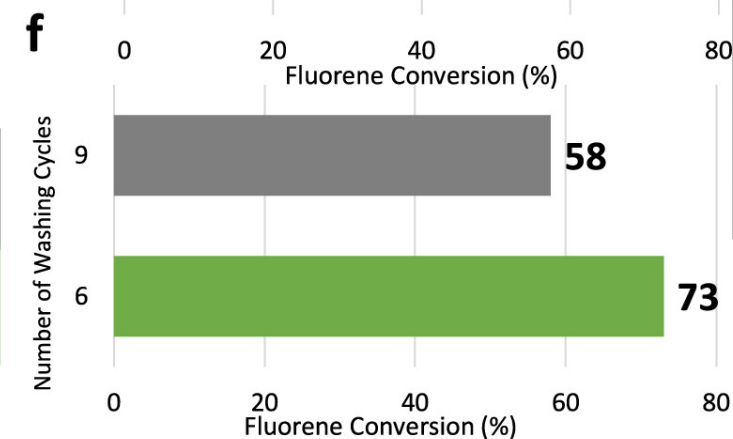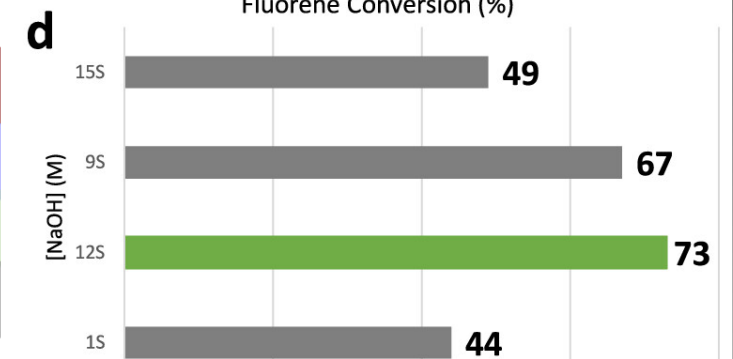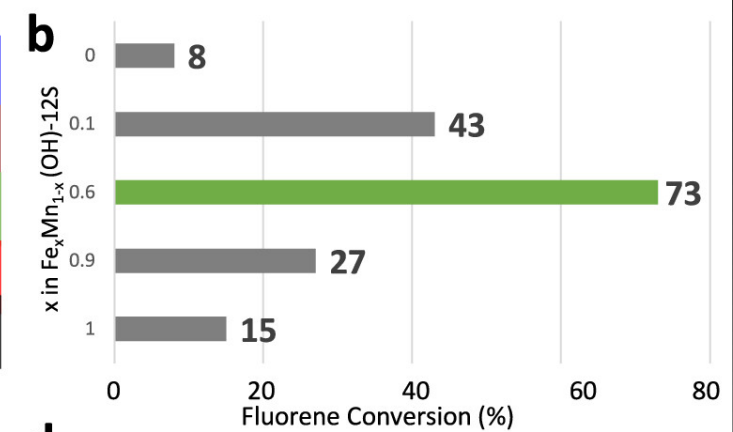
Elemental Composition & Oxidation State of Pd Nano-discs on Al$_2$O$_3$ Films After S-Poisoning
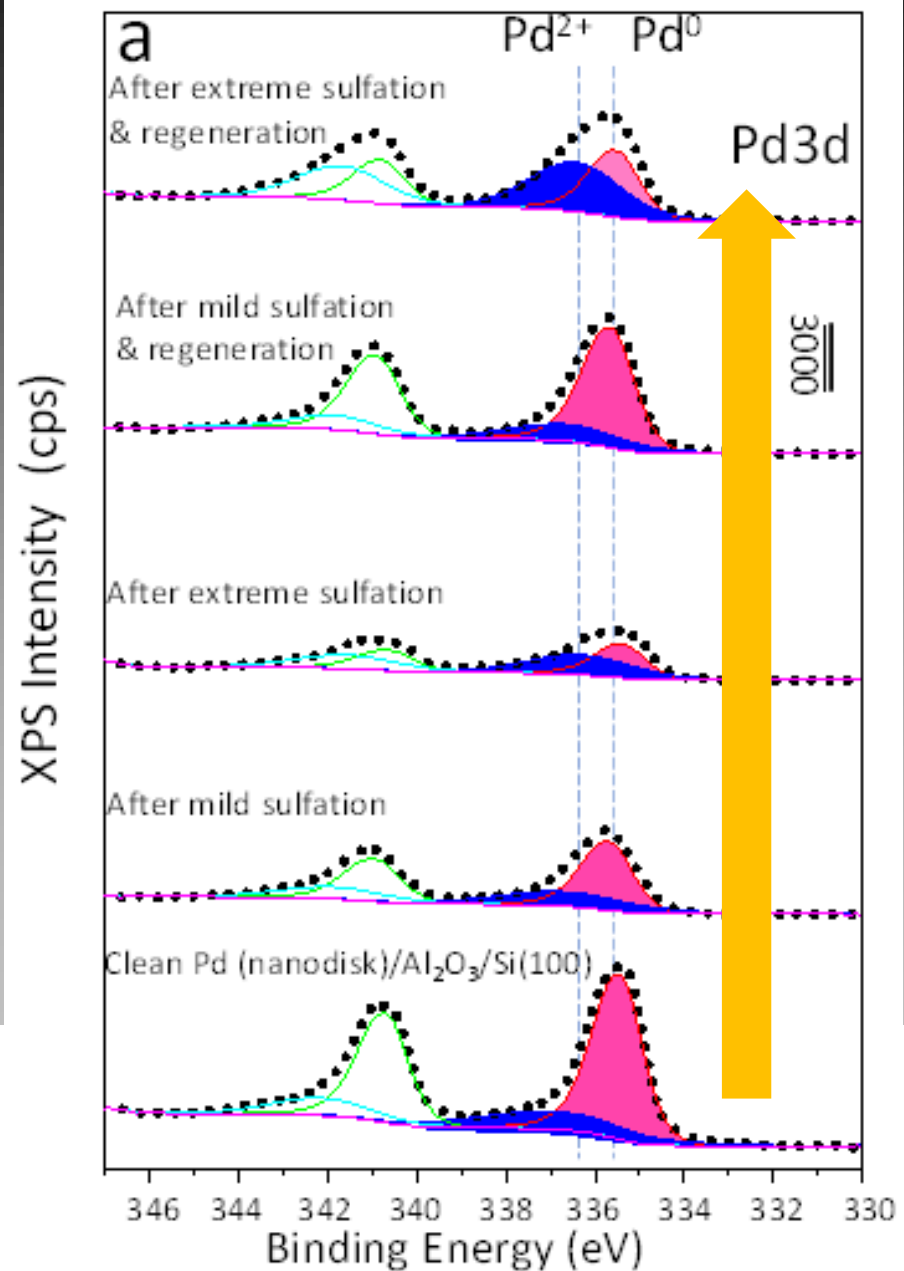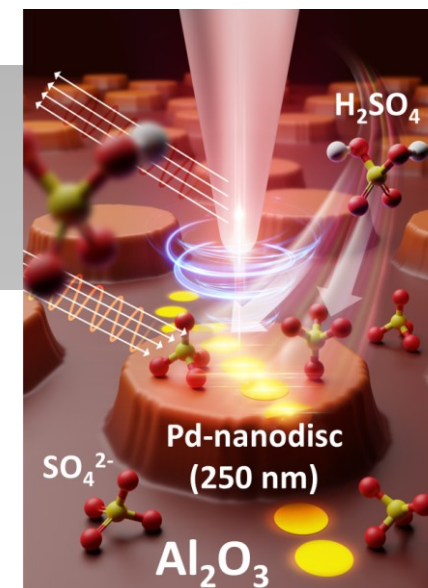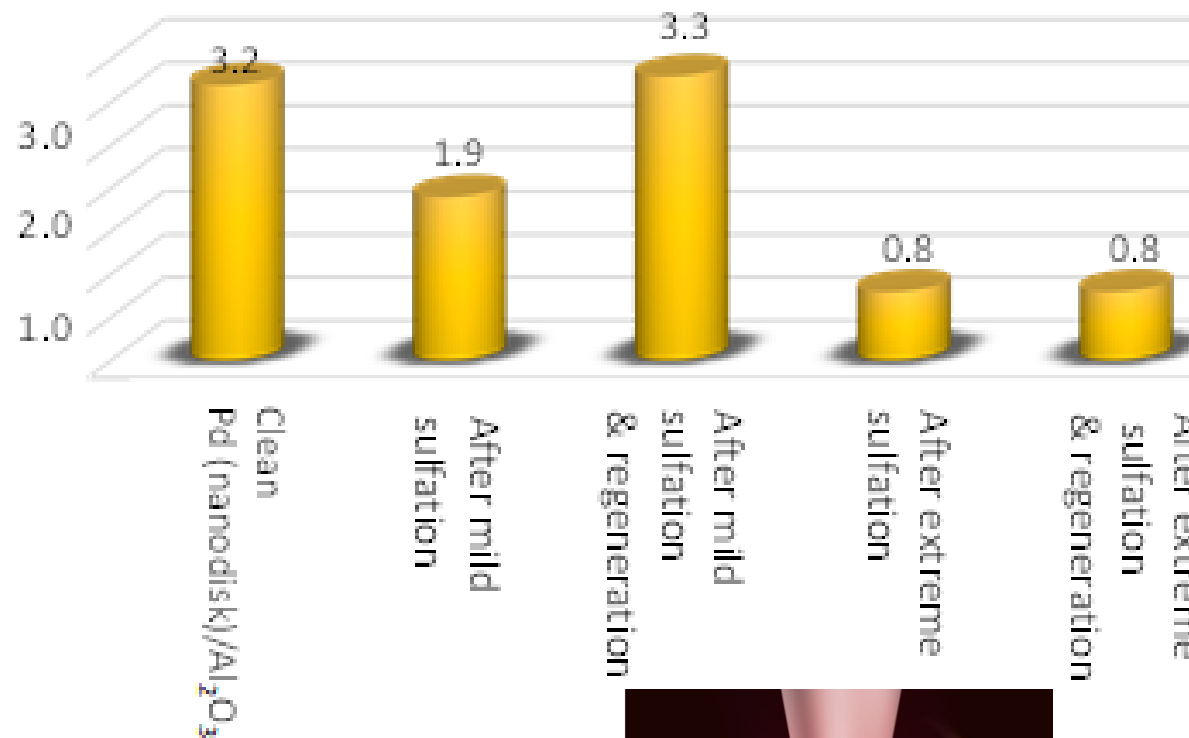
Say & Ozensoy et al. *J. Amer. Chem. Soc.*
2022, 144, 19, 8848

Emrah Özensoy
Bilkent University
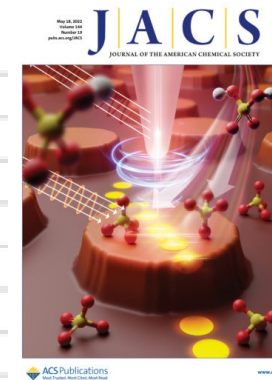
Interaction of NO$_2$ with Al$_2$O$_3$ Ultrathin Films Grown on NiAl(100) Substrate: Formation of Nitrite and Nitrate Surface Species with Temperature
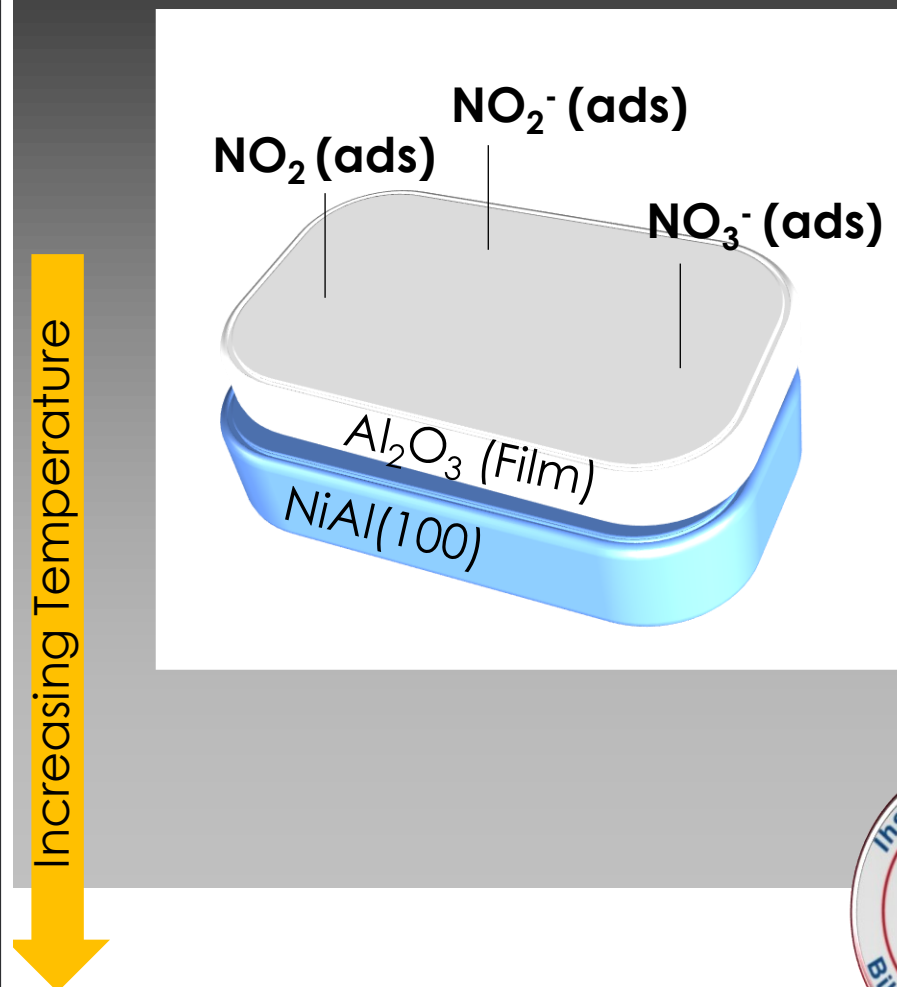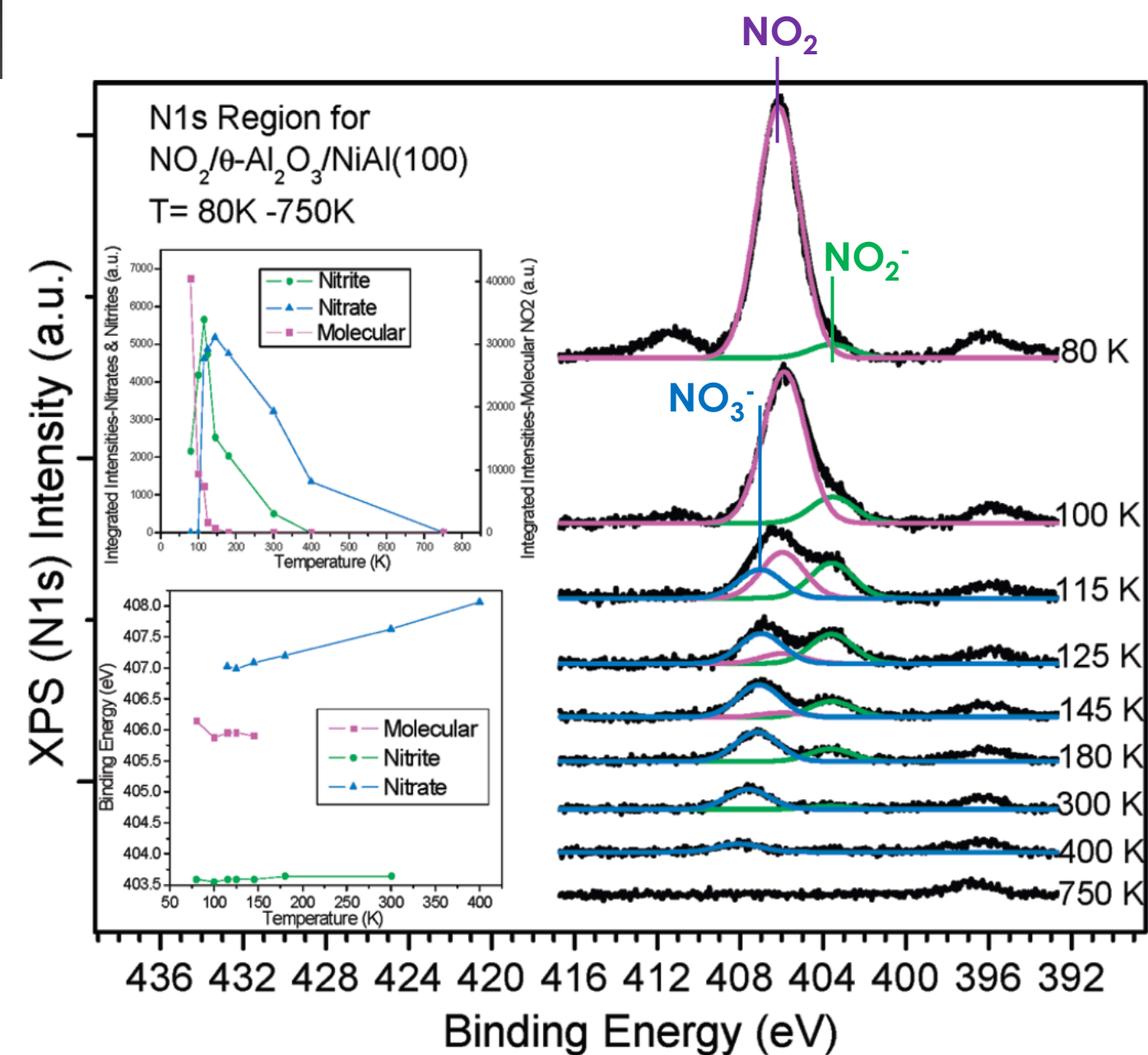
Ozensoy & Szanyi et al. J. Phys. Chem. B, 2005, 109, 33, 15977

Emrah Özensoy
Bilkent University

Oxide-Peroxide Transitions of BaO$_x$ Overlayer on Pt(111) Substrate upon NO$_2$ Adsorption & T

**Emrah Özensoy
Bilkent University**
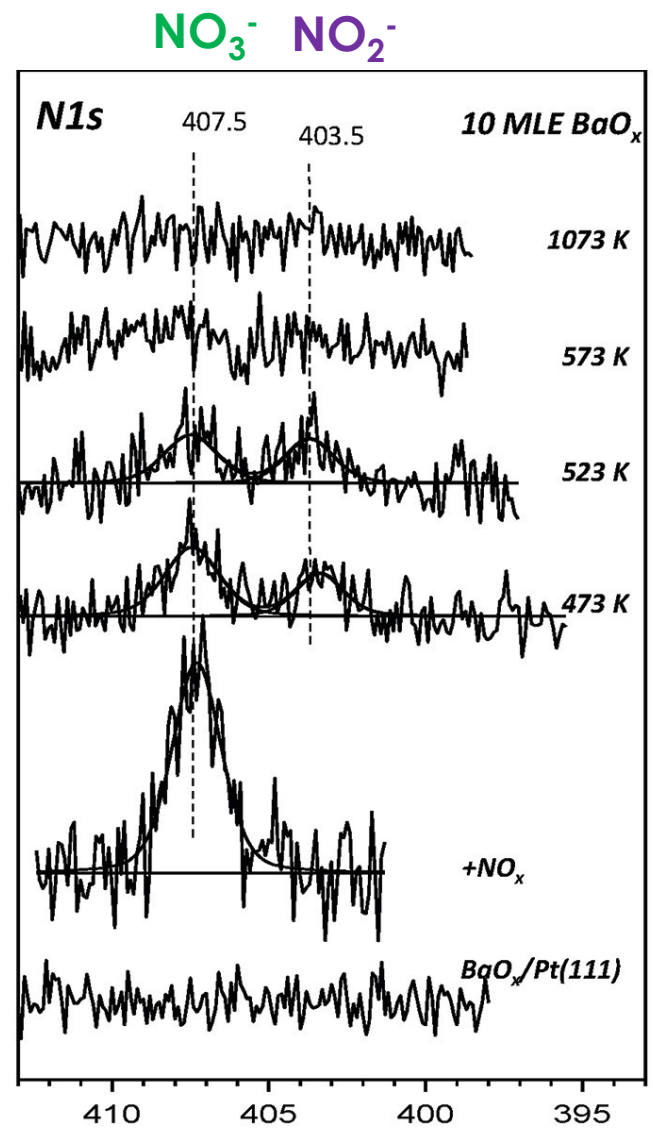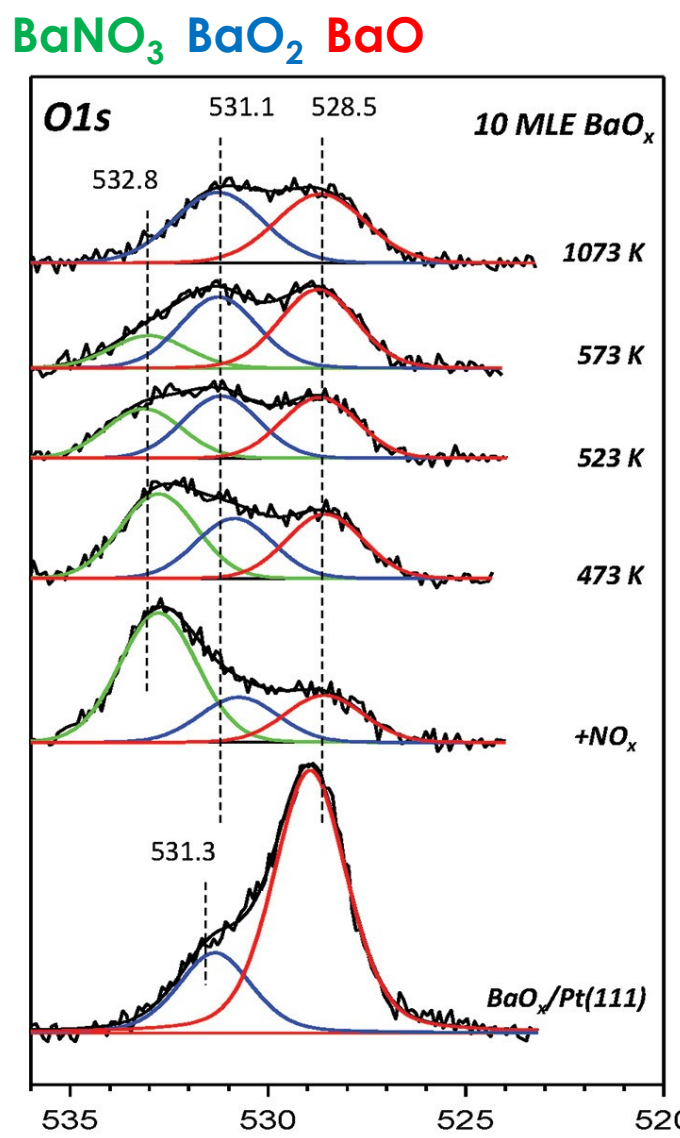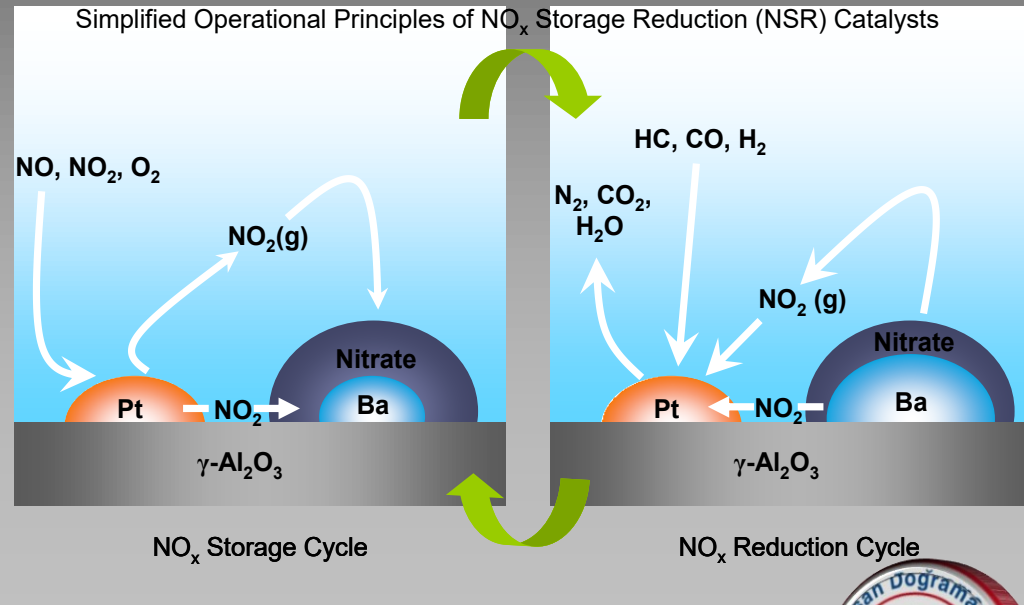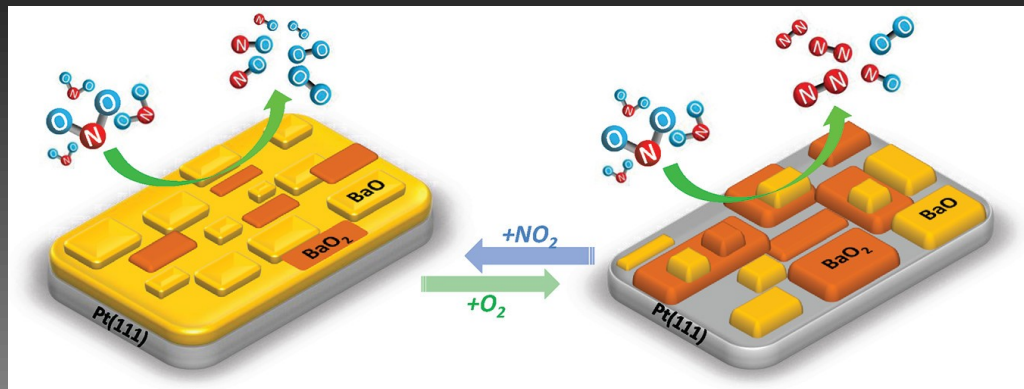
Functional Group Analysis of Mesoporous g-C$_3$N$_4$ Photocatalyst for NO$_x$ Oxidation & Storage
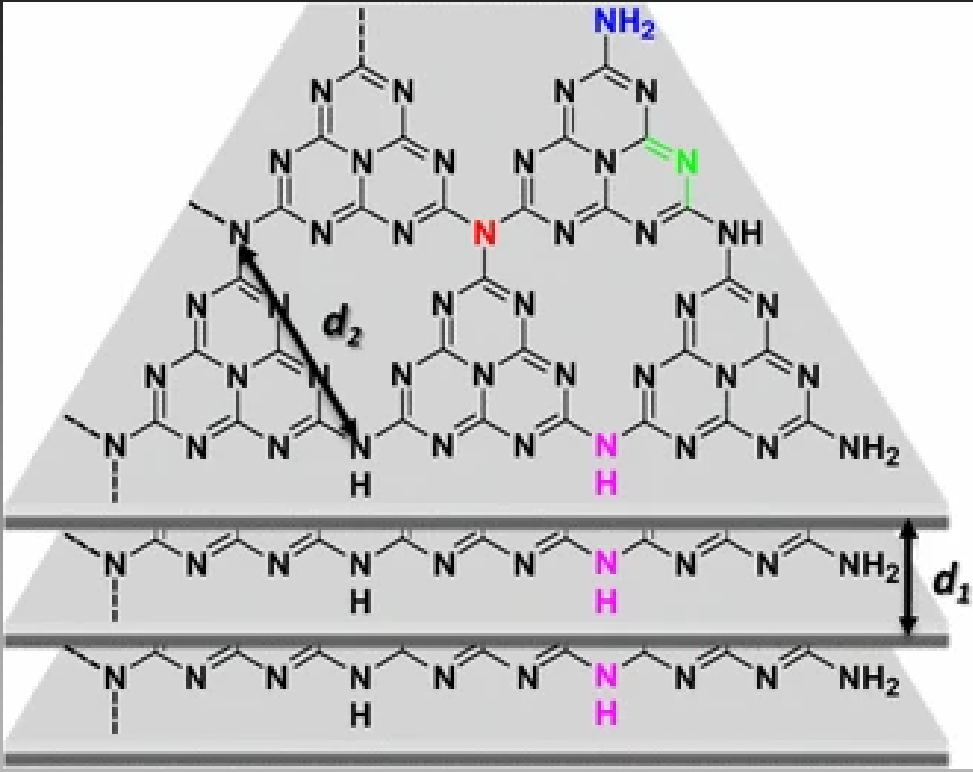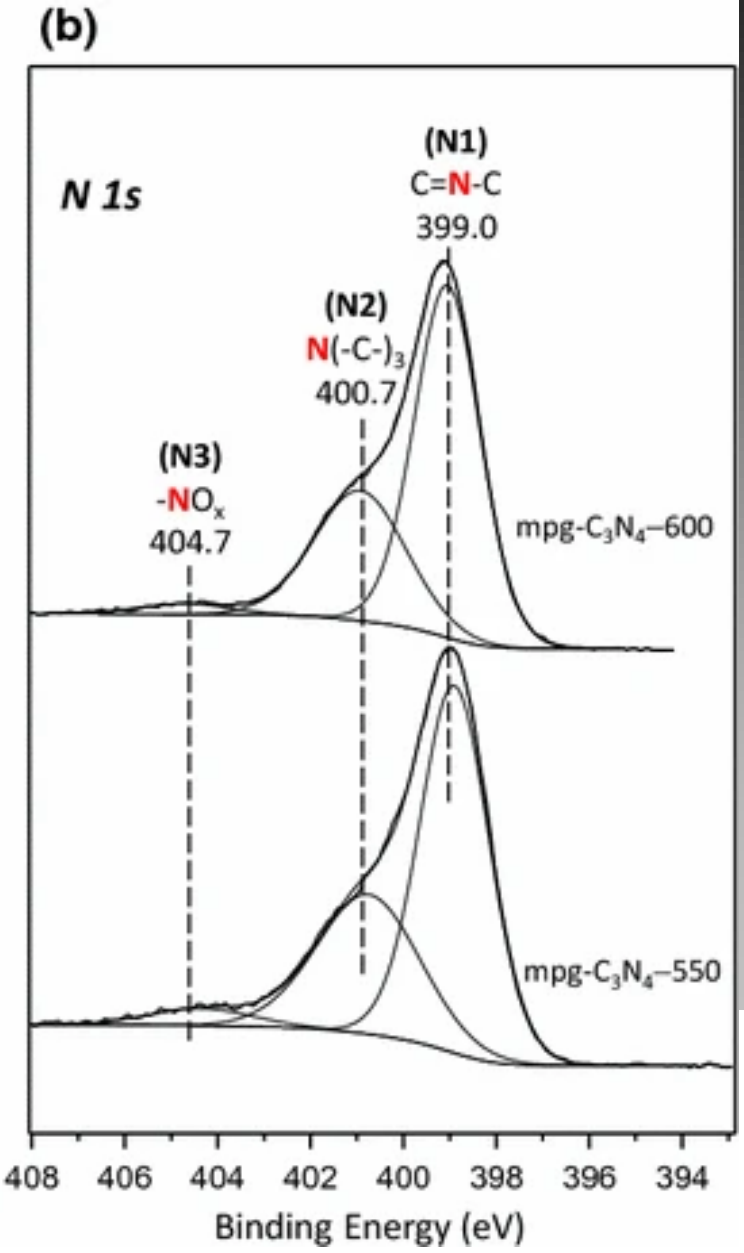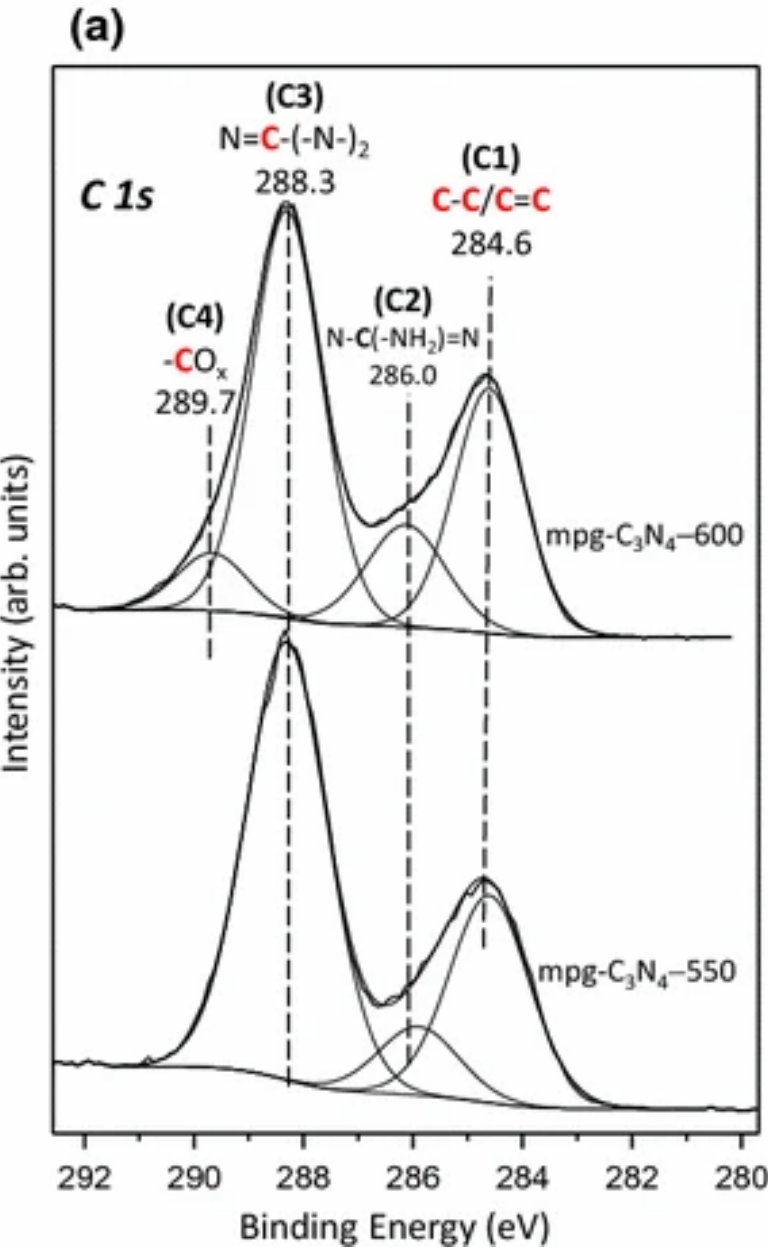
Mesoporous g-C$_3$N$_4$

Electronic Nature of Chemisorbed Oxygen Species on Ag(111) MeOH Oxidation Catalyst
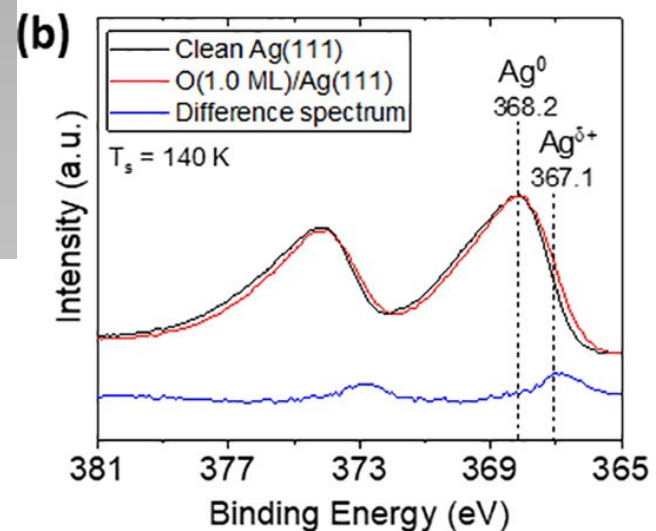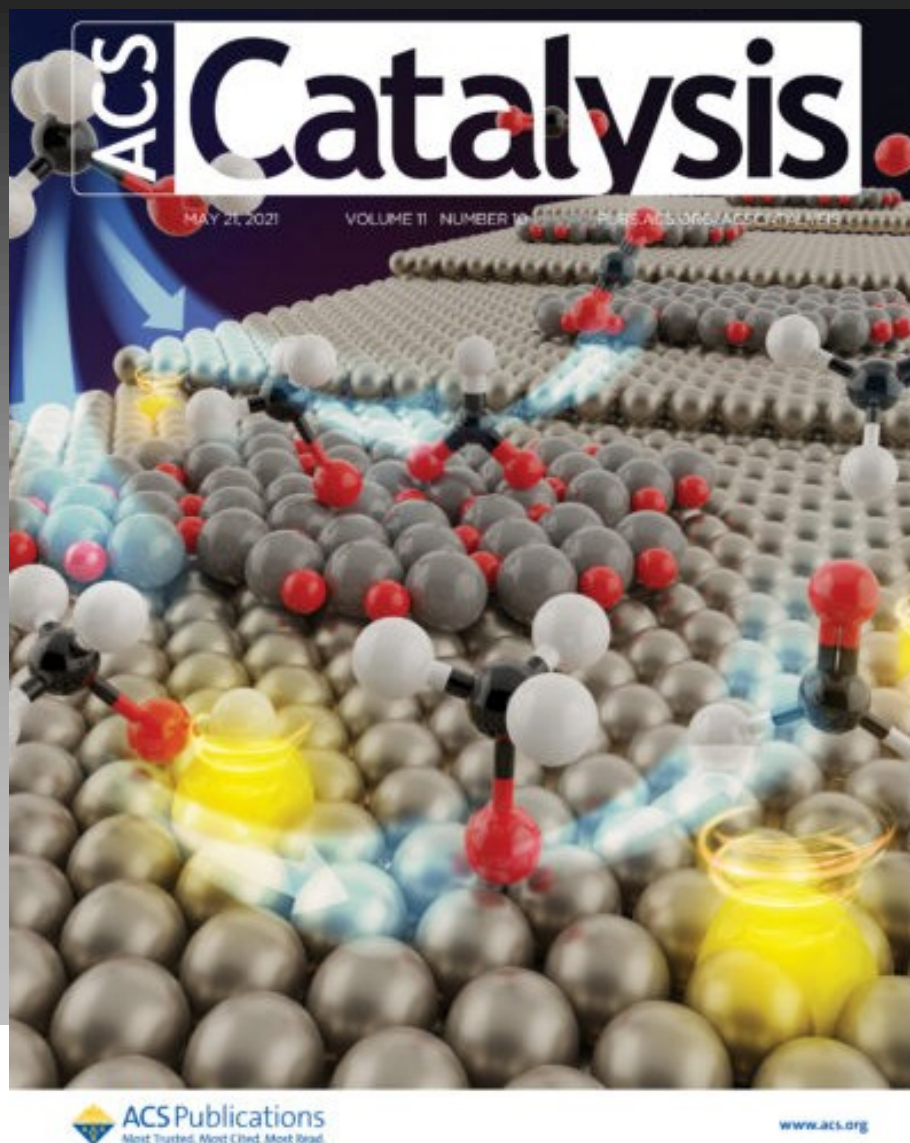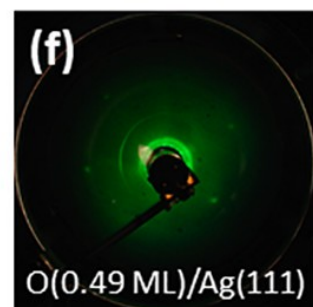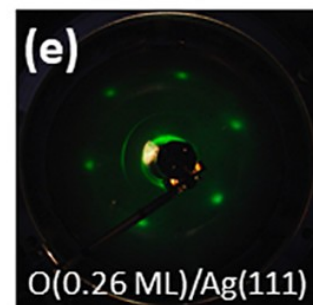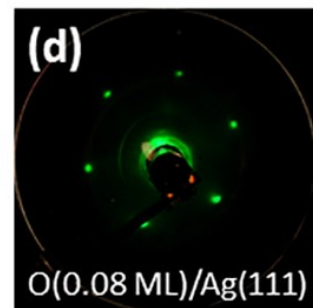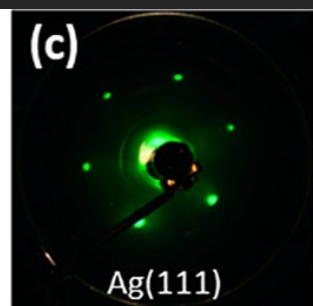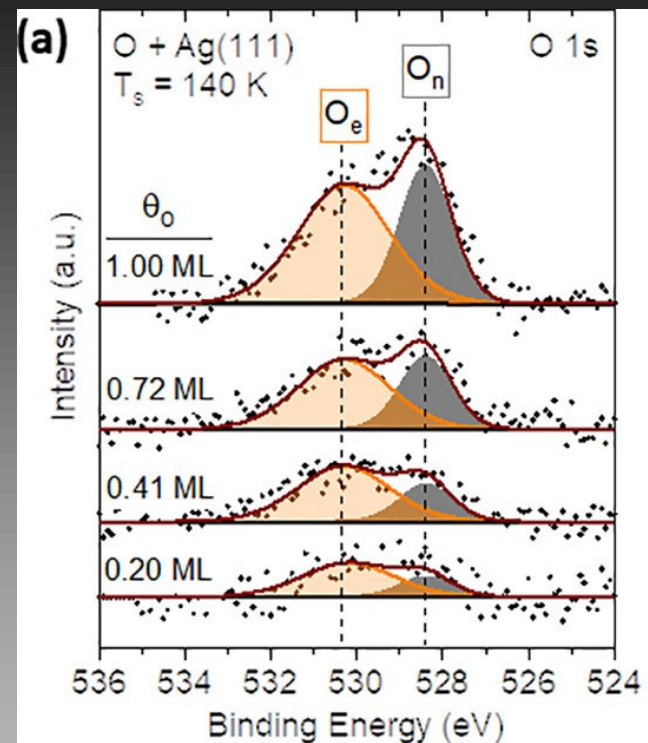
Karatok & Ozensoy et al. ACS Catalysis, 2021 (21) 6200

Emrah Özensoy
Bilkent University

Ozensoy & Szanyi et al. J. Phys. Chem. B, 2005, 109, 8, 3431

Emrah Özensoy
Bilkent University

Surface Chemistry of Quantum-Well CdSe/CdSeTe Photocatalyst for NO$_x$ Oxidation & Storage

Introduction to X-ray Photoelectron Spectroscopy (XPS)

Emrah Özensoy

Bilkent University

Chemistry Department
Ankara, Türkiye

Turkish Soft **X**-ray **P**hoto**E**lectron **S**pectroscopy Project

TXPES

SESAME

OzensoyLab
Catalysis for Energy, Environment and Sustainability

Thank You

https://ozensoylab.bilkent.edu.tr/